Heavy Ion Laboratory

ANNUAL REPORT 2021

UNIVERSITY OF WARSAW

HIL Heavy Ion Laboratory

Heavy Ion Laboratory

University of Warsaw

Annual Report

2021

Warszawa, June 2022

Various information concerning the Laboratory is distributed via the HIL mailing list.
In order to subscribe to the list please visit the page
`http://mail.slcj.uw.edu.pl/mailman`

Annual Report of the
Heavy Ion Laboratory, University of Warsaw
ul. Pasteura 5a, 02-093 Warszawa, Poland
phone (+48)22-8222123, (+48)22-5546000
fax (+48)22-6592714
`http://www.slcj.uw.edu.pl`

The editors thank Andrzej Tucholski
for his help in collecting and formatting
the Publications presented in the Appendices to the Report

Editors:
Nicholas Keeley, Michalina Komorowska, Justyna Samorajczyk-Pyśk,
Marzena Wolińska-Cichocka
e-mail: raport@slcj.uw.edu.pl
ISSN 1895-6726

Cover design:
Rafał Klęk

On the cover:
Nuclei of CHO-K1 cells irradiated at HIL with a dose of 4 Gy of C-12 beam
with an average LET in the cell area of 635 keV/µm.

Contents

Introduction . . . 5

A Laboratory overview and technical developments **7**

A.1 Cyclotron operation in 2021 and tasks carried out in order to improve the cyclotron infrastructure and efficiency . . . 9

A.2 Status of the 10 GHz ECR ion source at HIL . . . 12

A.3 Status of the EAGLE array . . . 15

A.4 NEDA at HIL . . . 16

A.5 A standalone station with automatic loading, dedicated to the PETtrace cyclotron, intended for the irradiation of various types of targets . . . 18

A.6 Status of the Radiobiology Laboratory at HIL . . . 19

A.6.1 Teaching in 2021 at the Radiobiology Laboratory . . . 19

A.6.2 Improvement of the Radiobiology Laboratory . . . 19

A.7 Upgrade of the radiobiological facilities at HIL UW – funded under the program for the research group at JINR and research centers in Poland . . . 22

A.8 Beam position monitoring system based on SiC detectors . . . 25

A.9 Commissioning of digitizers developed at HIL . . . 28

A.10 Polish Workshop on the Acceleration and Applications of Heavy Ions . . . 30

A.11 Fourth edition of the Nuclear Physics Innovation and brokerage event – Global Nuclear Physics Innovation . . . 32

B Research for medical and biological applications **35**

B.1 Improved synthesis of ^{18}FHBG for molecular imaging of progenitor cells in mice models . . . 37

B.2 Stability of selenium compounds in standard samples during storage under different conditions . . . 39

B.3 How the clean-up procedure influences the antioxidant activity of selenium nanoparticles . . . 41

B.4 Study of biological effects in glioblastoma radiosensitive and radioresistant cell lines after exposure to high LET radiation . . . 43

B.5 Porphyrin complexes as potential radiopharmaceuticals for PET . . . 46

B.6 Preliminary investigations of the mechanisms of radiochromic response in three-dimensional gel dosimeters as applied to hadron radiotherapy . . . 48

B.6.1 Goal . . . 48

B.6.2 Materials and Method . . . 48

B.6.3 Preliminary Tests . . . 48

B.6.4 Conclusions . . . 49

B.6.5 Investigations Planned for 2022 . . . 49

B.7 The HIL - ICHTJ Collaboration . . . 50

B.7.1 Production of $^{197/197m}$Hg . . . 50

B.7.2 Production of ^{44}Sc . . . 50

B.7.3 Production of ^{99m}Tc . . . 52

B.7.4 Production of ^{89}Zr . . . 52
B.7.5 Production of ^{135}La . . . 52
B.7.6 Production of ^{72}As . . . 53

C Nuclear physics **55**
C.1 Dissipation by transfer and its influence on fusion . . . 57
C.2 Coupling of ^{6}Li+^{10}B elastic scattering with the inelastic channels . . . 60
C.3 Asymptotic normalization coefficient for the ^{14}C→^{13}B+p overlap from the ^{14}C(^{11}B,^{12}C)^{13}B reaction . . . 61
C.4 Spin 3^+ of the 1415.5 keV level from the γ-band in ^{138}Nd measured using γ–γ angular correlations . . . 62
C.5 Collective isovector quadrupole excitation in ^{142}Sm - Identification via a γ-γ–corelation measurement after ϵ/β^+ decay . . . 65
C.6 Construction of 10 µm, self-biased epitaxial silicon detectors operated in a built-in-field bias potential for radiation hardness tests . . . 69
C.7 Radiation damage of PIN diode detectors irradiated with heavy ions studied using positron annihilation spectroscopy. . . . 72
C.8 Elastic scattering differential cross section for ^{6}He on protons at 26MeV/n 75
C.9 Collective bands in ^{128}Xe as seen from the 'beyond mean field' perspective 77
C.10 Comparison of Coulomb breakup effects on the elastic scattering of ^{6}He and ^{8}He using a Coulomb dipole polarization potential . . . 80

D Appendices **81**
D.1 List of experiments performed at HIL in 2021 . . . 83
D.2 Degrees and theses completed in 2021 or in progress . . . 84
D.2.1 PhD theses of students affiliated to HIL, of HIL staff members, and supervised by HIL staff . . . 84
D.2.2 Other PhD theses based on experiments performed at HIL . . . 85
D.2.3 MSc and BSc theses supervised by HIL staff members . . . 86
D.3 Publications . . . 88
D.3.1 Publications in Web of Knowledge and/or Scopus data bases . . . 88
D.4 Seminars . . . 94
D.4.1 Seminars co-organised by HIL . . . 94
D.4.2 Other seminars organised at HIL . . . 97
D.4.3 External seminars given by HIL staff . . . 97
D.4.4 Poster presentations . . . 98
D.4.5 Lectures for students and student laboratories . . . 99
D.5 Honours and Awards . . . 101
D.6 Laboratory staff . . . 102
D.7 Laboratory Council . . . 103
D.8 Programme Advisory Committee . . . 104
D.9 External HIL users . . . 105

List of Authors **107**

Introduction

Activity at our laboratory in the first half of 2021 was still strongly influenced by the COVID pandemic. The scientists were encouraged to work from home while the technical staff mostly worked on-call. This situation changed with the decision of our Rector that from the first of July the University of Warsaw should return to normal working conditions from before the pandemic period. Thus, after the summer holidays the laboratory, like many other university units, returned to work under normal conditions.

In October, after a one-year break, the traditional workshop for students from various Polish universities was organized. The number of students applying for participation was the largest in the history of this event (45 persons), although we able to host no more than 20 of them (see contribution A.10). Simultaneously with this event we hosted the international conference “New Trends in Nuclear Physics Detectors”, with about 80 participants from various countries. This conference was organized in collaboration with the Joint Institute of Nuclear Research, Dubna.

October 2021 was rich in meetings, as just before the student workshop mentioned above a two-day workshop devoted to the “NEDA at HIL” project was organized. This project is related to the foreseen installation of the NEDA neutron array at HIL, which will open up opportunities to use it in a series of experiments in combination with the standard HIL detectors, such as the gamma-detector array EAGLE. The fact that this very modern neutron-detector array consisting of 59 neutron detectors of 70% efficiency and very good gamma-neutron discrimination will be installed and used at HIL is due to the considerable efforts of Dr. Grzegorz Jaworski and Dr. hab. Marcin Palacz. This project is co-funded by the Polish National Science Centre.

Continuing with meetings hosted by HIL, at the beginning of December we co-organized the fourth edition of the brokerage event “Global Nuclear Physics Innovation” (contribution A.11). In a difference with previous editions, this meeting was organized on-line, as in 2021.

At the end of November we were able to return to our experimental activities, and the first experiment was the project HIL88 related to the study of collective excitations in ^{142}Sm (contribution C.5). The team of physicists consisted of scientists from the Technical University Darmstadt, the St. Kliment Ohridski University Sofia and HIL. A beam of ^{32}S was delivered by our U-200P heavy ion cyclotron. This successful run reduced our backlog of experiments accepted by the Programme Advisory Committee before the COVID pandemic period.

Since the beginning of 2021 our laboratory has engaged in the preparation of the EURO-LABS project to provide funding for access to European research infrastructure under the Transnational Access formula. The Heavy Ion Laboratory will provide 1,000 beam hours for 8 international experiments and will host 40 foreign researchers in the four year duration of the project. In addition, our laboratory took part in the preparation of streamlined access to facilities and contributed to a plan to establish a collaboration of target maker laboratories. The EURO-LABS proposal was submitted to the EC portal in September 2021 and in January 2022 the project was approved.

In December a meeting of the HIL Scientific Council was held, with new members nominated by the Rector of the University of Warsaw. During the meeting new members of the Programme Advisory Committee were elected. December also saw the termination of the tenure of Krzysztof Rusek as the director of HIL, so I (KR) would like to thank all my HIL colleagues for a very fruitful several years of collaboration and to congratulate my successor Dr. Pawel Napiorkowski, appointed by the Rector, and wish him all the best in the coming years. In accepting the duties of acting director of HIL, I (PJN) would like to express my deep gratitude to Prof. Rusek for over a decade of efforts to develop and establish our laboratory.

Unfortunately, the beginning of this year also brought the drama of war in Ukraine and a tragedy that affected our colleagues from Kiev. We hope that they will be able to return to research soon and that we will meet them all again during experiments at our Laboratory.

Part A
Laboratory overview and technical developments

A.1 Cyclotron operation in 2021 and tasks carried out in order to improve the cyclotron infrastructure and efficiency

J. Choiński, P. Gmaj, A. Bednarek, T. Bracha, A. Jakubowski, P. Jasiński, W. Kalisiewicz, M. Kopka, W. Kozaczka, P. Krysiak, K. Łabęda, K. Makowski, I. Mazur, J. Miszczak, O. Saeed Mohamed Nassar, B. Paprzycki, K. Pietrzak, B. Radomyski, K. Sosnowski, Ł. Standyło

Heavy Ion Laboratory, University of Warsaw, Warszawa, Poland

Operation:
Similarl to recent years the technical team of HIL was focused on the development of the cyclotron infrastructure and delivering beams to experiments recommended by the PAC and accepted by the Director of HIL. Limited financial resources means that the main effort of the technical staff was to increase the cyclotron's capacity and capabilities without investing in major modernization projects. This includes the maintenance of the whole cyclotron infrastructure and replacement of worn-out components.

ECR Ion source:
The ECR control system was upgraded to take advantage of the free experimental time introduced by the constraints of the Covid-19 pandemic. In addition to eliminating errors and deficiencies in the source software and replacing some of the hardware causing critical dysfunctions of the ECR system, the possibility of temporary beam chopping (macro-chopper with a period of repetition of a few minutes) was introduced as required by an international project approved by the PAC. The proper functioning of the source power supply system, which had been damaged during preparations for the experiment with the modulated beam, was restored.

Work to obtain a high current and stable Nickel beam was another affort made by the ECR team. Since the nickelocene which was tested before is very toxic and carcinogenic and needs special treatment, a new organonickel compound was obtained with collaboration from the Faculty of Chemistry (Warsaw University of Technology) and the Institute of Biochemistry and Biophysics (Polish Academy of Sciences). A new MIVOC chamber with external heating was designed. Since this compound is not a standard MIVOC compound which is volatile at room temperature, the evaporation point had to be found. Starting with 120°C, 9mA of $^{59}Ni^{9+}$ was produced but the beam was not stable. Tests will be continued because the results are not better than with nickelocene.

Cyclotron:
The condition of the resonators and duants was checked in accordance with the periodic inspection plans. It was found that both the resonators and the duants required re-adjustment. As a result, the position of the resonators is now parallel to the walls of the cyclotron vacuum chamber and the duants are symmetrically positioned with respect to the linings in both vertical and horizontal planes. A slight modification was made to the duant "A" puller. Taking advantage of the opening of the cyclotron, the shape of the cyclotron center was modernized in order to install a new inflector the following year. The

current inflector is powered by a socket that is damaged from time to time. Repairing it requires opening the cyclotron, which is time-consuming. It takes about 4-5 days from opening to re-creating a high vacuum in the cyclotron. Therefore, two types of inflector were designed, see Fig 1.

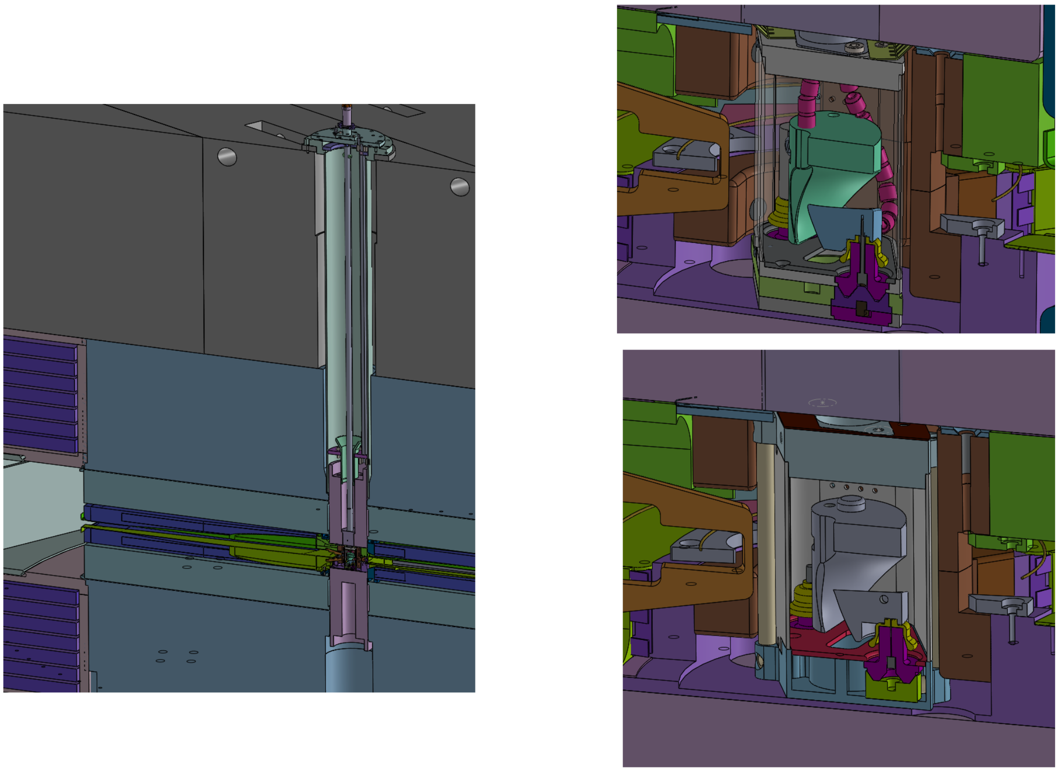

Figure 1: Cross sections. Left side – an inflector loading to the cyclotron from the top channel. Right side top – an inflector without a socket. Right side bottom - an inflector with a socket.

Both allow replacement by opening the top channel in the cyclotron yoke. Next year we will check which version allows for longer trouble-free operation of the cyclotron. As a result, the time for replacement and obtaining the final vacuum level will be shortened to 1.5 days. There are plans to develop a version of the inflector that will allow for its replacement without the need to break the cyclotron vacuum. The water flow meters in all the cyclotron correction coils were also replaced. The previous model began to be unreliable after many years of operation.

Our new system for target irradiation using internal beam which has a much more efficient cooling system and therefore allows irradiation with a more intense beam, necessary for experiments related to the production of radiopharmaceuticals, was expanded with a system for automatic transport of the irradiated target to a shielded transport container.

Magnetic measurement system:
A mechanical system for measuring the cyclotron magnetic field was put into operation. The software for controlling the movement of a cart with a measuring coil was developed and simulated tests of trolley runs were carried out. The tests showed improper functioning of the signal cable routing, which resulted in positioning errors and a reduced range of motion in relation to requirements. Further work is required which should allow for the

correct synchronization of the position of the coil cart with the position recorded by the Metrolab FDi2056 integrator.

Control system of the cyclotron:
As described in the 2020 HIL report [1], the main control system of the cyclotron now uses Linux as its core OS. There were numerous improvements and bug fixes to the control system in 2021, but it is the operator console that has changed the most during that time. Instead of one application tasked with gathering/propagating field data and presenting these data to the cyclotron operator, the latter task is now performed by a web browser. This approach allows for a smaller code base (fewer programming errors) and follows the general industry trend to break big programs into smaller, more manageable chunks. As a safety measure only computers on the laboratory LAN can access cyclotron data.

Experiments:
In 2021 two experiments recommended by the PAC were performed: HIL 088 and HIL 094. They were qualified for co-financing by the Trans-National Access program of the H2020-INFRAIA-1-2014-2015 project, ENSAR2 - European Nuclear Science and Applications Research (Agreement N°654002). Additionally, two other experiments were carried out from the pool of the Director of the HIL: one in the field of radiobiology and the other concerning materials research.

- HIL094 — Electromagnetic structure of low-lying states in ^{110}Cd - complementary Coulomb excitation measurements with a ^{14}N beam
- HIL088 — Collective Isovector Quadrupole Excitation in ^{142}Sm – Identification via a $\gamma - \gamma$ Correlation Measurement after ε/β^+ -decay on May 17-21, 2021
- Examination of radiation defects in Cu and Ag foils and in semiconductor detectors irradiated with a ^{12}C beam with an energy of 40MeV on May 24-28, 2021
- Study of the biological response of a glioblastoma cell line and the radiochromic response of polymer-gel dosimeters to ionizing radiation with high LET

The remaining five experiments planned for implementation in 2021 and recommended by the Experimental Committee had to be postponed due to various limitations caused by the pandemi, which made it very difficult or even impossible for experimental teams to come from abroad. Completing the accelerator service team due to unexpected isolation and quarantine of HIL employees was also a problem.

Like every year, the cyclotron division delivered beam for the students' workshop, which took place in the autumn.

Bibliography

[1] J. Miszczak, Z. Kruszyński, HIL Annual Report 2020, page 12 .

A.2 Status of the 10 GHz ECR ion source at HIL

L. Standyło, K. Sudlitz

Heavy Ion Laboratory, University of Warsaw, Warszawa, Poland

This report summarizes recent work that has been carried out to restart operation of the 9.55 GHz ECR [1] ion source. The source [2] delivered ion beams to the U-200P cyclotron until 2015. The problem was the failure of the Klystron microwave lamp in the RF generator. The lack of availability on the market and the high price of a replacement lamp forced the suspension of the source's operation for some time. A generator with an X-band Klystron, Fig. 1, borrowed from the HIL ECRIS test stand, was installed and tested with the current source. In the meantime, the broken microwave lamp was sent for repair.

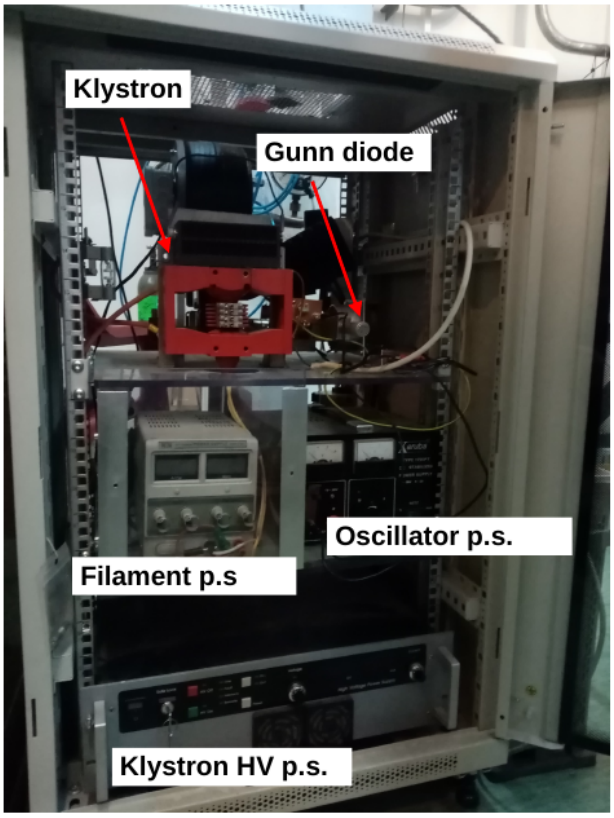

Figure 1: Generator rack with klystron lamp. The generator was built at HIL for experiments on the ECRIS test stand. The klystron is air-cooled - this type is typically used in military aviation. (p.s. - power supply)

Before the ECR ion source commenced operation, following steps were performed:

- RF generator: connection of the generator rack to the ion source. Tests with tuning and RF power injection to the plasma chamber. Stable work with maximum power for this generator is 250 W.
- ECR trap: water and thermal protection have been improved - the coil power supplies are turned off instantly when there is no coolant or when the coil temperature is exceeded.

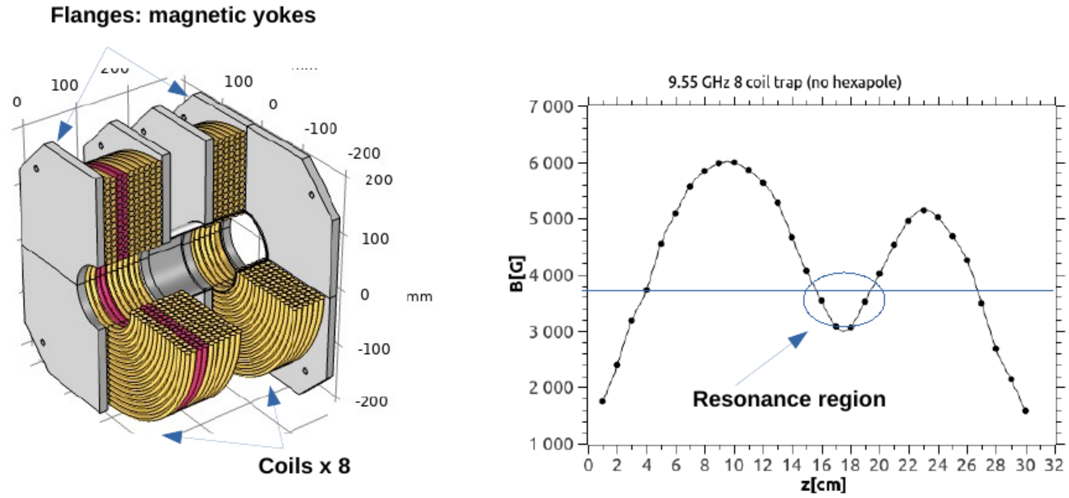

Figure 2: *(Left)* Magnetic trap (the hexapole layout is not shown) for the 9.55 GHz ECRIS. *(Right)* Axial magnetic field measurement for 8 coils configuration: 5 coils in the injection part and 3 in the extraction part.

- ECR trap: A measurement of axial magnetic field (without hexapole) was performed – Fig. 2 (left). The magnetic field from the trap flange - entrance to the chamber, to the flange on the puller side was measured. The current on the coils was 500 A maximum. The second coil has approx. 30% lower power than the others, but it can be assumed to work. The remaining coils catch up with the magnetic field on the RF inlet side (injection part). The positions of the resonance peaks and their values are consistent with measurements made earlier. It appears that the position of the resonant region in the trap has not changed.

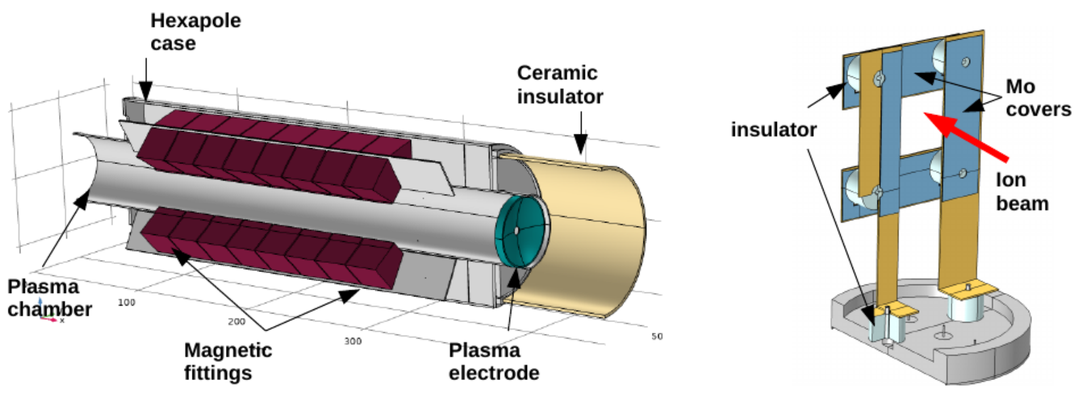

Figure 3: *(Left)* The hexapole setup is placed inside, in the center of themagnetic trap, between two sets of coils. The permanent magnet configuration creates a radial magnetic field which stabilizes the conditions for plasma confinement (MHD)[3]. *(Right)* Simple diagnostic collector for the extracted ion beam from the plasma chamber.

- The glass insulator separating the plasma chamber from the extraction system has broken and been replaced with a ceramic one, more resistant to mechanical and thermal damage – Fig. 3(left).

- The coils cooling system was upgraded and the magnetic field of the hexapole configuration checked, the hexapole cooling system improved, and the, pneumatic connections, buffer container and oil pump replaced. After all parts were assembled, the system was checked for vacuum tightness. A simple collector in the form of a frame (four isolated plates) – Fig. 3 (right) was mounted to check the spread and position of the beam coming out of the ECR chamber. The collector is located behind the correction coil and in front of the analyzing magnet, just after the source.

Ion source performance is still under test. ECR plasma ignition starts with 25 W of injected RF power and remains stable. The total beam current extracted from the trap was around 10 mA with 100 W RF power and 10 kV extraction voltage applied to the plasma chamber. Currently, it is planned to extend the source's range to the production of metallic ion beams.

Bibliography

[1] R. Geller, Rev. Sci. Inst. textbf71, 612 (2000).
[2] K. Sudlitz*et al.*, NUKLEONIKA 2003; **48**(Supplement 2):S105-S108.
[3] J.P. Blewett and E.J. Jones, Phys. Rev. C **50**, 465 (1936).

A.3 Status of the EAGLE array

M. Palacz, T. Abraham, M. Kisieliński, M. Kowalczyk, W. Okliński, for the EAGLE collaboration

Heavy Ion Laboratory, University of Warsaw, Warszawa, Poland

The central European Array for Gamma Levels Evaluations (EAGLE) is an array of High Purity Germanium (HPGe) detectors located at HIL [1], see also [2]. Up to 30 HPGe detectors with anti-compton shields can be installed in the EAGLE frame, and the setup can be augmented with various ancillary devices.

The Heavy Ion Laboratory operates a number of HPGe detectors on loan from GAMMAPOOL [3]. In 2021 an application to prolong the loan period until December 2023 was submitted to GAMMAPOOL and subsequently accepted. At present, 15 complete sets of a HPGe detector and its anti-compton shield are allocated by GAMMAPOOL to HIL, and an additional 3 HPGe detectors are supposed to be shared as spares between HIL and the University of Jyväskylä. HIL also owns 19 smaller detectors with anti-compton shields, which may also be installed in the EAGLE frame. The detectors located at HIL are routinely serviced in-house [4].

At the beginning of 2021 all experimental activities with EAGLE were on-hold due to the COVID-19 pandemic. In June a measurement was run which had a partly commissioning character for a new digitial data acquisition system developed at HIL for EAGLE [5, 6], see the separate contribution [8]. Functioning of the entire HPGe array and of the Coulex chamber with pin-diodes installed was tested at the same time, after a long period of inactivity of EAGLE. In November 2021 an experiment to study collective isovector quadrupole excitation in ^{142}Sm was performed, see Ref. [9]. Also in 2021, a project to install a collection of neutron detectors named NEDA in connection with EAGLE was initiated, see Ref. [10] and references therein.

Bibliography

[1] J. Mierzejewski *et al.*, Nucl. Inst. and Meth. **A659** (2011) 84.
[2] M. Palacz *et al.*, HIL Annual Report 2019, page 12
[3] T. Abraham *et al.*, HIL Annual Report 2016, page 17.
[4] T. Abraham *et al.*, HIL Annual Report 2017, page 14.
[5] M. Kowalczyk, HIL Annual Report 2017, page 16.
[6] T. Abraham *et al.*, HIL Annual Report 2018, page 51.
[7] M. Kowalczyk, HIL Annual Report 2014, page 14.
[8] K. Wrzosek-Lipska, this Report, page 28.
[9] T. Stetz, this Report, page 65.
[10] G. Jaworski *et al.*, this Report, page 16.

A.4 NEDA at HIL

G. Jaworski, M. Palacz, for the EAGLE-NEDA Collaboration
Heavy Ion Laboratory, University of Warsaw, Warszawa, Poland

A new, state-of-the-art system of neutron detectors, called NEDA [1, 2], was constructed over the last decade by an international collaboration. In the years 2022-2023 NEDA will be used in experiments at HIL in connection with the EAGLE γ-ray spectroscopy array [3].

The primary application of NEDA is the selection of rare fusion-evaporation channels in measurements in which very proton-rich nuclei are studied. In such experiments, nuclei of interest are produced with very small cross sections, both in absolute and relative terms. Efficient detector aggregates are thus needed and they should make possible very precise selection of the reaction products. The setups usually consist of a γ-ray spectrometer, neutron detectors and charged particle detectors. The role of the neutron detectors is in particular essential, as itis the efficiency and quality of the neutron detection which in most cases sets limits on the feasibility of the investigation of the most proton-rich and most interesting nuclear species.

NEDA has so far been used in one experimental campaign, in 2018, in connection with the AGATA γ-ray spectrometer at GANIL, Caen, France [4–7]. In December 2021 the NEDA equipment was shipped from GANIL to HIL, and its installation on site started. The NEDA detectors will be placed in the forward part of the EAGLE frame, while 15 HPGe detectors will be mounted in the the backward hemisphere, see Fig. 1. In some experiments this setup will be augmented with the DIAMANT charged particle detector [8], situated inside the EAGLE-NEDA ball.

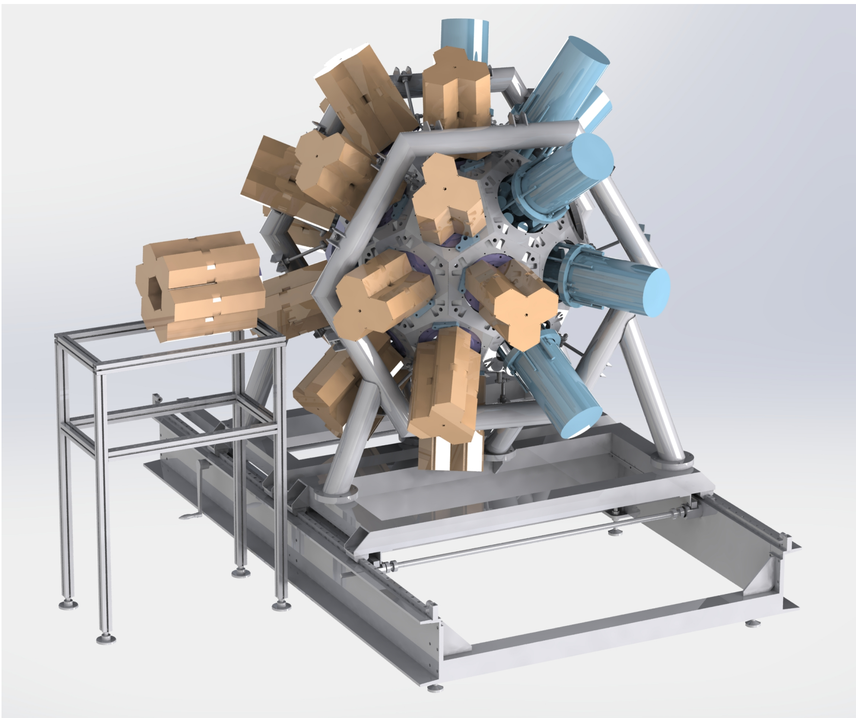

Figure 1: Visualisation of the EAGLE-NEDA array. The NEDA detectors are marked in light-brown.

In October 2021 a two-day workshop was organised at HIL, with the aim of disseminating information on new experimental opportunites which open with the instalation of NEDA and to discuss specific projects which can be realised using the new setup. About 50 participants from more than 20 European institutions took part in the workshop. Eight letters of intent were presented, and a few other possible projects emerged from the discussions.

Acknowledgement: the installation and use of NEDA at HIL are supported by the Polish National Science Centre grant no. 2020/39/D/ST2/00466, COPIN-IN2P3, COPIGAL, and POLITA projects.

Bibliography

[1] J.J. Valiente-Dobon *et al.*, Nucl. Inst. and Meth. **A927** (2019) 81.
[2] G. Jaworski *et al.*, Acta Phys. Pol. **B50** (2019) 585.
[3] M. Palacz *et al.*, this Report, page 15.
[4] A. Akkoyun *et al.*, Nucl. Inst. and Meth. **A668** (2012) 26.
[5] E. Clément *et al.*, Nucl. Inst. and Meth. **A855** (2017) 1.
[6] B. Cederwall *et al.*, Phys. Rev. Lett. **124** (2020) 062501.
[7] X. Liu *et al.*, Phys. Rev. C **104** (2021) L021302-1.
[8] J.N. Scheurer *et al.*, Nucl. Inst. and Meth. **A385** (1997) 501.

A.5 A standalone station with automatic loading, dedicated to the PETtrace cyclotron, intended for the irradiation of various types of targets

J. Choiński, T. Bracha, J. Kowalska, A. Stolarz, Ł. Świątek, R. Tańczyk

Heavy Ion Laboratory, University of Warsaw, Warszawa, Poland

The Radiopharmaceutical Production and Research Center houses a PETtrace cyclotron with a series of standard stations for the production of ^{18}F, ^{11}C and ^{15}O. The HIL team designed, constructed and operates a dedicated standalone external target system for the irradiation of targets composed both of metallic pieces/foils or of powder (elemental or compound), Figure 1. The target system is fully remotely controlled and protected by Polish patent no. 227402. The dual beam proton/deuteron cyclotron is primarily used for commercial production of fluorine, ^{18}F, provided by an external commercial company. The Heavy Ion Laboratory team, implementing its research program, carries out the production of other radioisotopes in the intervals between regular production of ^{18}F.

The external target system is connected to the cyclotron via a beam line consisting of: a drift tube of a total length of 3.4 m, two sets of steering magnets made of permanent magnets, one quadrupole doublet and a four-sector collimator, with shielding provided by a concrete wall of thickness of 0.25 m. This protective wall ensures the safety of the center staff. The beam line with the target station has its own autonomous vacuum system which allows a static vacuum of $4 \cdot 10^{-7}$ mbar to be reached.

Figure 1: The standalone station with the beam line attached to the PETtrace cyclotron

The beam transport efficiency to a target with a diameter of 10 mm is close to 95%. A fully remotely controlled robot loads the target into its position from an eight position carousel. It is an integral part of the target system. After irradiation the target drops into a lead container and is evacuated from the cyclotron vault on a remotely controlled trolley. Last year, despite the restrictions related to the COVID-19 pandemic still in force, we performed a dozen target irradiations for research groups cooperating with us, producing ^{43}Sc, ^{44}Sc, ^{72}As, ^{89}Zr, ^{99m}Tc, ^{135}La and ^{197}Hg isotopes.

A.6 Status of the Radiobiology Laboratory at HIL

U. Kaźmierczak[1], M Paluch-Ferszt[1], Z. Szefliński[1,2]

1) Heavy Ion Laboratory, University of Warsaw, Warszawa, Poland
2) Faculty of Physics, University of Warsaw, Warszawa, Poland

A.6.1 Teaching in 2021 at the Radiobiology Laboratory

Bachelor's thesis and master's thesis

In 2021, research was conducted at the Radiobiology Laboratory at HIL for the needs of a bachelor's (Survivability of cancer cells irradiated by alpha particles from a ^{241}Am source) and master's (Alpha radiation dosimetry of a flat 241-Am source and cellular response to alpha exposure) thesis from students of the Faculty of Physics of the University of Warsaw.

Prostate cancer is the most frequently diagnosed oncological disease in men and one of the most common causes of mortality in terms of malignant neoplastic changes. In order to select the appropriate treatment plan with radiotherapy, the biological response of cells should be assessed depending on the value of the dose deposited in the diseased tissues and in the adjacent critical organs. The DNA of the irradiated cell is damaged by ionizing radiation, which can lead to a reduction in its ability to proliferate.

In the above diploma theses the characteristics of the ^{241}Am flat source located at the Radiobiology Laboratory at HIL was studied. Furthermore, a series of experiments was performed in which prostate cancer cells (PC-3 cell line) were irradiated with different doses of high LET (Linear Energy Transfer) α radiation from a ^{241}Am flat source. The biological response of PC-3 cells exposed to alpha radiation was studied. A clonogenic test was used to evaluate the biological effects induced in the irradiated material. It allows the survival analysis and maintenance of the ability to proliferate irradiated cells.

Student internships

In 2021, a student internship took place at the Radiobiology Laboratory at HIL (a student from the Faculty of Physics of the University of Warsaw).

As part of this internship, the student underwent training in the field of good laboratory practice in the radiobiological laboratory, as well as training in the cultivation of animal cells. The student then examined the characteristics of the ^{241}Am flat surface source available in the lab. The duties of the student were independently to cultivate cells and to conduct a clonogenic test of irradiated biological material.

Research for the purposes of a doctoral dissertation

In 2021, research for the doctoral dissertation of Martyna Araszkiewicz (Doctoral School of Exact and Natural Sciences at the University of Warsaw) began at the Radiobiology Laboratory at HIL. The report on these studies is a separate article of this year's HIL Annual Report (see Ref. [1]).

A.6.2 Improvement of the Radiobiology Laboratory

Furniture replacement

In 2021, the entire radiobiological laboratory underwent modernization. Due to the continuous development and increasing demand for space, in 2021 the HIL Directorate allowed the use of a technical room located in the class III isotope laboratory for the needs of the radiobiology laboratory. The first step towards better space management was the replacement of the laboratory furniture. HIL financed the purchase of new cabinets along one wall with a sink and countertops (see Fig. 1a). Thanks to a furniture donation HIL received from Wiener TU S.A. it was possible to replace all laboratory tables in the room. Additional cabinets fitting beneath the desk tops were also obtained, enabling better space management and storage (see Fig. 1b). All this increased the storage space available for the radiobiology lab.

(a) New cabinet construction.

(b) Tables and donated by Wiener TU S.A.

Figure 1: New furniture in the Radiobiology Laboratory at HIL.

Purchase of new equipment

In addition to replacing the furniture in the laboratory new equipment was also purchased. Purchases of equipment in 2021 from the JINR Dubna grant are described in a separate article (see Ref. [2]), and the equipment financed from HIL's own funds will be presented here.

Water is a major component of all cell culture media and is therefore needed to prepare media, buffers, and additives. Thus, water quality plays an important role in the outcome of cell culture experiments. A Rephile Genie A system for purifying tap water into ultrapure water was installed at the Radiobiology Laboratory at HIL (presented in Fig. 2a). It generates type I ultrapure water on demand from the system and delivers consistently high water quality for reliable and reproducible results in the lab.

In order to create a cryogenic storage system in the radiobiological laboratory, enabling the storage of biological samples in liquid nitrogen (-196°C to -210°C), a special dewar with equipmment was purchased. Biological samples are transferred to cryogenic tubes and packaged in boxes. The boxes are placed in racks, which are then stored in liquid nitrogen in the dewar. The aluminium dewar with racks for storing biological samples available at the Radiobiology Laboratory at HIL is presented in Fig. 2b.

(a) Genie A Ultrapure Water System.

(b) Dewar with racks for storing biological samples.

Figure 2: Purchases of new equipment in 2021 financed from HIL's own funds.

Additionally, an old laboratory dryer has been acquired and restored, thus allowing all plastics and laboratory glassware to be dried faster and in a controlled manner after washing.

Bibliography

[1] M. Araszkiewicz *et al.* this Report, page 43.
[2] M. Paluch-Ferszt *et al.*, this Report, page 22.

A.7 Upgrade of the radiobiological facilities at HIL UW – funded under the program for the research group at JINR and research centers in Poland

M. Paluch-Ferszt, Z. Szefliński

Heavy Ion Laboratory, University of Warsaw, Warszawa, Poland

In order to meet the needs of radiobiological studies, experiments with α particles and heavy ion beam are carried out at the Heavy Ion Laboratory of the University of Warsaw. The Warsaw U-200P cyclotron offers many possibilities to perform radiobiological experiments for different ionizing particles with energies in the region of the Bragg peak. The facility provides beams of energies from 2 to 10 AMeV and intensities up to a few hundreds pnA. At an energy of $\sim$ 2AMeV the energy loss in the biological cells is $\sim$ 1MeV/mm and the range of ions in water is $\sim$ 10µm, which corresponds to a typical cell diameter. At an energy of $\sim$ 10AMeV the energy loss reaches a value of 200 keV/mm and the range of the ions is $\sim$ 400µm. An experimental set-up with a horizontal heavy ion beam designed for radiobiological research at HIL provides the possibility to irradiate biological samples at room temperature and atmospheric pressure by various ions at high linear energy transfer (LET). An ^{241}Am α-particle disc source is also used as an irradiator in radiobiological experiments at the Heavy Ion Laboratory, University of Warsaw.

With the creation of an experimental infrastructure for biological samples it was decided to establish a radiobiology laboratory. In 2018 a group dedicated to experiments in the field of radiobiology at HIL obtained funding for a research program involving the research group at JINR and research centers in Poland. From part of the funds obtained in 2018-2020, the equipment necessary to equip a Radiobiological Laboratory at HIL was purchased [1].

In 2021 the following equipment was bought:

- Radiochromic films – At HIL the dosimetry control system needed to be equipped with new detectors and materials. Since the dosimetric measurements of the radioactive sources are crucial for dose estimation in radiobiological experiments, we bought radiochromic films.
- Accessories/tools for cryopreservation of cell lines or biological samples – Cryopreservation is a method whereby cells are frozen, maintaining their viability, until they are defrosted months or years later. Cells are cryopreserved to minimize genetic change and avoid loss through contamination. Cryopreservation includes freezing, storage, and recovery. Best practices for successful cryopreservation have been established [2–4]. Cells should be frozen at early passage numbers, in an actively growing state (log phase) and at an appropriate concentration. The principle of successful cryopreservation is to freeze slowly and thaw rapidly. A controlled slow cooling at a rate of $-1°C$/min down to $-80°C$ before transferring to ultra-low temperature storage is required to prevent cell death by intracellular ice formation. Specialized containers paired with reliable Ultra-Low Temperature freezers allow for standardization of the freezing procedure [5–7].
- A centrifuge for biological samples, shown in Fig. 1. Centrifugation plays a vital role in cell culture workflows. In passaging, for example, cultures must be spun down

to concentrate cells and separate them from old growth media. When experiments are concluded, centrifugation is often used to support sample characterization and analysis. Another key use of the technology is to collect intra- and extracellular products such as antibodies and other proteins [8].

- Equipment necessary to maintain sterility: autoclave, ultrasonic cleaner, surface welding machine for autoclave material bags, shown in Fig. 2. Successful cell culture depends heavily on keeping the cells free from contamination by microorganisms such as bacteria, fungi, and viruses. Nonsterile supplies, media, and reagents, airborne particles laden with microorganisms, unclean incubators, and dirty work surfaces are all sources of biological contamination. Therefore, disposable or autoclavable sterile instruments are used. Autoclavable materials such as glass should be well washed first. An ultrasonic cleaner is indispensable for this process. Before putting the tools into the Autoclave, they should be sealed in special bags ensuring sterility even after taking them out of the device. An autoclave, also known as a steam sterilizer, is the most effective machine for the sterilization of lab equipment, water, or media. The machine uses steam under pressure to kill bacteria, viruses, and spores present in/on the equipment or culture media.

Figure 1: Centrifuge for biological samples.

Figure 2: Equipment necessary to maintain sterility: autoclave (left), ultrasonic cleaner (center), surface welding machine for autoclave material bags (right).

In the following years further expansion of the Radiobiology Laboratory is planned.

Bibliography

[1] M. Paluch-Ferszt *et al.*, HIL Annual Report (2020) 28-29.
[2] Animal Cell Culture Guide, Cryopreservation, `www.lgcstandards-atcc.org`.
[3] M. Thompson *et al.*, Cryopreservation and Thawing of Mammalian Cells, Wiley Online Library (2014).
[4] General Guide for Cryogenically Storing Animal Cell Culture, `www.corning.com/lifesciences`.
[5] CoolCell, ATCC, ACS-6000. `www.ATCC.org`.
[6] `www.eppendorf.com/freezers`.
[7] `www.abnova.com`.
[8] I. Place, Cell Culture Workflows In a Spin? How Next-generation Centrifuges Are Overcoming Common Challenges, (2019), `www.technologynetworks.com`.

A.8 Beam position monitoring system based on SiC detectors

E. Piasecki[1], J. Choiński[1], G. Colucci[1], H. M. Jia[2], M. Kisieliński[1], M. Kowalczyk[1], C. J. Lin[2], M. Matuszewski[1], N. R. Ma[2], K. Piasecki[3], A. Trzcińska[1], M. Wolińska-Cichocka[1], B. Zalewski[1], L. Yang[2], H. Q. Zhang[2]

1) Heavy Ion Laboratory, University of Warsaw, Warszawa, Poland
2) China Institute of Atomic Energy, Xinzhen, Fangshan, Beijing, China
3) Faculty of Physics, Warsaw University of Technology, Warszawa, Poland

A precise and stable experimental geometry is a necessary condition in some measurements, e.g. concerning fusion excitation functions. This is due to the very steep angular distribution of the fusion products, centered around the beam axis [1]. Because of this, even a slight change in the beam spot position on the target influences the detection angle and, consequently, the cross section. This can lead to serious consequences, in particular during changing the beam energy in measurements of fusion barrier distributions, where the second derivative of the excitation function is taken [2]. Planning this kind of experiment, we looked for a system enabling us to monitor the beam position on the target.

The idea was to base such a system on four detectors placed at relatively small angles, registering Rutherford scattered ions. One can determine the beam position from the ratios of the counting rates of ions hitting the detectors. The smaller the detection angle, the more sensitive the method is. However, radiation damage of the detector is also much faster. Because of this, we decided to use Silicon Carbide (SiC) detectors, owing to their extraordinary hardness to radiation damage [3, 4]. The detector active area is 5 x 5 mm, and the thickness 80 μm (produced by www.techjw.com).

The detector support (see Fig. 1) allows the monitor geometry to be changed depending on requirements. The detectors can be set at angles in the range of 8 – 15 degrees and the distance to the target from 10 to 15 cm. In the test, the SiC detectors were placed at

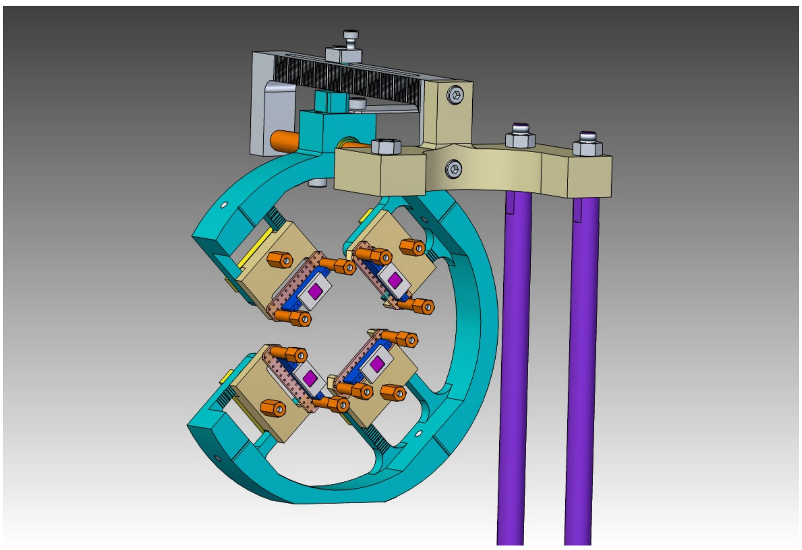

Figure 1: The support for the 4 SiC detectors designed for the ICARE scattering chamber.

10 degrees and 10 cm from the target.

Dedicated electronics were prepared for the SiC detectors. The purpose was a lossless counting of registered ions. The current signals from the reverse-biased SiC diodes at 150 V DC were amplified 30dB with Minicircuits ERA-8SM wideband amplifiers. After passing fast discriminators, the signals were fed to four channels of a CAEN C257 Camac scaler. A fifth channel, with an external clock, provided a time base for simultaneous counting and following readout sequence.

The first test was performed at the ICARE chamber with a ^{32}S beam of 85 MeV energy and 2 enA intensity, passing through a 2 mm diameter collimator, delivered by the U200-P cyclotron of the Heavy Ion Laboratory. The targets used were: ^{nat}Au (0.1 mg/cm^2), ^{nat}Sn (0.1 mg/cm^2) and ^{nat}Mo (0.6 mg/cm^2).

To monitor the beam position, a dedicated GUI application "BeamMon" was developed (see Fig. 2). This ROOT-based code calculates and visualizes online (as well as off-line) the position of the beam center, based on the ratios of the rates of Rutherford scattering events measured in the 4 SiC monitors. In the case of low statistics available in a

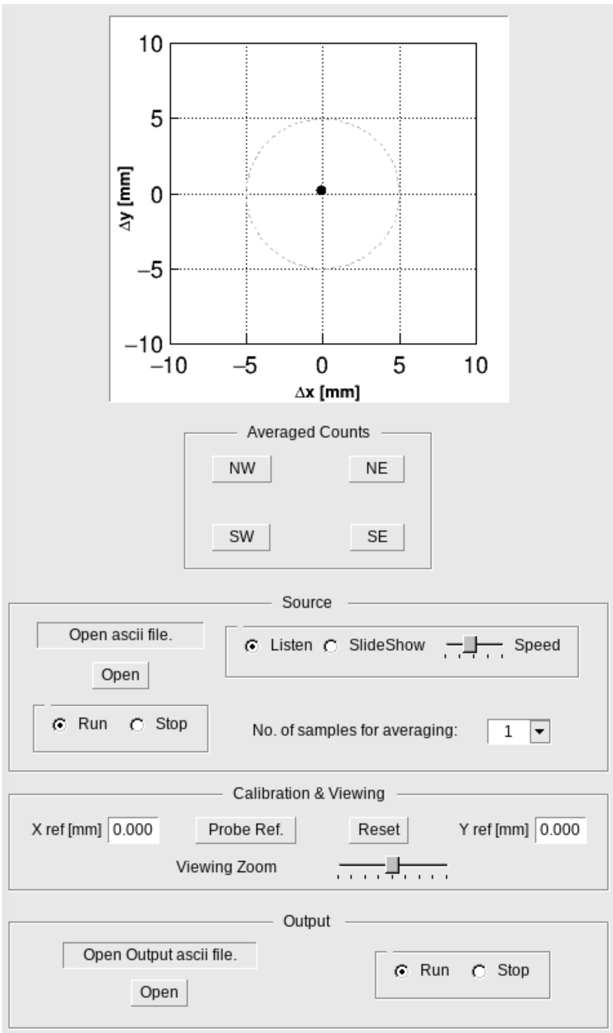

Figure 2: The BeamMon application displaying the beam position on the target online.

single measurement, the application can group in-flight series of data. The user can also reposition the "beam axis" reference point.

A preliminary analysis of the test has been performed and the results of the measurement on the ^{nat}Mo target are shown in Figure 3. The figure shows the vertical and horizontal distribution of the center of the beam position. The spot position was determined every 1 s, but the time interval could be changed depending on the count rate, which in the test run was in the range of 0.4 kHz – 4 kHz (depending on the target and the beam current). The beam spot position was stable during a 7 hour run with an uncertainty of 0.15 mm. In our geometry, this corresponds to an angle uncertainty of less than 0.1 degree.

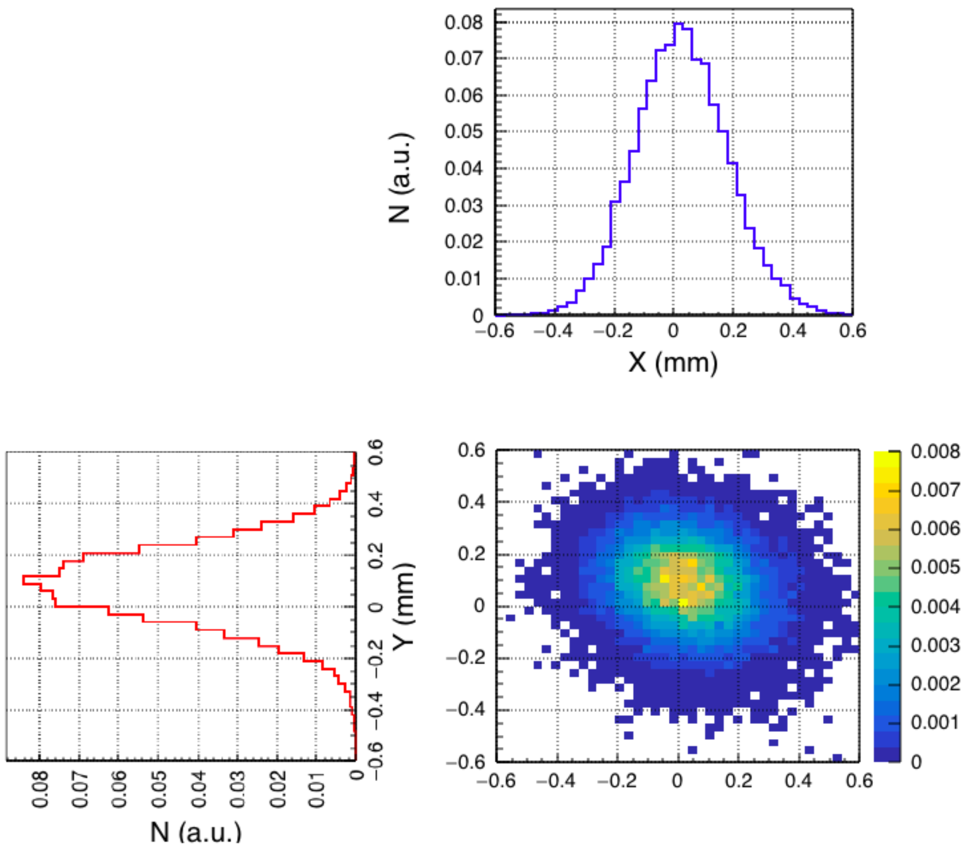

Figure 3: Distribution of the ^{32}S beam spot center on a ^{nat}Mo target, measured with 4 SiC detectors for 7 hours. The uncertainties in the horizontal and vertical positions are 0.15 mm and 0.14 mm, respectively. Preliminary results.

Bibliography

[1] J. X. Wei *et al.*, Nucl. Inst. and Meth. **A306** (1991) 557.
[2] N. Rowley *et al.*, Phys. Rev. Lett. **B254** (1991) 25.
[3] S. Tudisco *et al.*, European Physical Journal Web of Conferences **227** (2020) 01017.
[4] A. Benyagoub and A. Audren, Nucl. Inst. and Meth. **B267** (2009) 1255–1258.

A.9 Commissioning of digitizers developed at HIL

K. Wrzosek-Lipska[1], *M. Kowalczyk*[1], *I. Piętka*[2], *P.J. Napiorkowski*[1], *M. Palacz*[1], *T. Abraham*[1], *G. Colucci*[1], *K. Hadyńska-Klęk*[1], *K.Z. Krutul*[1] *G. Jaworski*[1], *M. Komorowska*[1], *A.M Quỳnh*[3], *J. Samorajczyk-Pyśk*[1], *A. Trzcińska*[1], *A. Tucholski*[1]

1) Heavy Ion Laboratory, University of Warsaw, Warszawa, Poland
2) Faculty of Physics, University of Warsaw, Warszawa, Poland
3) Nuclear Research Institute, Dalat, Vietnam

The first an in-beam measurement with the EAGLE array since November 2019 was carried out in mid June 2021. This measurement had a partly commissioning character of the entire setup after a long period of shutdown, including HPGe detectors, the ancillary detectors, and the data acquisition system.

A 35 MeV ^{14}N beam of and 4 pnA intensity was used to Coulomb excite a 2 mg/cm^2 thick ^{110}Cd target. The EAGLE array was equipped with 16 HPGe detectors. The germanium array was coupled to a scattering chamber with 48 PIN-diodes placed inside to detect backscattered beam particles.

Data from the HPGe detectors were acquired in parallel by standard analog ADCs and, for the first time, with the EFE (EAGLE Front End) digitizers developed at HIL [1]. The analog CAMAC system was running in coincidence mode using a CEFE module [2] as trigger source while the EFE modules were running triggerless (singles mode). Both systems were started and stopped simultaneously and used synchronized clocks for the event time stamp.

Data from the HPGe detectors acquired with the use of the afore-mentioned digital units were utilized to perform an analysis of the γ-γ coincidence events. In the analog system the γ-γ coincidence window width was always set to 200 ns. The digital system allows the window to be set offline using the event time stamp. In our tests the coincidence matrices were created using two different window lengths, 37.5 ns and 75 ns (the time step was 6.25 ns). No significant differences between the two settings were observed.

The analysis of the in-beam γ-γ coincidence data allowed us to identify additional γ ray transitions as a result of nuclear reactions of the ^{14}N beam on the aluminium target frame as well as light target contaminants: ^{16}O and ^{12}C. The strongest identified γ lines are marked in the spectrum and shown in Fig. 1.

In aditional to the in-beam measurements, 3.5 hour after off-beam the natural background γ-ray spectrum was also collected. The latter was acquired in the so called *single-γ mode*. It is interesting to note the observation of an intense 1369-keV transition which cannot be atributed to the natural Ra and Th decay chains [3]. Moreover, the 1369-keV line was a few times stronger compared to the well known background 1461-keV γ line which follows the β decay of ^{40}K. The only possible origin of the 1369-keV γ-ray transition was that it results from long-lived radioactivity produced in-beam via the afore-mentioned nuclear reactions.

As shown in Fig.1, the 1369-keV γ-ray transition is clearly visible in the γ-γ coincidence spectrum. The analysis showed that the 1369-keV γ depopulates the first excited 2^+_1 state in ^{24}Mg, which is strongly produced in the ^{12}C(^{14}N,pn)^{24}Mg reaction. In addition to this, the 1369-keV 2^+_1 state in ^{24}Mg is also fed following the β decay of ^{24}Na from its 4^+ ground state. The ^{24}Na isotope is the reaction product of the ^{12}C(^{14}N,2p)^{24}Na reaction. The lifetime of the 4^+_{gs} state in ^{24}Na is $T_{1/2}$=15 hours, giving rise to the 1369-keV γ line observed in the background spectrum.

The analysis of the in-baem γ-γ coincidence data and off-beam background spectra, both acquired with the use of the in-house developed digital units, was the subject of the student internship of I. Piętka, performed at HIL in September 2021.

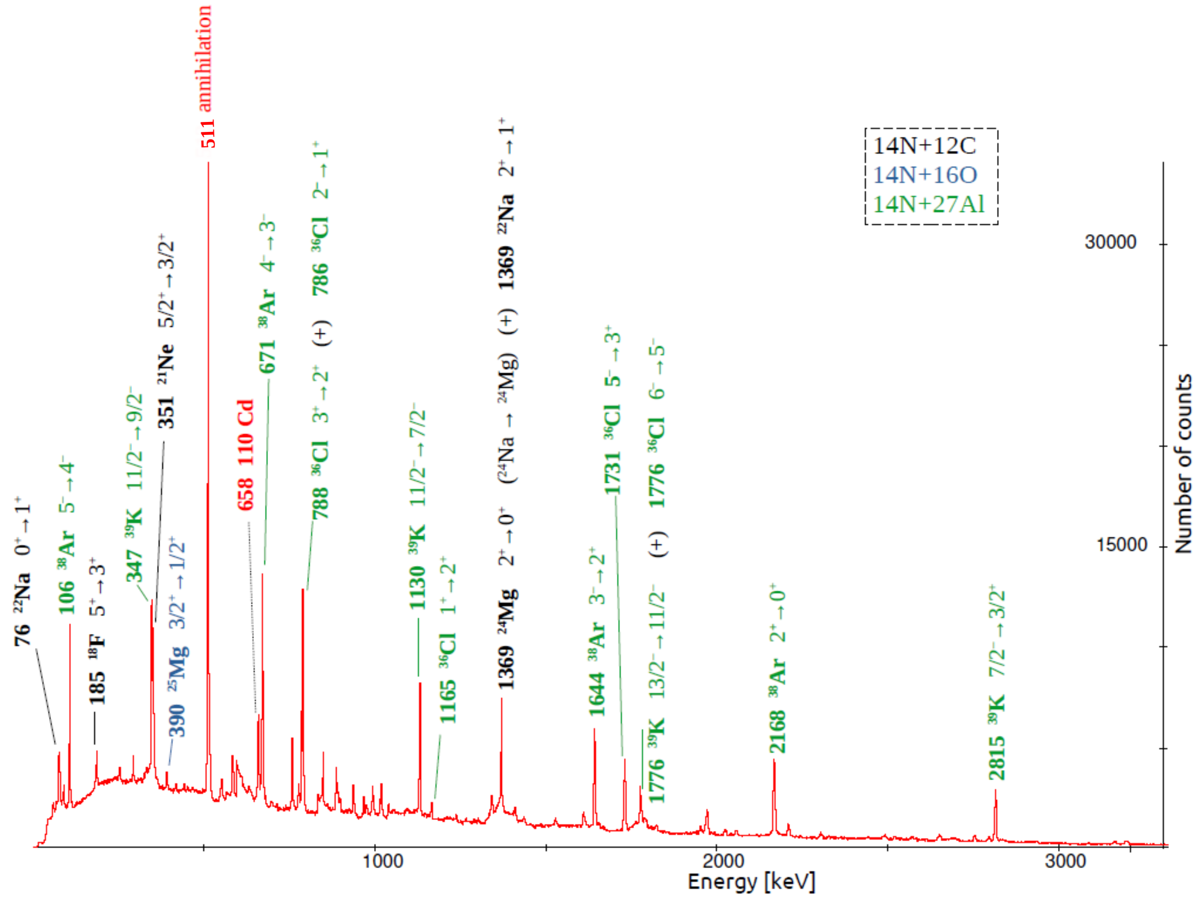

Figure 1: The total projection of the γ-γ coincidence matrix. The coincidence time window was set to 37.5 ns. The strongest of the identified γ ray transitions arising from the ^{14}N+^{16}O (blue), ^{14}N+^{12}C (black), ^{14}N+^{27}Al (green) reaction channels are marked. In addition the 658-keV γ-ray transition coming from the Coulomb excitation of the 2_1^+ state in ^{110}Cd and the 511-keV anihilation γ line are visible.

Bibliography

[1] M. Palacz *et al.*, HIL Annual Report 2020, page 10.

[2] M. Kowalczyk *et al.*, HIL Annual Report 2014, page 17.

[3] K. Debertin amd R. G. Helmer *Gamma- and X-ray spectrometry with semiconductor detectors* Elsevier Science Publisher B. V., Amsterdam 1988

A.10 Polish Workshop on the Acceleration and Applications of Heavy Ions

J. Samorajczyk-Pyśk[1], T. Abraham[1], M. Araszkiewicz[2], K. Hadyńska-Klęk[1], M. Kowalczyk[1], K. Kilian[1], U. Kaźmierczak[1], M. Komorowska[1], K.Z. Krutul[1], P.J. Napiorkowski[1], M. Palacz[1], M. Paluch-Ferszt[1], K. Rusek[1], O. Saeed Mohamed Nassar[1], A. Sentkowska[1], A. Stolarz[1], Z. Szefliński[1], R. Tańczyk[1], A. Trzcińska[1], K. Wrzosek-Lipska[1], B. Zalewski[1]

1) Heavy Ion Laboratory, University of Warsaw, Warszawa, Poland
2) Faculty of Physics, University of Warsaw, Warszawa, Poland

After a one-year break caused by he COVID-19 pandemic, the XVI session of the Polish Workshop on the Acceleration and Applications of Heavy Ions at HIL took place in the autumn of 2021. The workshops are dedicated to physics students (3rd and 4th year) interested in nuclear physic and its applications. They offer a unique opportunity to gain experience in acquiring and analyzing experimental data, the techniques of gamma radiation detection (off-line and on-line) low background gamma spectra, and the impact of radiation on PiN detectors. Students also had the opportunity to use tools such as a gamma camera and were also able to irradiate and examine cancer cells and prepare experimental targets.

These workshops have met with great interest, however the number of participants is limited. The 16th edition of the event welcomed seventeen students from:
- University of Warsaw (5 students)
- Warsaw University of Technology (3 students)
- Poznan University of Technology (2 students)
- Jagiellonian University (2 students)
- University of Zielona Góra (2 students)
- University of Gdansk (1 student)
- University of Silesia (1 student)
- Maria Curie-Sklodowska University (1 student)

In 2021, the programme of lectures was as follows:

- HIL in a nutshell (K. Rusek);
- Introduction to heavy ion acceleration and elements of ion optics (O. Saeed Mohamed Nassar);
- Radioprotection at the HIL (R. Tańczyk);
- Targets for research in nuclear physics (A. Stolarz);
- Detection of gamma radiation, charged particles and neutrons (M. Palacz);
- In-beam gamma spectroscopy (P. Napiorkowski);
- Radiopharmaceuticals for Positron Emission Tomography (K. Kilian);
- Nuclear reactions (K. Rusek);

- The uncertain Heisenberg – scientists facing the realities of World War II (A. Sentkowska);

Students took part in the following experimental tasks:

- Study of the Radiation Hardness Performance of PiN diodes in interaction with heavy ions;
- Gamma spectroscopy with the EAGLE multidetector setup;
- Targets: production and thickness measurements;
- Measurement of ^{137}Cs activity in environmental samples;
- Gamma camera — a medical imaging tool.

As usual, the Workshop was completed by the student presentations session.

Figure 1: Participants in the 16th Polish Workshop on the Acceleration and Applications of Heavy Ions (photo. P. Jasiński).

A.11 Fourth edition of the Nuclear Physics Innovation and brokerage event – Global Nuclear Physics Innovation

T.J. Krawczyk[1,2], *M. Paluch-Ferszt*[1], *D. Jankowski*[2], *K. Rusek*[1], *J. Matuszczak*[1],
the organisers of the workshop

1) Heavy Ion Laboratory, University of Warsaw, Warszawa, Poland

2) Enterprise Europe Network

The University of Warsaw co-organized the 4^{th} edition of the Nuclear Physics Innovation and brokerage event: "Global Nuclear Physics Innovation" on 1-2 December 2021 in Warsaw, Poland (Digital Edition). The brokerage event at Global Nuclear Physics Innovation (Digital Edition) brought together scientists and companies (buyers as well as suppliers) from all over the word.

The event supported the workshop: "Nuclear Physics and Innovative Technologies" which was proposed as a space for the presentation of Academia-Industry results and technology. Keynote speakers from nuclear physics research centres and technology companies presented the current state of the art in research techniques and proposed commercial solutions. Achievements from both fields were presented to attract prospective customers and collaborators, but requisites for future projects and directions of necessary developments were also addressed to the partners. The workshop gave the opportunity to find partners for future research and development projects.

Meetings took place online and were arranged in advance by means of the website: `https://gnpi2021.b2match.io/`. Nuclear physics laboratories had the chance to establish links with international industry and SMEs. During the workshop, 25 bilateral meetings (brokerage meetings) were organized between researchers and companies in which 45 participants took part. The purpose of the bilateral meetings was to establish initial contacts that may lead to further research cooperation and to intensify the transfer of innovative technologies.

The forum explored recent achievements and challenges in the following areas:

- Radiobiology.
- Radiopharmaceutical production and molecular imaging.
- PET diagnosis.
- Ionizing radiation.
- Scientific instrumentation and medical physics.
- Medical imaging.
- Computation and information technology sciences.

- Data acquisition and analysis of software development.
- Energy and environmental technologies.
- Laser-plasma acceleration.
- Radiation resistance studies of electronic systems.
- Radiation detection.
- Detector electronics development.
- Ion source developments for radioactive ion beam production.
- Monitoring of environmental radioactivity.
- R and D for gamma radiation detectors.
- Big data applications (Data Mining, Data Science, Machine Learning, Deep Learning, Neural Networks, Genetic Algorithms).
- Machines (CNC and other technical tools necessary for the exploitation of research facilities).
- CAD/CAM/CAE, FEM software and applications to nuclear research.
- Special engineering construction services for nuclear facilities.
- Research cooperation and transfer of knowledge and technology.
- COVID-19: virus protein structure analysis (synchrotron).
- Development of Ion Beam Analysis (IBA) Techniques for materials analysis.
- Development of irradiation trials of technological components and biological samples.
- Development of radiation detectors and nuclear instrumentation.

This 4^{th} edition of the brokerage event was organized in a special time. To the different areas of research activity was added a special subject in reference to fighting against the COVID-19 - virus protein structure through analysis with the use of synchrotrons.

62 people participated in all events (brokerage meetings and workshop), including: 24 people from universities and 38 people from companies and other institutions.

Part B
Research for medical and biological applications

B.1 Improved synthesis of ^{18}FHBG for molecular imaging of progenitor cells in mice models

K. Kilian[1], *K. Koszel*[2], *K. Milewska*[2]

1) Heavy Ion Laboratory, University of Warsaw, Warszawa, Poland

2) Faculty of Physics, University of Warsaw, Warszawa, Poland

Recently, a procedure for [^{18}F]FHBG ((9-(4-^{18}F-Fluoro-3-[hydroxymethyl] butyl)guanine) synthesis was developed [1]. Detailed studies showed three different compounds in the mixture of products before purification. In the course of further research it was shown that during synthesis an formed unstable labeled compound had been fomed which decomposed to release free ^{18}F-, thus the procedure required careful and long lasting purification. Detailed analysis of animal images in papers published to date using [^{18}F]FHBG indicated that the authors neglected this problem, allowing for an increased concentration of free fluoride-18, which resulted in abnormal accumulation in the skeletal system.

The aim of this study was to eliminate the by-product and obtain better radiochemical purity and stability of [^{18}F]FHBG. The difference in solubility of the final product, synthesis intermediates and solubility of fluorides was used to separate the [^{18}F]FHBG from the impurities. An additional cleaning step before hydrolysis of intermediate products effectively eliminated the main impurities and resulted in better radiochemical purity of the final product. This allowed better purity of the reaction mixture to be reached at this stage and increased the synthesis yield from 20 - 30% to 60 - 85%, which facilitated purification of the final product and improved the quality of imaging.

A further step was to develop and experimentally verify the quality of the [^{18}F]FHBG, with particular emphasis on the determination of radiochemical purity. The broader goal was to obtain confirmation of the quality and stability of the manufactured radiopharmaceutical, to evaluate applicability in preclinical studies.

For this purpose, radiochemical purity was determined and exceeded 99%. Stability tests were performed at the following time points: after 1h, 2h, 3h, 6h, 12h, 18h and 24h and showed the stability of the manufactured compound for more than 12h, where radiochemical purity stayed above 99%, dropping to 98.5% after 24h, which proved the stability of the product and the effective removal of the unstable byproduct.

For animal studies fluorine-18 was obtained from the ^{18}O(p,n)^{18}F reaction with radiochemical purity $>$ 99.9%. The input activity per synthesizer was 10 GBq. Product quality control comprised testing radiochemical and chemical purity. High-performance liquid chromatography (HPLC) with a radiometric detector was used to determine these parameters. During HPLC analysis, a C18-RP column was used. The Atomlab 500 dose calibrator was used for all activity measurements. We obtained the product with a radiochemical purity $>$ 98.5%.

[^{18}F]-FHBG was used as a reporter probe for imaging HSV-TK. The mechanism comprised trapping the cyclic analogues of guanosine because of the phosphorylation catalysed by the HSV-TK protein product with consequent visible accumulation in tissues expressing HSV-TK15. Using a dedicated small-animal PET probe for the reporter gene, [^{18}F]-FHBG was used for non-invasive imaging of stem cells transplanted to the healthy and post-infarction myocardium. [^{18}F]-FHBG accumulates in cells when it is phosphorylated by

HSV-TK, resulting in trapping the compound inside the cell, where it cannot diffuse outward. The fusion of PET and CT images illustrates the exact location of activity derived from [^{18}F]-FHBG uptake in the apex region. The retention of stem cells was observed in both control and post-infarction mice. Recorded images demonstrated positive imaging of stem cells in the mouse myocardium within a month of cell implantation. The cell retention in control and post-infarction hearts varied; however, the radiotracer uptake did not fall below 50%. [^{18}F]-FHBG was used for long-term imaging of transplanted genetically modified stem/progenitor cells in the post-infarction small animal myocardium [2].

Bibliography

[1] Lenartowicz A. *et al.*,HIL Annual Report 2020 page 23.
[2] Wargocka-Matuszewska W. *et al.*, Sci. Rep.**11(1)** (2021) 19825.

B.2 Stability of selenium compounds in standard samples during storage under different conditions

A. Sentkowska[1]*, K. Pyrzyńska*[2]

1) Heavy Ion Laboratory, University of Warsaw, Warszawa, Poland

2) Faculty of Chemistry, University of Warsaw, Warszawa, Poland

Selenium is an important element for the proper functioning of the human body. As this element is essential as well as toxic in narrow concentration range, the procedure of its extraction as well as determination should be reliable. Sample preparation is the first crucial step for successfully assessing the concentration and range of selenium species. Different extraction media are used to extract selenium form various matrices, eg. hot water, an aqueous solution of HCl, methasulfonic acid, ammonium. However, the problem is that the stability of selenium species is limited. In such a situation, the time from sample preparation to analysis can have a huge impact on the analysis result.

The stability of two inorganic (selenite Se(IV) and selenate Se(VI)) as well as four organic (selenomethionine (SeMet), selenocystine (SeCys$_2$), selenomethylocysteine (MeSecys) and selenomethionine selenoxide (SeMetO)) selenium species was investigated in standard solutions. The structures of the studied selenium compounds are presented in Fig. 1. All of the samples were without any stabilizer addition. Samples were stored in the dark at -18°C, -4°C and +20°C as well as in the light at +20°C. Stability was also investigated in terms of the pH of the sample solution. The samples were prepared in hydrochloric acid (pH 4.5), in deionized water (pH 5.8) and in ammonium acetate (pH 7). The stability of selenium compounds was investigated by Hydrophilic Liquid Chromatography coupled to mass spectrometry detection (HILIC-MS).

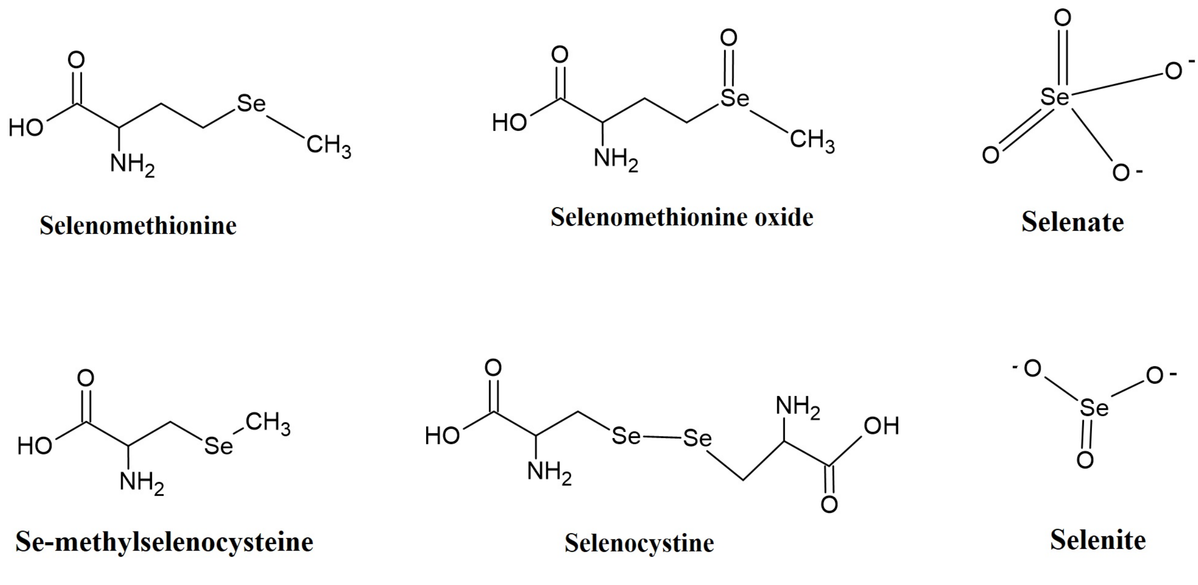

Figure 1: The structures of selenium compounds used in the study.

Inorganic selenium seems to be the least stable in water. About a 10% decrease in concentration of Se (IV) as well as Se(VI) is observed after 7 days of storage in aqueous solution. After 21 and 28 days of storage of Se(IV) the highest concentration is observed in solutions kept at room temperature. Our results showed that in water the highest losses are observed when the standards are kept in the light. For long term storage of Se(VI) it is recommended to keep the solution in the freezer. It should be highlighted that the stability of selenium depends on the container in which the standards are kept. Methylselenocysteine (MeSeCys) was found to be stable for 7 days in aqueous solution while kept in darkness at 20°C. Access to light affects its stability and causes a 10% loss. Also, low temperature is not advisable for storage of MeSeCys aqueous solutions but it is significantly more stable at -18°C degrees than at +4°C. MeSeCys is highly unstable in acidified solutions, but here it is more digestible at lower temperatures. In buffer solution its stability is moderate and it rather should be kept at lower temperatures. $SeCys_2$ is stable in water and acidic solutions up to 14 days at lower temperatures. Storage in buffered solution with 5% loss is possible up to 7 days at +4°C. $SeCys_2$ is totally unstable in water and it was not detected in solutions kept for 28 days (with the exception of a sample kept in the freezer). The problem with oxidation of SeMet during the extraction step and storage is well known, but still not completely explained with a clear indication of the origin of SeMetO in the sample. It can be speculated that SeMet in aqueous solution is oxidized to selenooxide during storage. A more rapid degradation of selenomethionine is observed in an acidic medium, but only a slight increase in SeMetO concentration is observed. It was stated that the first stage of the oxidation process of SeMet is a stable intermediate Se-dihydroxy-selenomethionine formulation After that, cyclization occurs and C-Se bond cleavage to form 2-amino-4-butyrolactone. The CH_3-Se is transformed to methane seleninic acid.

Due to the importance of selenium in the proper functioning of the human body and the differences in toxicity between its speciation forms, its analysis is very important. However, due to the instability of selenium in samples, its analysis should be performed immediately after sample preparation. In general, the lowest stability of selenium is observed in aqueous solutions. Acidification of the solution significantly increases the stability of selenium compounds, although such treatment caused a drastic decomposition of SeMet in the sample. Access to light has no impact on the stability of selenium forms. Also, the temperature of storage strictly depends on the sample matrix, but in our opinion, keeping samples in the fridge is the best solution. However, the storage time should be as short as possible.

B.3 How the clean-up procedure influences the antioxidant activity of selenium nanoparticles

A. Sentkowska[1], *K. Pyrzyńska*[2]

1) Heavy Ion Laboratory, University of Warsaw, Warszawa, Poland

2) Faculty of Chemistry, University of Warsaw, Warszawa, Poland

Selenium nanoparticles (SeNPs) have attracted great attention in recent years due to their unique properties and potential bioactivities. While the production of SeNPs for various application has been long reported, little has been written about the impact of the clean-up procedure after synthesis on their antioxidant properties. In this study the influence of such procedures (centrifugation force and additional heating) on the antioxidant properties using DPPH and radical scavenging assay was examined. SeNPs were synthesised via reduction of Na_2SeO_3 with ascorbic acid. The procedure was performed with polyvinyl alcohol (pVa) as stabilizing agent. After synthesis SeNPs were purified from the surrounding liquid containing dissolved materials using different procedures: (*i*) centrifugation with two units of rotational speed (8000 and 12000 rpm) for 10 min, decantation and rising three times with 10 mL of deionized water; (*ii*) additional heating with magnetic stirring at 70°C for 1h, then rising three times with 10 mL of deionized water.

According to previous reports, SeNPs are strong free radical scavengers or inhibitors that can be used as an active form of selenium in food supplements. Their antioxidant activity was mainly evaluated in a dose-dependent manner. The antioxidant activity obtained for SeNPs formed in the reaction of ascorbic acid and pVa was found to be 37.2 ± 0.21 µmol TR L^{-1}. The influence of the cleaning procedure for SeNPs on the scavenging of DPPH radicals was positive. The highest results were obtained for centrifugation at 8 000 rpm after synthesis with ascorbic acid (56.2 ± 0.99 µmol TR L^{-1}). However, with an additional heating step higher results were obtained (46.3 ± 1.09 µmol TR L^{-1}). An SEM image of the SeNPs with the highest antioxidant activity is presented in Fig. 1.

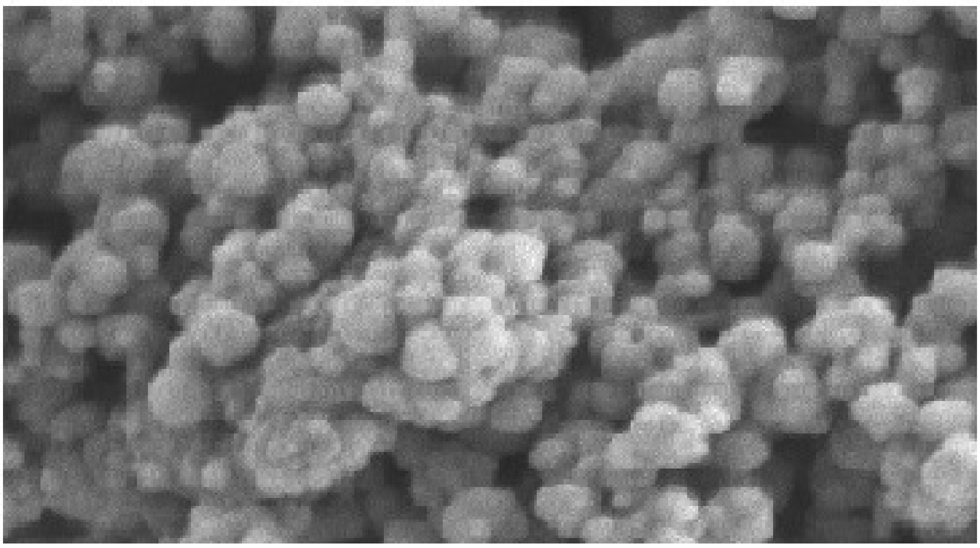

Figure 1: SEM image of SeNPs cleaned using centrifugation at a speed of 8000 rpm

Selenium nanoparticles can be treated as a nanoantioxidant due to their antioxidant properties. However, the synthesis method itself is only the first step to maximize the antioxidant activity of selenium nanostructures. Our results clearly show that every analytical procedure that is used during clean-up step has a great impact on the properties of the final product.

B.4 Study of biological effects in glioblastoma radiosensitive and radioresistant cell lines after exposure to high LET radiation

M. Araszkiewicz[1,2], U. Kaźmierczak[3], A. Korgul[1], A. Lankoff[4], K. Maliszewska-Olejniczak[5], M. Paluch-Ferszt[3], Z. Szefliński[3], K. Tymińska[2], M. Wojewódzka[4]

1) Faculty of Physics, University of Warsaw, Warszawa, Poland
2) National Centre for Nuclear Research
3) Heavy Ion Laboratory, University of Warsaw, Warszawa, Poland
4) Institute of Nuclear Chemistry and Technology
5) Warsaw University of Life Science, Warszawa, Poland

Glioblastoma (GBM) is considered the most common and the most aggressive primary brain tumor. It is characterized by rapid progression and short patient survival time of about 15 months despite being exposed to maximum treatment. GBM is highly difficult to treat because of its resistance to current therapeutic approaches [1]. In 2021, at the Heavy Ion Laboratory at the University of Warsaw (HIL), preliminary research devoted to the biological response of glioblastoma cell lines after exposure to high LET (Linear Energy Transfer) radiation took place and two GBM cell lines, radiosensitive M059J (Fig. 1) and radioresistant M059K, were irradiated with a carbon ion beam (^{12}C) and alpha particles.

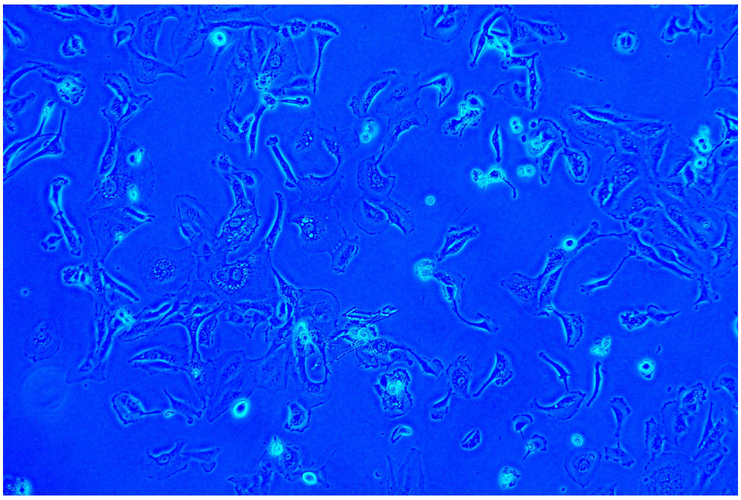

Figure 1: Radiosensitive M059J glioblastoma cells seen in an inverted microscope at the HIL radiobiological laboratory.

Ionizing radiation (IR) induces different types of DNA damage such as DNA single-strand breaks (SSBs) and the most cytotoxic DNA double-strand breaks (DSBs). Unrepaired damage can cause cell death while misrepaired DSBs lead to chromosomal rearrangement and mutagenesis [2]. Radiation represented by high LET like alpha particles or carbon ions where the average amount of energy lost per unit track length in tissue is higher, forms clustered DNA lesions of higher complexity than low LET radiation (e.g., X-rays and γ-rays) [3].

To characterize the biological responses of the GBM cells irradiated with high LET radiation, a colony formation assay was performed. This test allows the ability of single cells to survive and reproduce to form colonies to be assessed. M059K and M059J cell lines primarily isolated from a 33-year-old male patient, although obtained from ATCC American Type Culture Collection [4], were cultured at the properly equipped HIL Radiobiological Laboratory which meets all restricted conditions necessary for cell culture. According to ATCC protocols cells were incubated at 37°C and 5% CO_2 in an air atmosphere in DMEM F12 medium, containing 10% fetal bovine serum (FBS) and 1% penicillin and streptomycin.

Prior to irradiation, depending on the radiation source, an appropriate number of cells were seeded on mylar-bottom dishes (for the horizontal carbon beam) that allowed irradiation of adherent cells in an upright position, whereas for alpha irradiation, cells were seeded on 30 mm diameter coverslips. Both of the cell lines were irradiated by a carbon ion beam of energy 45.3 MeV generated by the HIL U-200P cyclotron according to the irradiation procedure described previously [5] and by alpha particles of energies 5388 keV, (1.7%) 5443 keV (13.1%), 5485 keV (0.4%), and 5544 keV (84.8%) [6] emitted from a surface ^{241}Am source, Fig. 2. M059J and M059K cells were irradiated with dose ranges of 1-3 Gy and 0.5-6 Gy respectively.

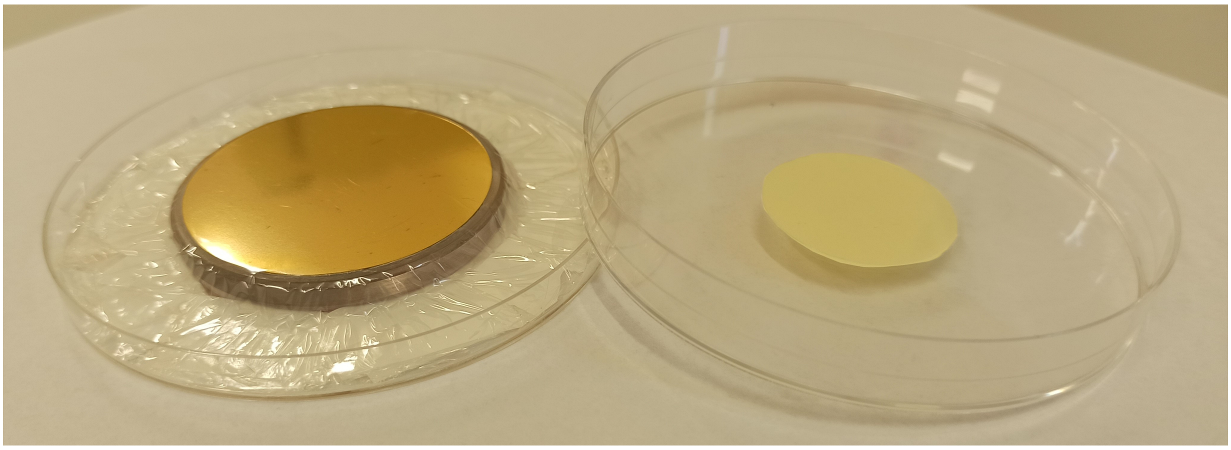

Figure 2: Surface ^{241}Am source mounted by Mylar foil on the inner side of the top part of the Petri dish (left) and coverslip (yellow circle) in the center of the bottom part of the Petri dish.

To obtain the desired doses, the radiation field parameters and the time of irradiation were estimated by Monte Carlo simulations using the MCNP6.2 code [7]. Computational calculations took account of the particle energy, irradiation geometry, and beam intensity or source activity respectively.

After irradiation the cells were trypsinized (with Trypsin-EDTA), to make single-cell suspensions from a monolayer of irradiated cells. Next, these were seeded on Petri dishes and incubated at 37°C and 5% CO_2 in air atmosphere. After 14 days of incubation colonies were fixed with formaldehyde, stained with Giemsa violet (Fig. 3) and counted to determine the surviving fraction of irradiated cells.

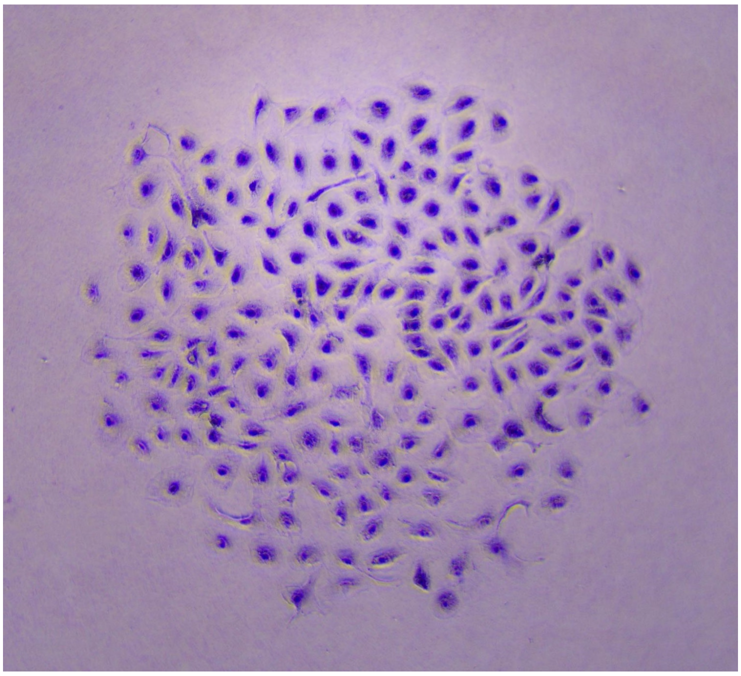

Figure 3: Colony of M059K cells from the control (0 Gy) stained with Giemsa violet.

In 2022 it is planned to repeat the survival analysis at HIL with GMB cell lines to obtain appropriate statistics in a biological experiment. Future experiments will also be focused on immunofluorescence analysis of phosphorylated histone H2AX (γ-H2AX) that appears in the immediate vicinity of DBSs as well as on irradiation of M059J and M059K cell lines with low LET radiation.

Bibliography

[1] F. E. Bleeker, R. J. Molenaar, J. Neu. -Onc. **108**(2012) 11–27.
[2] Cheng, L. *et al.*, PLoS ONE **13** (2018) e0204068.
[3] E. Sage, N. Shikazono, Free Radic. Biol. Med **107** (2017) 125–135.
[4] `https://www.atcc.org/products/crl-2365`
[5] U. Kaźmierczak *et al.* Rep Pract Oncol Radiother**19** (2014) 37–41.
[6] `https://www.nndc.bnl.gov/nudat3/decaysearchdirect.jsp?nuc=241AM&unc=nds`
[7] C.J. Werner, *et al.*, Los Alamos National Laboratory, report LA-UR-18-20808 (2018).

B.5 Porphyrin complexes as potential radiopharmaceuticals for PET

M. Pęgier[1], K. Kilian[1], K. Pyrzyńska[2]

1) Heavy Ion Laboratory, University of Warsaw, Warszawa, Poland

2) Faculty of Chemistry, University of Warsaw, Warszawa, Poland

Porphyrins are promising agents which can potentially be used as ligands for positron emission tomography (PET). They can serve as bifunctional ligands that on the one hand can effectively coordinate positron emitting radionuclides, and on the other hand can be covalently linked to other targeting molecules for imaging biochemical processes of interest. Porphyrin complexes occur naturally in the human organism (iron complex in heme, cobalt complex in vitamin B12). One of the popular radionuclides used in PET is ^{68}Ga which has a half-life of 68 min and decays 87.94% through positron emission (mean energy 0.89 MeV). Gallium forms stable complexes which allows for kit development. It is easily available from the ^{68}Ge/^{68}Ga generator, which facilitates its application in clinical practice, mainly for diagnosis of neuroendocrine tumors [1]. It can also be produced in a cyclotron via the ^{68}Zn(p,n)^{68}Ga reaction [2].

This study refers to the synthesis of gallium complex with porphyrins for potential applications in PET diagnostics. Four different hydrophilic porphyrins: anionic *meso*-tetrakis(4-carboxyphenyl)porphyrin (TCPP), anionic *meso*-tetrakis(4-sulfonatophenyl)porphyrin (TSPP,), anionic protoporphyrin IX (PPIX) and cationic *meso*-tetrakis(N-methyl-4-pirydyl)porphyrin (TMPyP) were used (Fig. 1).

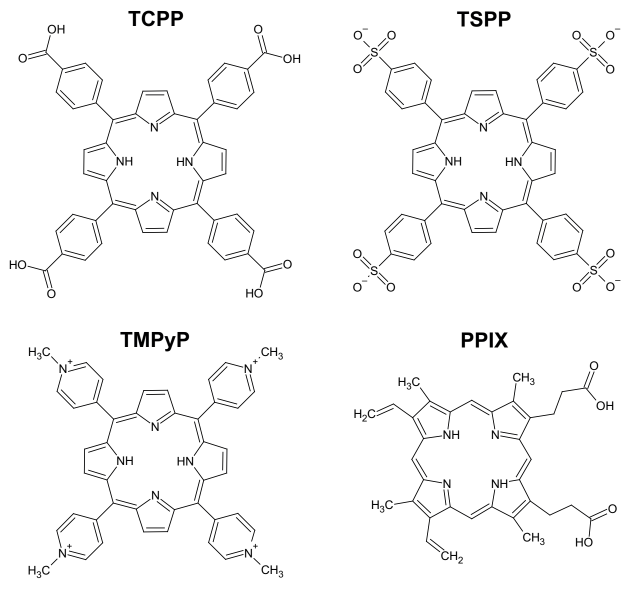

Figure 1: Structures of the investigated porphyrins.

The reaction was conducted in three different pH buffers (acetate pH 4, phosphate pH 7, borate pH 9) and monitored using a UV-VIS spectrophotometer. Protoporphyrin IX turned out to be unstable in solution and the characteristic peak in the Soret band (λ_{max} = 381 nm) diminished in time, while TCPP in acetate buffer at pH 4 precipitated shortly after preparation. Even 24 h after mixing of Ga^{3+} with porphyrins no characteristic changes in spectra were observed. To increase the reaction rate synthesis using sitting-a-top complex was performed in two steps [3]. The first step was formation with a large metal ion (Cd^{2+}) and then addition of the gallium ion, but the porphyrins remained unreactive towards gallium. To overcome this issue microwave synthesis at 150°C was applied. TCPP was thermally unstable and spectra after microwave heating showed decomposition of the porphyrin ring. Reaction of Ga with TSPP, TMPyP and PPIX ([Ga]=[Porphyrin]=$5{\cdot}10^{-6}$ mol/L) in acetate buffer at pH 4 was conducted at a temperature of 150°C with microwave power of 300 W. The results for Ga-TMPyP and Ga-TSPP aren shown in Fig. 2.

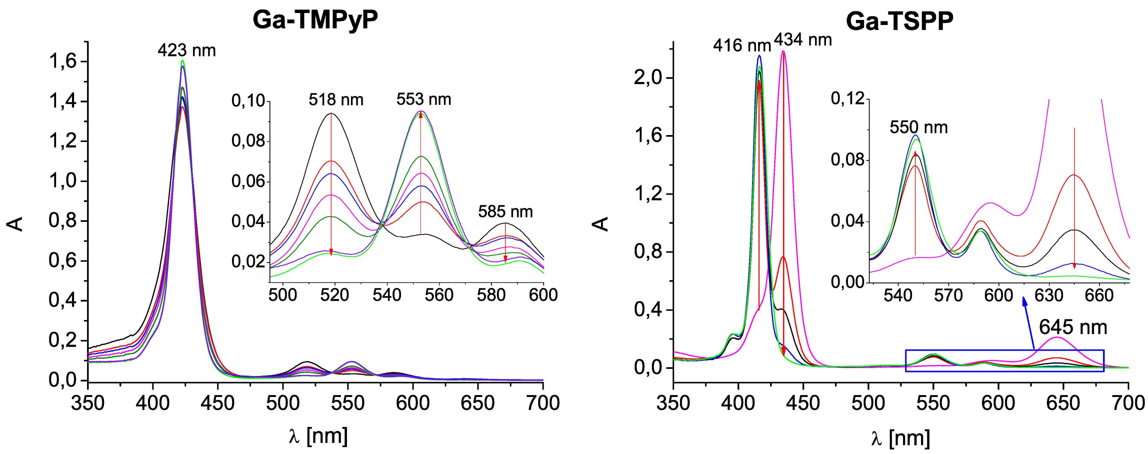

Figure 2: Changes in UV-VIS spectra during formation of Ga-TMPyP and Ga-TSPP complex

Microwave heating led to formation of Ga-TMPyP and Ga-TSPP complex. In the case of Ga-TMPyP the Soret band remained unchanged (with slight decrease in intensity), while in the Q-band a new peak appeared at 553 nm, while the porphyrin bands at 518 and 585 nm disappeared. Ga-TSPP shows a shift in the Soret band from 434 nm for free TSPP to 416 nm for the complex. Characteristic changes in the Q-band manifest through the formation of a new band at 550 nm and the disappearance of the free porphyrin bands. In the case of PPIX changes characteristic for formation of Ga-PPIX could also be observed, but most of the complex (or free porphyrin) precipitated on the magnetic stirring bar, which makes this reaction inadequate for potential applications in radiopharmaceutical synthesis.

Bibliography

[1] Martiniova L. *et al.*, Current Radiopharmaceuticals **9** (2016) 187-207.

[2] Pandey M.K. *et al.*, Am J Nucl Med Mol Imaging **4** (2014) 303-310.

[3] Kilian K., Pęgier M., Pyrzyńska K., Spectrochim. Acta A Mol. Biomol. Spectrosc. **159** (2016) 123-127.

B.6 Preliminary investigations of the mechanisms of radiochromic response in three-dimensional gel dosimeters as applied to hadron radiotherapy

J. Czubek[1], M. Marszewska[1], M. Cichacka[1], B. Mielewska[1], M.J. Maryański[1], U. Kaźmierczak[2], M. Paluch-Ferszt[2], Z. Szefliński[2]

1) Faculty of Applied Physics and Mathematics, Gdańsk University of Technology
2) Heavy Ion Laboratory, University of Warsaw, Warszawa, Poland

B.6.1 Goal

The goal is to investigate the mechanisms of radiochromic response in three-dimensional gel dosimeters as applied to hadron radiotherapy.

B.6.2 Materials and Method

These dosimeters have elemental composition and density that approximate human muscle tissue. Radiation-induced polymerization of acrylic monomers whose concentration in the gel is on the order of 1 M, forms stable polymer clusters of a size comparable to the wavelength of visible light. Therefore, these clusters scatter light such that the 3D distributions of the optical extinction coefficient in the gel represent the 3D distributions of the radiation absorbed dose. Previous investigations by one of the authors have shown that the angular distribution of laser light scattered on polymer clusters formed by 160 MeV proton beams strongly depends on Linear Energy Transfer (LET) [1]. It is therefore likely that the sizes of the polymer clusters, aligned along the tracks of ionization and electronic excitation in the gel, correlate with the LET. If true, this would enable tomographic imaging of the 3D distributions of the LET, i.e. mapping a significant factor of radiobiological effectiveness. Potential applications in hadron radiotherapy treatment planning could also be considered. In the proposed experiments at HIL we intend to investigate such phenomena induced by 90 MeV carbon ion beams.

B.6.3 Preliminary Tests

In 2021, we performed a pilot experiment (at HIL) using a 22 MeV carbon ion beam. The purpose was first to identify and then to minimize those factors related to the sample preparation and the geometry of their exposure to the ion beams, that might hamper the interpretation of the results. Preliminary results revealed two such factors:

1) atmospheric oxygen diffusion into the gel samples and

2) the angle between the carbon ion beam incident on the sample during exposure and the light beam incident on the exposed gel sample in the light scattering experiment.

The former relates to the inhibition of radiation-induced free-radical polymerization of acrylic monomers in the gel by the dissolved molecular oxygen. The latter – to the dependence of the total cross section for light scattering at the angle mentioned above. One of the significant consequences of this dependence is the necessity of modifications to the model of local dose deposited in the gel by beams of heavy ions. It emphasizes the importance of microdosimetric and nanodosimetric analyses in this field of research.

B.6.4 Conclusions

1) It is necessary more effectively to protect thin samples of dosimetric gels from atmospheric oxygen.

2) The use of at least 90 MeV carbon ion beams is recommended, to increase the depth of penetration of the beam into the gel.

3) Setting up the angle of incidence of the carbon ion beam on the surface of the gel sample at 45 degrees is recommended.

B.6.5 Investigations Planned for 2022

In experiments planned for 2022 the modifications described above will be implemented. Investigations will include:

1) the dependence of the total cross section for light scattering on exposed gels on the angle between the carbon ion beam and the laser beam with respect to the gel sample surface,

2) the angular dependence of the intensity of light scattered on radiation-induced polymer clusters as a function of LET,

3) its spectral dependence.

Bibliography

[1] M.J. Maryański *et al.*, 59thANNUAL CONFERENCE OF THE PARTICLE THERAPY CO-OPERATIVE GROUP Online Meeting, Poster Presentation P083, (2021) Prague.

B.7 The HIL - ICHTJ Collaboration

E. Majka[1], R. Walczak[1], A. Majkowska-Pilip[1], A. Bilewicz[1], K. Wawrowicz[1], M. Gumiela[1], E. Gniazdowska[1], P. Koźmiński[1], M. Łyczko[1], J. Choiński[2], A. Stolarz[2], T. Bracha[2], J. Kowalska[2], Ł. Świątek[2], R. Tańczyk[2], A. Matuszyńska[3]

1) Institute of Nuclear Chemistry and Technology, Warszawa, Poland
2) Heavy Ion Laboratory, University of Warsaw, Warszawa, Poland
2) Faculty of Chemistry, University of Warsaw, Warszawa, Poland

Medical radionuclides for studies of the processes of their separation from the targets and of the procedure of radiolabelling the molecules that act as isotope carriers were produced in proton induced reactions, i.e. the so called cyclotron method. The production of appropriate targets and their irradiation were performed at the Heavy Ion Laboratory, University of Warsaw. The thickness of the targets used for radioisotope production, regardless of their chemical form, was in the range assuring the complete stopping of the protons within the target body. The hot targets were transported to the Institute of Nuclear Chemistry and Technology for further processing.

B.7.1 Production of $^{197/197m}$Hg

The mercury radionuclides $^{197/197m}$Hg are obtained in the ^{197}Au(p,n)$^{197/197m}$Hg nuclear reaction using metallic targets made of pure ^{197}Au. In two irradiation runs 5 MBq and 8.25 MBq of $^{197/197m}$Hg was achieved. The activities of the mercury radioisotopes obtained in the first irradiation run are listed in Table 1.– around 5 MBq. We plan to extend the irradiation time in order to increase the radioactivity after obtaining the approval of the relevant authority.

Isotope	Activity [MBq]
^{197}Hg	4.9
^{197m}Hg	0.054
^{203}Hg	0.142

Table 1: Activity of radionuclides produced in the first run

The irradiated target was dissolved in 1 mL of aqua regia and was loaded onto a column filled with 3.6 g of LN resin (Di(2-ethylhexyl)orthophosphoric acid (HDEHP) impregnated onto an inert support. The resin was previously conditioned with 6 M HCl overnight. The $^{197/197m}$Hg was eluted with 6M HCl. We collected 20 fractions, each of half a mL, and measured their activity. The measured activities are presented in Table 2. We managed to recover $\sim$ 4 MBq of $^{197/197m}$Hg merging together fractions 7 to 15.

B.7.2 Production of ^{44}Sc

The scandium radionuclide ^{44}Sc is obtained in the ^{44}Ca(p,n)^{44}Sc nuclear reaction. For irradiation, we used targets made of $^{nat}CaCO_3$ pressed into a graphite support. In the production run the activity of ^{44}Sc produced was of the order of 120 MBq. After irradiation the target was dissolved in 3 mL 1 M HCl and subsequently 400 µL of ammonia water (25%) was added to the solution to precipitate the Sc compounds. The colloidal suspension of the target material obtained was pressed through a Whatman 0.2 µm filter to trap the Sc. The filter was washed with 2 mL water. The loss of Sc activity in this process was lower

No	Activity[Bq]	No	Activity[Bq]
1	0.01	11	0.49
2	0.01	12	0.54
3	0.01	13	0.49
4	0.07	14	0.40
5	0.11	15	0.22
6	0.18	16	0.12
7	0.27	17	0.09
8	0.38	18	0.06
9	0.50	19	0.05
10	0.70	20	0.04

Table 2: Activities of mercury radionuclide fractions collected from the target material

than 15%. In order to dissolve the Sc radionuclide trapped in the filter, it was washed with two portions of 0.5 mL of 1 M HCl. 99% of the ^{44}Sc was in the first collected fraction. The solution containing ^{44}Sc was loaded on to Dowex-50X Cation Exchange resin (200 mg) which was then washed with 2 mL of water. For elution of ^{44}Sc, ammonium acetate solution (0.4 M, pH=4.5) was used. The eluent was collected in 8 fractions of 1 mL each (Tab.3).

Fractions	Activity of ^{44}Sc[%]
1	0
2	0
3	40.8
4	45.9
5	1.4
6	0.32
7	0.13
8	0.07

Table 3: Percentage of ^{44}Sc activity in collected eluent fractions

Fractions 3 and 4, which hade the highest activity, were merged.

Radiolabelling Procedure

C-Fe3O4-SiO2-HPG-NH2-EDTMP@PSMA-617 (NP-EDTMP@PSMA-617) and C-Fe3O4-SiO2-HPG-NH2-DPAPA@PSMA-617 (NP-DPAPA@PSMA-617) nanoparticles were radiolabelled the ^{44}Sc obtained in this work. The stock samples were prepared from 1 mL NP (41 mg) suspensions that were centrifuged at 13500 rpm for 5 min to remove supernatant and replace it with 100 µL of 1 M ammonium acetate buffer. Finally, the ^{44}Sc was added to each NP and the samples were incubated for 30 minutes at 95°C. After incubation, the samples were centrifuged to remove the unbound ^{44}Sc. The radiolabelling efficiency was found to be almost 98% for EDTMP-PSMA, while for DPAPA-PSMA it was found to be almost 97%.

B.7.3 Production of ^{99m}Tc

The technetium radionuclide ^{99m}Tc is formed in the ^{100}Mo(p,xn)^{99m}Tc nuclear reaction. For irradiation, we used metallic targets made of natural Mo. Two targets irradiated in two separate runs were dissolved in 3.5 M HNO3. Triammonium phosphate (88 mg/mL) and ammonium nitrate (25%) were added to the solution to precipitate the Mo in the form of a yellow solid (ammonium molybdenum phosphate, AMP). After filtration of the AMP, the solution containing the ^{99m}Tc was divided into two portions. One was used in radiolabelling procedures. The other one was used in further purification steps. Cyclotron-produced ^{99m}Tc after the one step purification process (precipitation of AMP) was directly used in the synthesis of two complexes: [^{99m}Tc]Tc-(EDDA/tricine)-HYNIC-SP(1,11) (RCY, radiochemical yield = 64.4 ± 6.4%) and [^{99m}Tc]Tc-MIBI (RCY = 67.8 ± 1.1%). A three column purification system based on AnaLig® Tc-02 resin, a cation exchanger Dowex® 50 WX2 and an alumina column was used. With this system the ^{99m}Tc was recovered with 30% yield. The final saline solution of pertechnetate met radiochemical, chemical and radionuclide requirements. The ^{99m}Tc, after a four-step purification process, was also used for radiolabelling. The radiolabelling efficiency was 100% for [^{99m}Tc]Tc-DTPA.

B.7.4 Production of ^{89}Zr

The zirconium radionuclide ^{89}Zr is obtained in the ^{89}Y(p,n)^{89}Zr nuclear reaction. Using metallic targets made of natural Y 142 MBq of ^{89}Zr was produced in a 2 h irradiation The irradiated target was dissolved with 7 mL 4 M HNO3. A small black dust remains after dissolution. The dissolved target was loaded on 200 mg UTEVA resin that was conditioned with 4 M HNO3 for 12 h. After loading the target solution, the bed was washed with 5 mL of 4 M HNO3. The loss of Zr activity in the process of dissolving and loading onto resin was lower than 5%. In order to elute the Zr radionuclides from the resin it was washed with HCl (0.1 M, 1 M, 2 M, and 6 M). Unfortunately, the ^{89}Zr stuck on the resin. Studies on the separation process will be continued.

B.7.5 Production of ^{135}La

In the cyclotron method, the lanthanum radionuclide ^{135}La is produced in the ^{135}Ba(p,n)^{135}La nuclear reaction. For irradiation, we used targets made of ^{nat}BaCO_3 mixed with a small addition of graphite. Based on the results a student from the of Warsaw University Faculty of Chemistry, Antonina Matuszyńska, defended her MSc thesis: "Biomolecule DOTATATE labeled with ^{135}La radionuclide for Auger electron therapy of neuroendocrine tumors." The abstract of her work is presented here. Lanthanum 135 was obtained by the cyclotron method in the ^{135}Ba(p,n)^{135}La nuclear reaction. Column chromatography was used to separate the lanthanum from the target. The solid phase was a Chelex100 cation exchange resin and the mobile phase was an aqueous solution of hydrochloric acid. The recovery efficient of ^{135}La was 72.41% ± 11.79%. In the next step, the DOTATATE biomolecule was labeled with the obtained ^{135}La radionuclide at pH 4.5 with an efficiency of 100%. The stability of the obtained radiobioconjugate in saline, PBS, and human serum after 1, 2, 24, 48, 72 and 96 hours was over 90%. Receptor affinity studies on rat pancreatic cancer cells (AR42J cell line) showed the specificity of the preparation for SSTR2* receptors.
* SSTR2 receptor is a receptor of Somatostatine, type 2

B.7.6 Production of ^{72}As

In the cyclotron method, arsenic radionuclides were obtained in the $^{nat}Ge(p,n)^{*}As$ nuclear reaction. ^{72}As isotope was produced using a natural GeO_2 target. The total produced activity of *As(*As=^{70,72,74,76}As) was 800 MBq, and the activity of ^{72}As was 143 MBq. The dissolution of the irradiated target in 5 ml of concentrated HF took 1 h, then 50 mg of KI was added to the solution and stirred for another 10 minutes. The solution prepared in this way was applied to a BOND ELUT column in order to separate the formed $^{*}AsI_3$ remaining on the column under these conditions from the $[GeF_6]^{2-}$ ions, which were formed during the dissolution of the target material. $^{*}AsI_3$ was then eluted with 500 µl of ethanol. The eluted solution had an activity of 120 MBq, of which the activity of ^{72}As was approx. 64 MBq. In this procedure, 45% of the activity of ^{72}As in the form of $^{72}AsI_3$ was recovered from the target. The solution prepared this way was ready for further synthesis. Due to the volatility of arsenic compounds, the work was carried out in a glove box.

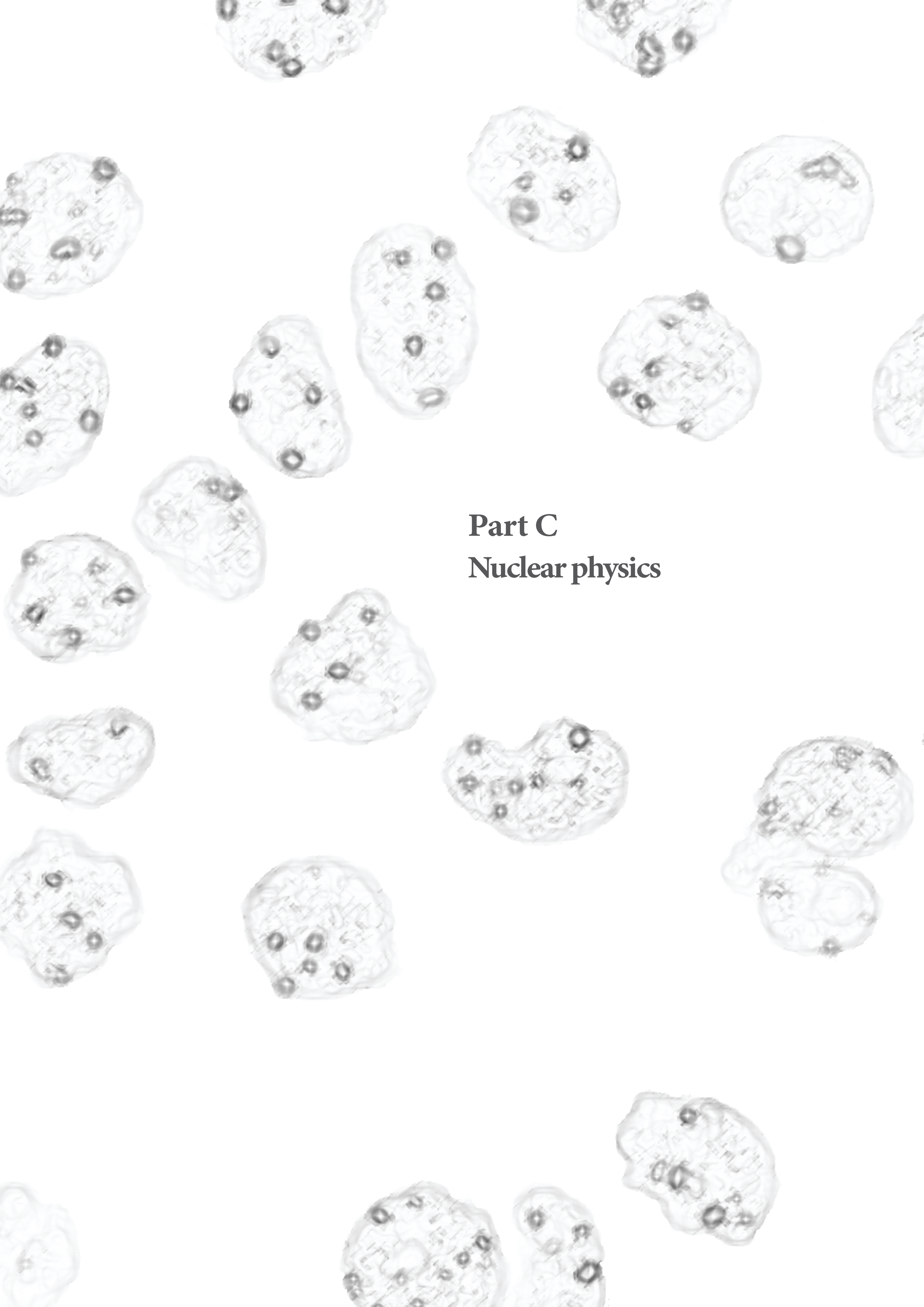

Part C
Nuclear physics

C.1 Dissipation by transfer and its influence on fusion

E. Piasecki[1], G. Colucci[1], A. Trzcińska[1], P. W. Wen[2], K. Hagino[3]

1) Heavy Ion Laboratory, University of Warsaw, Warszawa, Poland
2) China Institute of Atomic Energy, Xinzhen, Fangshan, Beijing, China
3) Department of Physics, Kyoto University, Kyoto, Japan

The influence of the limited number of projectile and target collective excitations on fusion has been studied for many years by the Coupled Channels (CC) method [1, 2]. The influence of dissipation, i.e. of the partial conversion of the projectile-target kinetic energy into their heating is much less understood.

There are two main mechanisms of dissipation: excitation of non-collective levels by nuclear and electromagnetic interactions [3–5] and mutual projectile-target transfer of light particles. Up to now, the first has beens treated by combining the CC method with the Random Matrix Theory (model CCRMT), with promising results [4, 5]. The influence of transfer has been both experimentally and theoretically investigated, but the conclusions are still contradictory. The reason is the complicated nature of this many-body time-dependent phenomenon, requiring both unknown information as well as an enormous computer calculation power. This forces the introduction into the models of approximations, which might influence the results.

The CCFULL [6], as well as the CCQEL codes, are widely used to calculate respectively the fusion and the quasielastic cross sections, under the influence of the coupling of the relative motion to several nuclear collective motions. These calculations are then used to extract the fusion and quasielastic barrier distributions (D_{fus} and D_{qe} [7, 8]). Both codes are able to include transfer channels, treated as transfer coupling between the ground states. Under this condition, it is assumed that transfer coupling is given by the expression F_{tr} * dV/dr, where V is the nuclear potential. The coefficient F_{tr} is the coupling strength and according to this simplified model, is independent of:

- the type of the transferred light particle(s);
- the Q-value of the reaction (usually g.s. to g.s. transfer is assumed);
- the projectile energy.

Moreover, it is frequently assumed that 2n transfers with positive Q_{gg} dominate, so usually only they are taken into account.

While the potential V is calculated using the Akyuz-Winther parametrization, the transfer coupling strength F_{tr} is fitted or simply assumed. Sometimes this is sufficient to reproduce the enhancement of the experimental fusion excitation function over the theoretical one, however there is a rising number of cases, which contradict the model expectations.

The D_{fus} and D_{qe} shapes are frequently, as expected, grosso modo similar to each other, although they could be different in detail due to the different time scales of fusion and scattering, and in particular of dissipation processes in the reactions. From the experimental point of view D_{qe} is much simpler to determine. In the context of the present subject, even more important is the fact that in scattering one can easily determine the Q-value distribution, while in fusion we know only the fixed final Q value.

We presented in [9] the Q-value distributions for various transfer channels measured in the backscattering of the ^{20}Ne+^{208}Pb and ^{24}Mg+^{90,92}Zr systems at near barrier energies at backward angles. The choice of a ^{208}Pb target is particularly interesting because of the disagreement between the experimental barrier distributions (without any trace of structure in the measured D_{qe} and D_{fus} distributions) and the strong structures expected by the theoretical results of the CCRMT calculations [5]. As the relatively low-level density of the ^{208}Pb nucleus can smooth out neither the D_{qe} nor the D_{fus} structure, we suspect that the disagreement can be caused by by neglecting in the calculations the transfer channels.

Measurements of the Q-value distribution for transfers at near-barrier energies are rather rare, but almost always they have a significant part above the Q_{gg} value, corresponding to negative excitation energy E*. This, clearly nonphysical, effect was observed also in our measurements. It results from the experimental resolution, which for the ^{20}Ne+^{208}Pb measurements was 2.4 MeV (FWHM). Thus, to exploit the information contained in the Q distributions the deconvolution of experimental Q-value distributions was performed, taking into account the cut-off at Q_{gg}. An example of the effect of deconvolution on the Q distributions in the one and two neutron pick-up transfers is shown in Fig. 1.

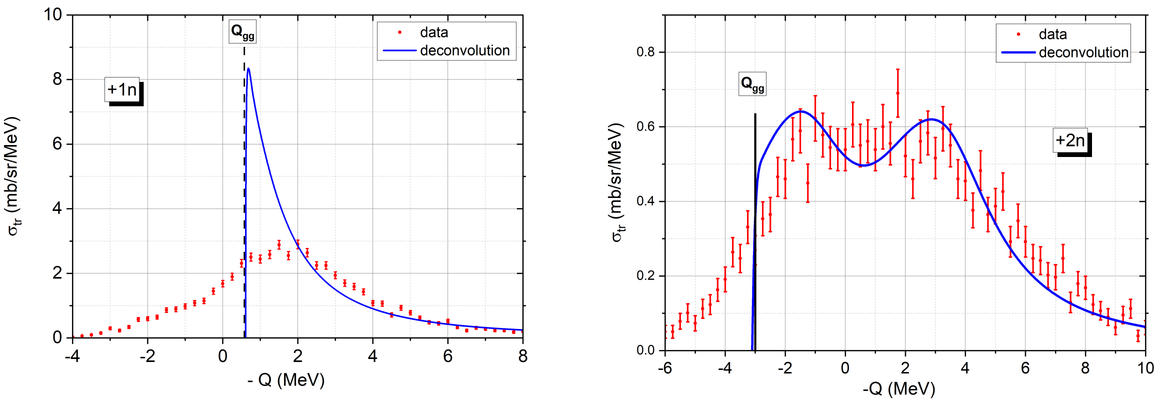

Figure 1: Examples of deconvolution of the Q-value distributions for the +1n and +2n transfers in ^{20}Ne+^{208}Pb system at the near-barrier energies.

A modified CCQEL code, able to include several particle transfers as well as their Q distributions, was used to determine the F_{tr}(Q) dependence for a given projectile energy and scattering angle. The calculations included the collective excitations of the target and projectile nuclei [10] and four transfer channels (+1n, +2n, -1p, -1α). The F_{tr} coefficients were estimated through an iterative procedure by comparing the calculated transfer cross sections for each transfer with the measured ones. The comparison of the theoretical and experimental transfer cross sections is shown in Fig. 2a.

Using the obtained F_{tr} (Q, E$_{beam}$) dependence for various transfer reactions (see example in Fig. 2b), we should be able to verify the importance of the above assumptions on fusion and quasielastic backscattering excitation functions. In particular, we plan to test:

a) how much the approximations in the treatment of transfer in the standard CCQEL code influence the results of the calculations, and more generally,

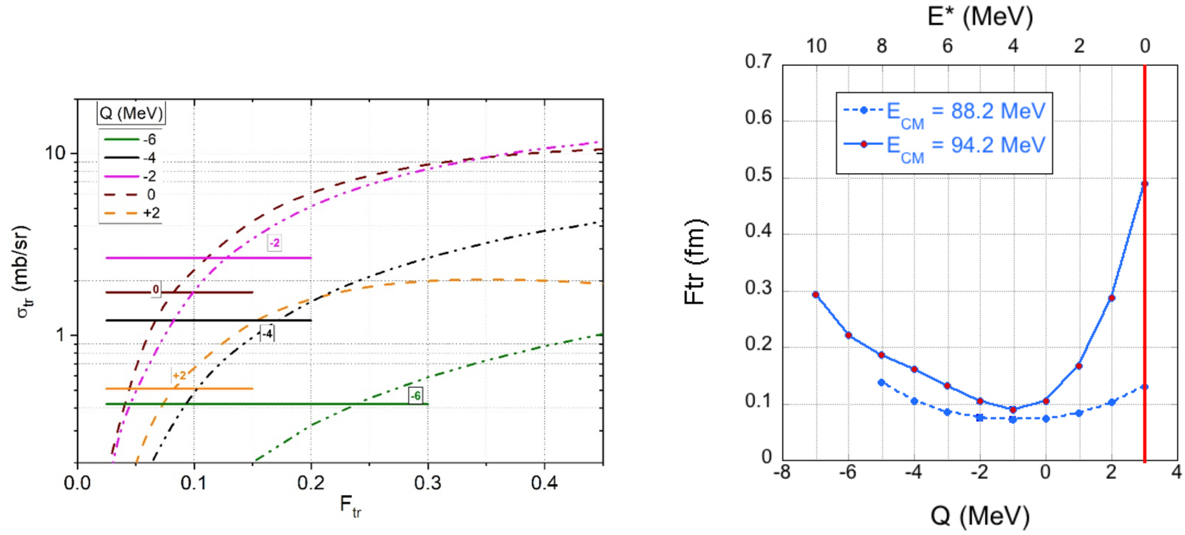

(a) **(b)**

Figure 2: (a) Principle of the F_{tr}determination. The straight lines give experimental transfer cross sections at a given Q value, the dashed ones are the results of the CCQEL calculations. (b) Example of the F_{tr} (Q) dependence for the 2n transfer in the ^{20}Ne+^{208}Pb scattering for two beam energies. The vertical red line denotes the Q_{gg} (equivalent to E* equal to zero). We also obtained the corresponding functions for +1n, -1p and -1α.

b) whether dissipation via transfer influences significantly the fusion and Coulomb barrier distributions.

A similar analysis will be performed for the ^{24}Mg+^{92}Zr system. However, in this case, the smoothing of the barrier distribution is mainly caused by the non-collective excitations as shown in [11]. The work is in progress.

Bibliography

[1] M. Dasgupta *et al.* Annu. Rev. Nucl. Part. Sci. **48** (1998) 401.
[2] B. Back, H. Esbensen, C. Jiang, and K. E. Rehm, Rev. Mod. Phys. **86** (2014) 317.
[3] E. Piasecki *et al.*, Phys. Rev. C **80** (2009) 054613.
[4] S. Yusa, K Hagino, and N. Rowley, Phys. Rev. C **88** (2013) 054621.
[5] E. Piasecki *et al.*, Phys. Rev. C **100** (2019) 014616.
[6] K. Hagino *et al.*, Comp. Phys. Comm. **123** (1999).
[7] N. Rowley *et al.*, Phys. Lett. B **254** (1991) 25.
[8] H. Timmers *et al.*, Nucl. Phys. A **584** (1995) 190.
[9] A. Trzcińska *et al.*, HIL Annual Report (2020) 41.
[10] E. Piasecki *et al.*, Phys. Rev. C **85** (2012) 054608.
[11] A. Trzcińska *et al.*, Phys. Rev. C **102** (2020) 034617.

C.2 Coupling of ^{6}Li+^{10}B elastic scattering with the inelastic channels

A.T. Rudchik[1], A.A. Rudchik[1], O.O. Chepurnov[1], K.W. Kemper[2], N. Keeley[3], K. Rusek[4], E.I. Koshchyi[5], S. Kliczewski[6], S.Yu. Mezhevych[1], V.M. Pirnak[1], O.A. Ponkratenko[1], R. Siudak[6], H.M. Maridi[4], A.P Ilyin[1], B.V. Mishchenko[1], Yu.M. Stepanenko[1], V.V. Uleshchenko[1], Yu.O. Shyrma[1], K.A. Chercas[1], B. Zalewski[4]

1) Institute for Nuclear Research, The National Academy of Sciences of Ukraine, Kyiv, Ukraine
2) Physics Department, Florida State University, Tallahassee, USA
3) National Centre for Nuclear Research
4) Heavy Ion Laboratory, University of Warsaw, Warszawa, Poland
5) Cyclotron Institute, Texas A&M University, Collage Station, USA
6) The H. Niewodniczański Institute of Nuclear Physics PAN, Kraków, Poland

New experimental data of cross section angular distributions for the elastic and inelastic scattering of ^{6}Li+^{10}B nuclei were measured in inverse kinematics, with a ^{10}B beam of $E_{\mathrm{lab}}(^{10}\mathrm{B}) = 51$ MeV from the U-200P cyclotron at the Heavy Ion Laboratory of the University of Warsaw. The reaction products were detected with two types of ΔE-E telescopes - one where both ΔE and E stages consisted of silicon detectors and one consisting of an ionization chamber(ΔE) plus silicon detector (E). The inelastic scattering data corresponded to the excitation of ^{6}Li to the 2.19 MeV, 4.31 MeV and 5.65 MeV resonant states and the excitation of ^{10}B to the low-lying states at 0.72 MeV, 2.15 MeV and 3.59 MeV.

The data were analysed in two ways:
- using a global ^{6}Li optical model potential (OM) and the method of Coupled-Channels (CC) with fitted parameters;
- with the ^{6}Li+^{10}B interactions calculated from phenomenological α, d+^{10}B optical model potentials and the cluster model wave functions of ^{6}Li, with fixed parameters (Continuum-Discretized Coupled-Channels, CDCC) .

The total reaction cross section and complete fusion cross section, as well as cross sections for ^{10}B excitation and ^{6}Li$\rightarrow \alpha + d$ breakup were derived and are listed in the Table 1. The effective OM potential for ^{6}Li+^{10}B elastic scattering was found. The effects of couplings between various reaction channels were studied.

Table 1: Cross sections for various processes obtained from the data analysis by different models.

Process	cross section [mb]	Model
tot. reaction	1518.0	OM
complete fusion	820.0	BPM
tot. ^{10}B excitation	24.8	CDCC+CC
tot. breakup ^{6}Li$\rightarrow \alpha + d$	179.0	CDCC+CC
res. breakup $^{6}\mathrm{Li}_{3+}\rightarrow \alpha + d$	18.4	CDCC+CC
res. breakup $^{6}\mathrm{Li}_{2+}\rightarrow \alpha + d$	8.7	CDCC+CC
res. breakup $^{6}\mathrm{Li}_{1+}\rightarrow \alpha + d$	4.4	CDCC+CC

C.3 Asymptotic normalization coefficient for the $^{14}C \rightarrow ^{13}B+p$ overlap from the $^{14}C(^{11}B,^{12}C)^{13}B$ reaction

S.Yu. Mezhevych[1], N. Keeley[2], A.T. Rudchik[1], K. Rusek[3], K.W. Kemper[4], A.A. Rudchik[1], O.A. Ponkratenko[1], E.I. Koshchyi[5], S.B. Sakuta[6]

1) Institute for Nuclear Research, The National Academy of Sciences of Ukraine, Kyiv, Ukraine
2) National Centre for Nuclear Research
3) Heavy Ion Laboratory, University of Warsaw, Warszawa, Poland
4) Physics Department, Florida State University, Tallahassee, USA
5) Cyclotron Institute, Texas A&M University, Collage Station, USA
6) National Research Center "Kurchatov Institute", Moscow, Russia

In an experiment performed at the Heavy Ion Laboratory, University of Warsaw, with a 45 MeV ^{11}B beam scattered from a ^{14}C target, in addition to data for the elastic and inelastic scattering [1, 2], an angular distribution for the $^{14}C(^{11}B,^{12}C)^{13}B$ proton pickup reaction was obtained. Such a comparatively complete data set enables a determination of the $^{14}C=^{13}B+p$ asymptotic normalization coefficient (ANC) using the coupled reaction channel (CRC) technique. The complete nature of the data set allows two-step contributions to the reaction mechanism to be controlled while a set of $^{12}C=^{11}B+p$ overlaps obtained from a consistent analysis of (d,^{3}He) and (e,e'p) data fixes the projectile overlaps [3]. We find that the level of completeness of the modeling of the reaction mechanism has a significant effect on the value obtained for the ANC, with a distorted wave Born approximation (DWBA) analysis yelding a significantly larger ANC than the full CRC calculation. The final result obtained, when compared with the theoretical value calculated within the source term approach, is in accord with the trends for proton removal from similar p-shell nuclei [4].

Table 1: Values of ANC^2 obtained from DWBA and CRC calculations.

Model	ANC^2 [fm^{-1}]
DWBA	2044
CRC	1532
Theory [4]	803

Bibliography

[1] S.Yu. Mezhevych *et al.*, Nucl. Phys. A **724**, 29 (2003).
[2] S.Yu. Mezhevych *et al.*, Eur. Phys. J. A **50**, 4 (2014).
[3] G.J. Kramer, H.P. Blok, L. Lapikás, Nucl. Phys. A **679**, 267 (2001).
[4] N.K. Timofeyuk, Phys. Rev. C **88**, 044315 (2013).

C.4 Spin 3^+ of the 1415.5 keV level from the γ-band in ^{138}Nd measured using γ–γ angular correlations

J. Samorajczyk-Pyśk[1], *Ch. Droste*[2], *J. Srebrny*[1] *L. Próchniak*[1]

1) Heavy Ion Laboratory, University of Warsaw, Warszawa, Poland
2) Faculty of Physics, University of Warsaw, Warszawa, Poland

The experimental data [1, 2] suggest the presence of a γ-band in ^{138}Nd. This band is built on the second 2^+ level (Fig. 1) and it extends up to spin I=(6^+) but the spins of the levels, except for that of the bandhead, are not well established.

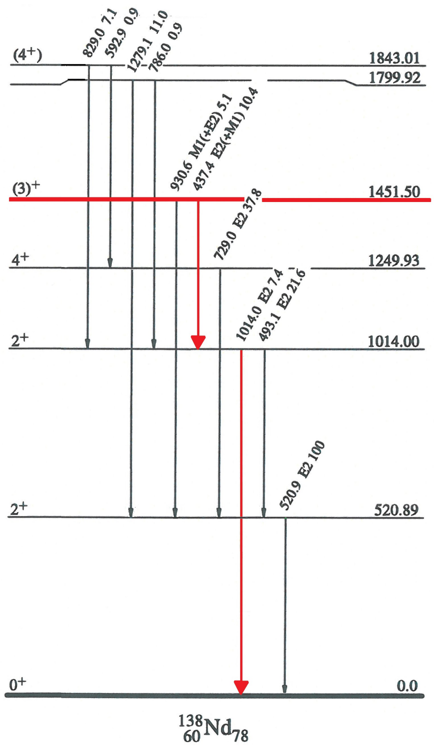

Figure 1: Partial level scheme of ^{138}Nd[2] relevant to our work. The red arrows and the red line indicate γ transitions and the level studied in this work.

Among the states of the γ-band is the 1451.5 keV level with a tentative spin assignment I=$(3)^+$ (Fig. 1). In our experiment this state was populated in the β^+/EC decay ^{138}Pm ((5^-) isomeric state with $T_{1/2}$=3.24(5) min) that were produced in the ^{104}Pd + ^{40}Ar reaction. The experiment was focused on the ^{140}Sm isotope and the ^{138}Pm nuclei were a by-product [1]. The ^{40}Ar beam was provided by the U-200P cyclotron of the Heavy Ion Laboratory. The γ rays were registered using 12 HPGe detectors of the EAGLE array. More details about this experiment and its analysis may be found in Ref.[1].

The spin of the 1451.5 keV level was established by studying γ–γ angular correlations between 437 keV (transition from the studied level to the 2_2^+level) and 1014 keV ($2_2^+ \rightarrow$g.s.) photons (Fig. 1). The obtained γ–γ angular correlation coefficients are equal to $A_{22} = -0.45(7)$ and $A_{44} = -0.13(7)$ (see the red diamond in Fig. 2). This result leads to the following conclusions:

a) there are two possible solutions for the spin of the 1451.5 keV level, namely I=1 or 3,

b) in the 1→2→0 cascade the upper transition (E_γ=437 keV) has a strong M1 component because of the low value of the δ(E2/M1) parameter. For a pure M1 transition (δ(E2/M1)=0) the A_{44} coefficient equals zero.

c) solutions with I=2 or 4 are excluded.

d) spin I=0 is excluded since for a 0→2→0 cascade A_{22}=0.357 and A_{44}=1.143 whereas the experimental values are $A_{22} = -0.45(7)$ and $A_{44} = -0.13(7)$

It turns out that the results of the experiment in which the internal conversion electrons were measured helps to solve the spin question (I=1 or 3). According to the result of Ref. [3], the experimental value of $\alpha_k(\gamma 437$ keV) equals 0.0160(15). From the BrIcc code [4] it is known that for 437 keV photons α_k^{th}(M1)=0.02195 and α_k^{th}(E2)=0.01397. Based on these values and using the following equation:

$$\alpha_k^{exp} = \frac{\alpha_k^{th}(M1) + \delta^2 \alpha_k^{th}(E2)}{1+\delta^2} \tag{1}$$

the mixing ratios δ(E2/M1)=$1.71^{+2.04}_{-0.49}$ or δ(E2/M1)=$-1.71^{-0.49}_{+2.04}$ were obtained.

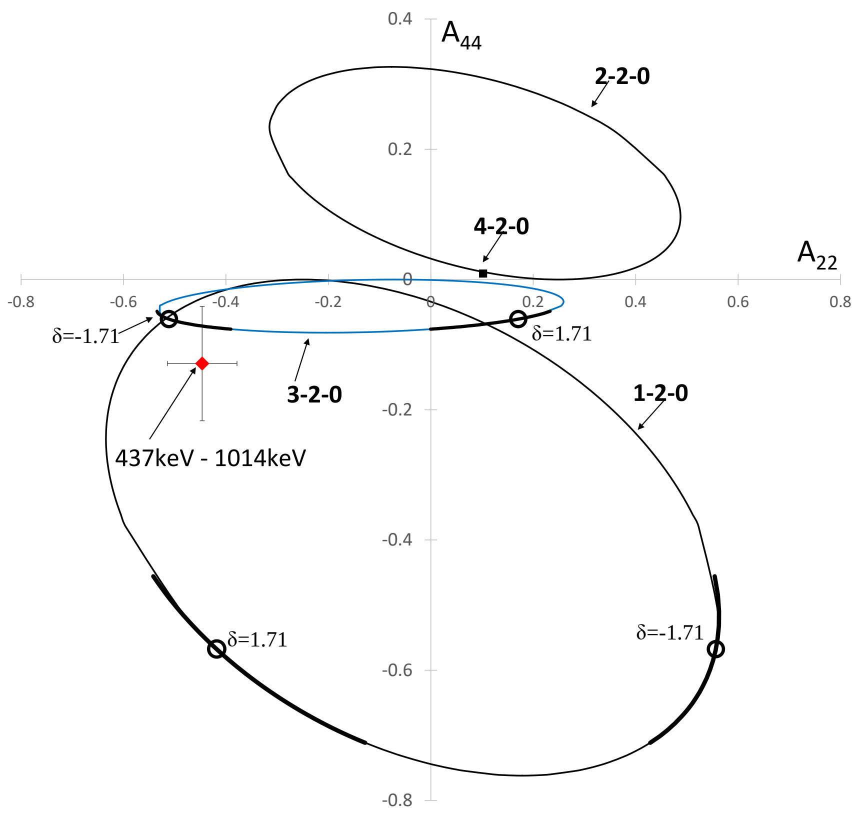

Figure 2: Parametric plot of the $A_{22}(\delta)$ and $A_{44}(\delta)$ angular correlation coeffcients for the I→2→0 cascades (for initial spins I=1, 2, 3, 4). The experimental results are compared with the theoretical predictions. The red diamond indicates the experimental values of A_{22} and A_{44} obtained in our work. Open black circles and thick black lines denote the experimental values of the mixing ratios $\delta = \pm 1.71$ obtained from the conversion electrons measurements [3].

Such values of δ mean that for the $1 \to 2 \to 0$ cascade the 437 keV γ-transition has a strong E2 component. In the case of I=1 this result is in contradiction with the result of the γ–γ correlation (see point b) above). There is no such contradiction in the case of I=3 (see the $3 \to 2 \to 0$ contour), where the point with $\delta(E2/M1) = -1.71$ (open black circle) lies in the vicinity of the (A_{22}, A_{44}) point (red diamond). Therefore, one may conclude that the spin value of the 1415.5 keV level equals 3^+. This supports the existence of a γ-band based on the 2_2 level in ^{138}Nd.

Bibliography

[1] J. Smorajczyk-Pyśk *et al.*, Phys. Rev. C **104** (2021) 034322.
[2] Data from the NNDC database, revision as of March 2022. `https://www.nndc.bnl.gov/ensdf/`
[3] J. Deslauriers *et al.*, Zeitschrift für Physik **303** (1981) 151.
[4] BrIcc code from NNDC database, revision as of March 2022.

C.5 Collective isovector quadrupole excitation in ^{142}Sm - Identification via a γ-γ–corelation measurement after ϵ/β^+ decay

T. Stetz[1], *T. Abraham*[2], *U. Ahmed*[1], *G. Colucci*[2], *M.L. Cortes*[1], *K. Hadyńska-Klęk*[2], *G. Jaworski*[2], *R. Kern*[1], *M. Kisieliński*[2], *M. Komorowska*[2], *M. Kowalczyk*[2], *P.J. Napiorkowski*[2], *C. Nickel*[1], *M. Palacz*[2], *N. Pietralla*[1], *G. Rainovski*[3], *J. Samorajczyk-Pyśk*[2], *J. Srebrny*[2], *M. Stoyanova*[3], *A. Trzcińska*[2], *V. Werner*[1], *K. Wrzosek-Lipska*[2], *B. Zalewski*[2], *R. Zidarova*[1]

1) IKP, Technical University Darmstadt, Darmstadt, Germany
2) Heavy Ion Laboratory, University of Warsaw, Warszawa, Poland
3) Sofia University "St. Kliment Ohridski", Sofia, Bulgaria

The 2^+_3 state of ^{142}Sm is a promising candidate for the one-quadrupole phonon mixed-symmetry state. In order to obtain the M1 strength of the $2^+_3 \rightarrow 2^+_1$ transition from a projectile Coulomb-excitation experiment at HIE-ISOLDE at CERN, a complementary β-decay experiment was performed at the Heavy Ion Laboratory in Warsaw with the intention of determining the multipole mixing ratio of the transition of interest.

1. Scientific motivation - nuclear valence-shell stabilization in N=80 isotones

The origin of quadrupole collectivity in most heavy open-shell nuclei is the attractive quadrupole-quadrupole interaction between valence protons and neutrons. This interaction results in a coherent mixing of collective quadrupole excitations of the proton and neutron subspaces. Geometrical models can well describe this collective motion. The nucleus is considered as a homogeneous object with a certain shape which can vibrate or rotate [1]. This approach neglects the nucleonic degrees of freedom to a large extent.

A theoretical approach to the modeling of quadrupole-collective heavy nuclei which provides an attempt to bridge the calculation of nuclear properties from fundamental nucleon-nucleon interactions to the collective model is the interacting boson model (IBM) [2]. The IBM-1 describes the lowest-lying excitations in even-even nuclei, which are called full-symmetry states (FSSs). The IBM-2 [3], which distinguishes between proton and neutron bosons, predicts another class of states, the mixed-symmetry states (MSS). The proton and neutron motions of these states are partly out of phase. To quantify the degree of coherence of the proton-boson and neutron-boson contributions the F spin is introduced. The F spin is the analog of the isopsin for bosons. The F spin of FSSs, $F=F_{max}=(N_\pi+N_\nu)/2$ equals the maximum F spin, whereas MSSs occupy a lower value, $F=F_{max}-1$. MSSs represent a physics case in which the balance and interplay between the nuclear phenomena of collectivity and shell structure, and the isospin degrees of freedom can be studied. In addition, the quality of the F spin as a good quantum number can solely be probed by measuring the mixing between MSSs and FSSs.

According to the IBM-2 the lowest-lying MSS in vibrational nuclei is the $2^+_{1;\mathrm{ms}}$ state. The most indicative experimental signature of the $2^+_{1;\mathrm{ms}}$ state is the strong M1 transition strength to the full-symmetry 2^+_1 state. In contrast to isoscalar transitions between two FSSs with $\Delta F=0$, the M1 strength of isovector transitions between MSSs and FSSs with $\Delta F=\pm1$ is not suppressed. Available information on MSSs in the mass regions A≈90, 130 of vibrational nuclei has been summarized in a review article [4] and was recently extended to

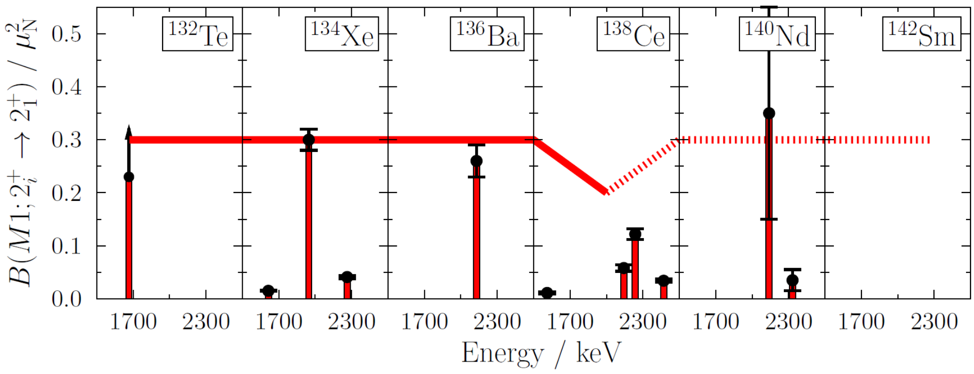

Figure 1: M1-strength distributions of N=80 isotones up to ^{138}Ce. A possible trend shows the restoration of the isolation of MSSs for ^{142}Sm. Picture taken from Ref. [12]

the mass A≈200 region [5–7]. The determination of the multipole-mixing ratio $\delta(2_i^+ \rightarrow 2_1^+)$ is indispensable for the identification of the $2^+_{1;\mathrm{ms}}$ state.

The study of MSSs of the N = 80 isotonic chain reveals an unsolved physics case. The nuclei ^{132}Te, ^{134}Xe and ^{136}Ba [8–10] form isolated $2^+_{1;\mathrm{ms}}$ states. In contrast, the ^{138}Ce $2^+_{1;\mathrm{ms}}$ strongly mixes with a nearby full-symmetry 2^+ state [11], see Fig. 1. This dramatic change in the properties of MSSs when only two protons are added to the system suggests that the strength concentration of collective-isovector excitations in the valence shell reflects the underlying single-particle structure through a mechanism dubbed shell stabilization [11]. The observed mixing in ^{138}Ce is attributed to the lack of shell stabilization at the $\pi(g_{7/2})$ sub-shell closure. All these experimental data lead to the conclusion that a direct experimental confirmation of the mechanism of shell stabilization in the N=80 isotones, which is a phenomenon related to the proton structure, should be sought for by identifying the MSSs in radioactive ^{140}Nd and ^{142}Sm.

The properties of MSSs of stable N=80 isotones were theoretically studied with the quasiparticle-phonon model (QPM) [13] and the large-scale shell model (SM) [14]. Both models have demonstrated that the splitting of the M1 strength in ^{138}Ce is a genuine shell effect caused by the specific shell structure and the pairing correlations [13, 14]. The theoretical predictions of the degree of mixing [14] and the experimentally observed mixing [16] of the MSS differs a lot for ^{140}Nd, while they are lacking for ^{142}Sm. To bring full clarity to the evolution of the F-spin mixing in N = 80 isotones, a measurement of the multipole-mixing ratio of the $2_3^+ \rightarrow 2_1^+$ transition is without an alternative.

A projectile Coulomb-excitation (CoulEx) experiment was performed at HIE-ISOLDE at CERN, with ^{140}Nd and ^{142}Sm as radioactive ion beams (RIB) [15]. Due to the naturally low statistics of RIBs the determination of the multipole mixing ratio of the $2_3^+ \rightarrow 2_1^+$ transition is not feasible; but there are strong indications that the 2_3^+ state is the most promising candidate for the MSS of both isotones. The necessary multipole mixing ratio of ^{140}Nd was determined by a $\gamma - \gamma$ angular-correlation measurement following a ϵ/β-decay [16]. For ^{142}Sm the multipole mixing ratio of the $2_3^+ \rightarrow 2_1^+$ transition is sought to be obtained by the evaluation of the present experiment, performed at the Heavy Ion Laboratory in Warsaw.

2. γ-γ-correlation measurement after ϵ/β^+ decay

The experiment was conducted at the Warsaw Cyclotron of the Heavy Ion Laboratory in Warsaw, Poland. It aimed at the identification of the MSS of ^{142}Sm and the corresponding

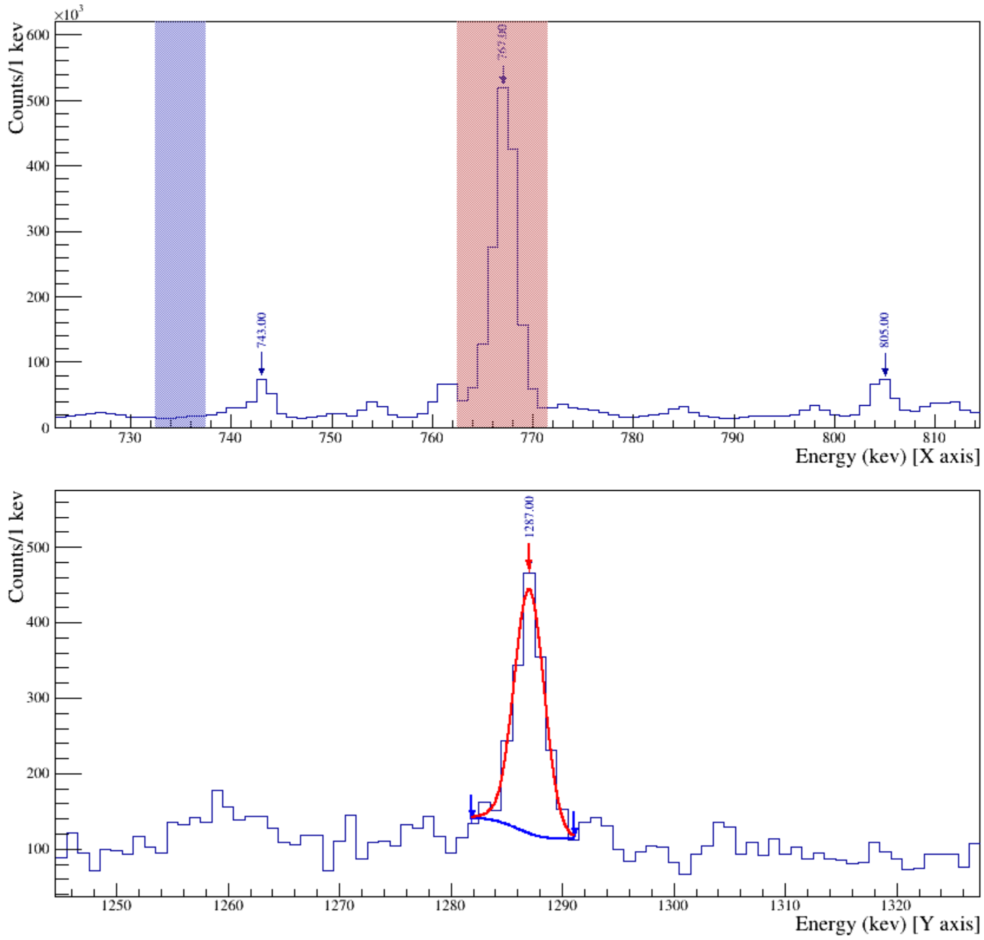

Figure 2: Top: The range of the coincidence condition set on the ground-state transition of the 2_1^+ state can be seen marked in red. Marked in blue is the range of the background deduction. Bottom: The $2_3^+ \rightarrow 2_1^+$ transition at 1287 keV clearly stands out above the background events. Both spectra contain the data of all detectors combined.

upper limit for the F-spin mixing matrix element via the obtained multipole mixing ratios in combination with an already perfomed CoulEx experiment at HIE-ISOLDE. The state of interest is the 2_3^+ of ^{142}Sm at 2140 keV. The population of this state was achieved via a four-neutron transfer reaction followed by two β-decays. A beam of ^{32}S ions in combination with a $4\,\mathrm{mg/cm^2}$ ^{114}Cd target formed the compound nucleus ^{142}Gd ($T_{1/2} \approx 70\,\mathrm{s}$), which is the grand-mother nucleus of ^{142}Sm. The four-neutron transfer reaction was followed by a ϵ/β^+-decay to the short living isomer of ^{142}Eu ($T_{1/2} \approx 2.4\,\mathrm{s}$).

During a timespan of 8 days the ^{32}S beam at 144 MeV was periodically stopped in a cycle of 150 s in order to obtain data in the off-beam periods. The EAGLE high-purity germanium (HPGe) array was ideally suited for the γ-ray detection. The high total efficiency of EAGLE (≈1%) was necessary to obtain a reasonable γ-γ-coincidence efficiency. The HPGe detectors of the EAGLE array are arranged in 5 angular groups with respect to the beam axis. A γ-ray coincidence condition on the $2_1^+ \rightarrow 0_1^+$ transition of ^{142}Sm at 768 keV can be set, as shown in Fig. 2. The desired $2_3^+ \rightarrow 2_1^+$ transition at 1287 keV can clearly be observed. From these data, obtained at the Heavy Ion Laboratory, an angular γ-γ-correlation between the two transitions can be determined. The multipole-mixing ratio can be obtained by analyzing the angular dependency of the coincidence intensity.

3. Ongoing analysis and outlook

As shown in Fig. 2, the desired $2_3^+ \rightarrow 2_1^+$ transition at 1287 keV can be observed in the coincidence spectrum with a condition set on the ground-state transition of the 2_1^+ state. By looking at this transition in different angular detector pairs, the multipole mixing ratio of the 2_3^+ state can be obtained. The analysis of the multipole mixing ratio is currently in progress. This is the last missing quantity in obtaining the M1 transition strength, conclusively to identify the MSS state of ^{142}Sm. It is the last missing piece of the puzzle of the nuclear valence-shell stabilization for the N=80 isotonic chain.

Bibliography

[1] A. Bohr and B. Mottelson *Nuclear Structure* (Benjamin, Reading, MA, 1975) Vol. 2
[2] A. Arima *et al.*, Phys. Lett. B **66** (1977)205
[3] F. Iachello, Phys. Rev. Lett. **53** (1984) 1427.
[4] N. Pietralla *et al.*, Phys. Rev. C **64** (2001) 031301.
[5] D. Kocheva *et al.*, Phys. Rev. C **93** (2016) 011303.
[6] R. Stegmann *et al.*, Phys. Lett. B **770** (2017) 77.
[7] R. Kern *et al.*, Phys. Rev. C **99** (2019) 011303.
[8] M. Danchev *et al.*, Phys. Rev. C **84** (2011) 061306.
[9] T. Ahn *et al.*, Phys. Lett. B **679** (2009) 19.
[10] N. Pietralla *et al.*, Phys. Rev. C **58** (1998)796.
[11] G. Rainovski *et al.*, Phys. Rev. Lett. **96** (2006) 122501.
[12] R. Stegmann Ph.D. thesis, Technische Universitat Darmstäd, 2017.
[13] N. Lo Iudice *et al.*, Phys. Rev. C **77** (2008) 044310.
[14] K. Sieja *et al.*, Phys. Rev. C **80** (2009) 054311.
[15] R. Kern *et al.*, European Physical Journal Web of Conferences **194** (2018) 03003.
[16] E. Williams *et al.*, Phys. Rev. C **80** (2009) 054309.
[17] A. Gavron, Phys. Rev. C **21** (1980) 230.
[18] H. Geissel *et al.*, ATIMA pogram, GSI Darmstad, 1997.
[19] `http://slcj.uw.edu.pl/en/available-beams/` .

C.6 Construction of 10 µm, self-biased epitaxial silicon detectors operated in a built-in-field bias potential for radiation hardness tests

A. Kordyasz, Z. Szefliński, M. Paluch-Ferszt, M. Kowalczyk, P.J Napiorkowski

Heavy Ion Laboratory, University of Warsaw, Warszawa, Poland

The problem of detector radiation hardness is very important for experimental physics. In an attempt to improve detector radiation hardness special detector technologies and new materials like diamond or silicon carbide have been tried. The aim of this work is the construction for test purposes of thin (10 µm) silicon epitaxial detectors operated in a built-in-bias potential. They seem to be more resistant to radiation damage due to the extremely low detector bias potential generated by the internal built-in-field potential and the low detector thickness. Low detector thickness prevents doping of the detector material since all heavy ions are not stopped in it. Previously conducted tests with a 23 µm self-biased detector show that it works correctly with 90 MeV ^{14}N ions and a total dose of about $7.1 \cdot 10^{11}$ ions/cm^{-2} [1].

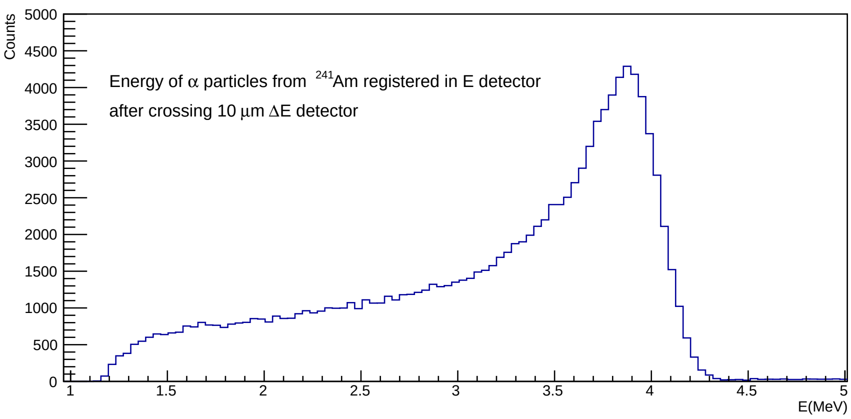

Figure 1: Energy of α particles from ^{241}Am registered in the E detector after crossing the 10 µm ΔE detector.

The thin detectors were constructed using silicon epitaxial n+ - n structures of resistivity epitaxial layer $> 20\ \Omega \cdot$ cm and thickness about 10 µm. The detector n$^+$-n-p$^+$ junction was obtained using B$^+$ implantation into the epitaxial n type side using the low-temperature technique [2]. To reduce the detector electric capacitance of self-biased detectors, the large-area self-biased detector (in the form of a thin 10 µm epitaxial membrane with n$^+$-n-p$^+$ junction) was broken down into smaller detector pieces (small self-biased detectors with n$^+$-n-p$^+$ junctions). The selected detectors were mounted in detector housings supplied with collimation entrance windows of diameter 1 mm. After gluing 50 µm silver wire contacts to the detector Al surfaces using two component silver paste hardened at a temperature of about 80°C, the self-biased thin detectors operating with internal built-in-potential (without any external bias potential) were ready to work with α particles and heavy ions. Preliminary measurements with a ΔE-E telescope consisting of a 10 µm self-biased ΔE detector followed by a thick E detector irradiated by 5.486 MeV α particles from an ^{241}Am source are presented in the following pictures:

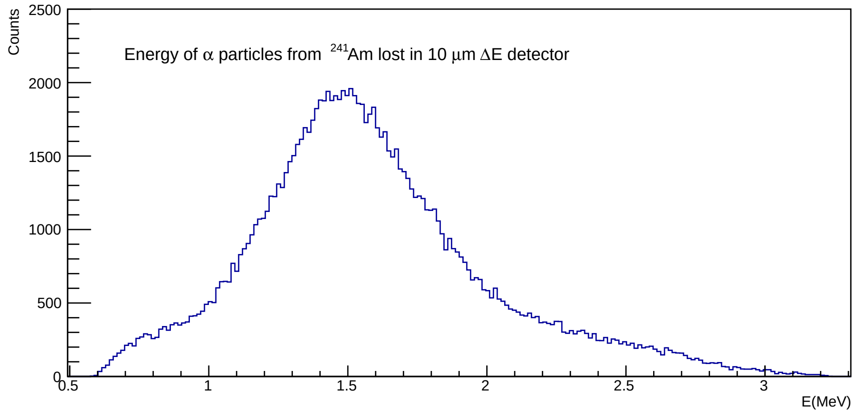

Figure 2: Energy of α particles from ^{241}Am lost in the 10 µm ΔE detector.

The radiation damage tests will be performed using a 90 MeV ^{14}N ion beam directly hitting the detectors during 20 eight hour shifts. The difference in carrier concentration between the detector substrate (n^-) and epitaxial layer (n^+) created the built-in potential difference as [3]:

$$V = (kT/q)ln((n^+/n^-) \tag{1}$$

where k is the Boltzman constant, T is the absolute temperature and q is the electron charge. Since 90 MeV ions punch through a thin detector, the carrier concentrations of n^+ and n^- remain unchanged. According to the above formula the built-in potential

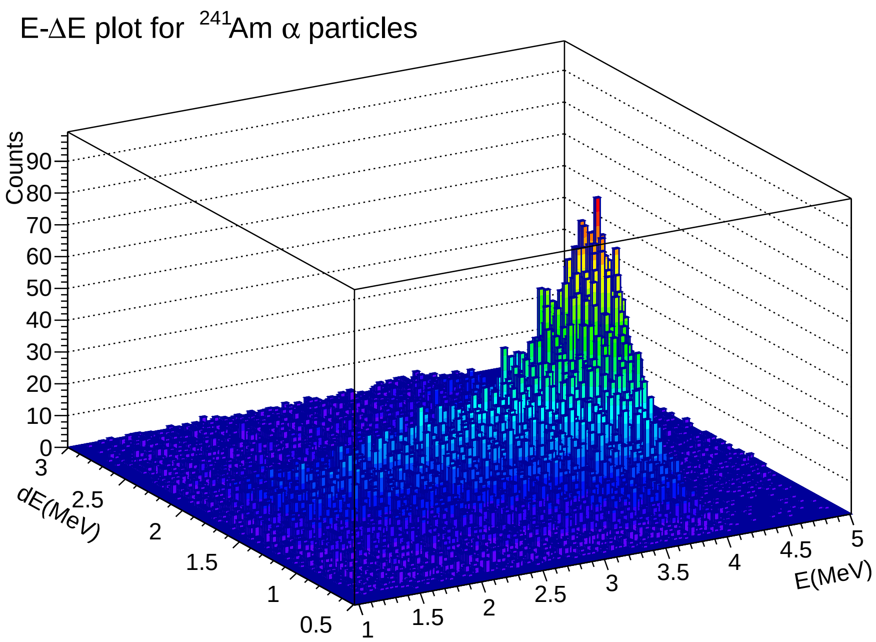

Figure 3: E-ΔE plot for ^{241}Am α particles.

difference should not be sensitive to the 90 MeV ^{14}N ion exposed dose. It is very important to check this conclusion with large doses. For this reason a thin detector will be directly irradiated with an ion beam of ^{14}N at the Exposure Station (on Beamline A at the Heavy Ion Laboratory of Warsaw University) followed by a control measurement with 5.487 MeV α particles from an ^{241}Am source. Radiation damage will be continued until degradation of the thin detector energy resolution is achieved.

Bibliography

[1] A. J. Kordyasz *et al.*, HIL Annual Report 2018 page 69.
[2] A. J. Kordyasz *et al.*, Eur. Phys. J. A **51** (2015) 15.
[3] A. J. Kordyasz *et al.*, Nucl. Inst. and Meth. A **539**(2005) 262.

C.7 Radiation damage of PIN diode detectors irradiated with heavy ions studied using positron annihilation spectroscopy.

K.Z. Krutul[1], P. Horodek[2], K. Hadyńksa-Klęk[1], M. Komorowska[1], T.N.M. Le[4], P.J. Napiorkowski[1], A. Olejniczak[3], M. Paluch-Ferszt[1], K. Siemek[2], Z. Szefliński[1], K. Wrzosek-Lipska[1]

1) Heavy Ion Laboratory, University of Warsaw, Warszawa, Poland
2) The H. Niewodniczański Inst. of Nucl. Phys. PAN, Kraków, Poland
3) Faculty of Chemistry, Nicolaus Copernicus University, Toruń, Poland
4) Institute of Physics, Viet Nam Academy of Science and Technology, Hanoi, Vietnam

PIN diode semiconductor silicon detectors are used at the Heavy Ion Laboratory (HIL) in Coulomb excitation experiments as heavy ion sensors. The deterioration of the quality of the registered particle energy spectrum determines the scope of the detector applicability. This is especially important when designing detection systems that are foreseen to operate with a large fluence of charged particles. Little information on the radiation destruction of PIN diode silicon semiconductor detectors is available in the literature. Qualitative deterioration of the acquired energy spectrum of the registered particles was found, which, for the first time, was associated with the increase of the dark current [1]. Therefore, at the HIL in Warsaw [2] an attempt was made to document at which point the detector is destroyed. The following ion fluences were used for these studies:

- ^{12}C, ^{20}Ne from the U-200P cyclotron at the HIL, Warsaw in the range to $1{\cdot}10^{13}$ ions/cm^2.
- ^{131}Xe, ^{209}Bi from the IC100 cyclotron at the JINR, Dubna in the range $1{\cdot}10^{12}$ up to $2{\cdot}10^{14}$ ions/cm^2.

The process of the deterioration of a PIN diode detector was studied in detail during the irradiation with a 45 MeV ^{12}C beam [3, 4]. Heavy ions scattered on a (9 mg/cm^2 thick) gold foil irradiated the PIN detector placed 30° with respect to the beam axis. Beam intensity was controlled with a Si detector (monitor) placed at 22.5°. Saturation of black current was observed at a fluence of $5{\times}10^9$ ions/cm^2. The spectroscopic properties of the PIN diode detector irradiated with the heavy ion beam i.e. FWHM, peak position and dark current were monitored by measuring the spectrum collected outside the beam with a ^{241}Am α source (Fig. 1).

Structural defects induced by the exposure to the heavy ion beam were further examined at the Joint Institute for Nuclear Research (JINR) in Dubna, Russia, using the positron annihilation spectroscopy technique. It is a sensitive tool for studying defects in crystals, i.e., vacancies and their clusters [5–7].

A set of four irradiated PIN diodes and the chosen reference PIN diode, which was not exposed to the high-flux heavy-ion beam, were measured. In the conducted experiment, the positron lifetime (LT) technique was used. More details related to the experimental setup used are given in ref. [7]. The results of positron annihilation spectroscopy are shown in Figure 2.

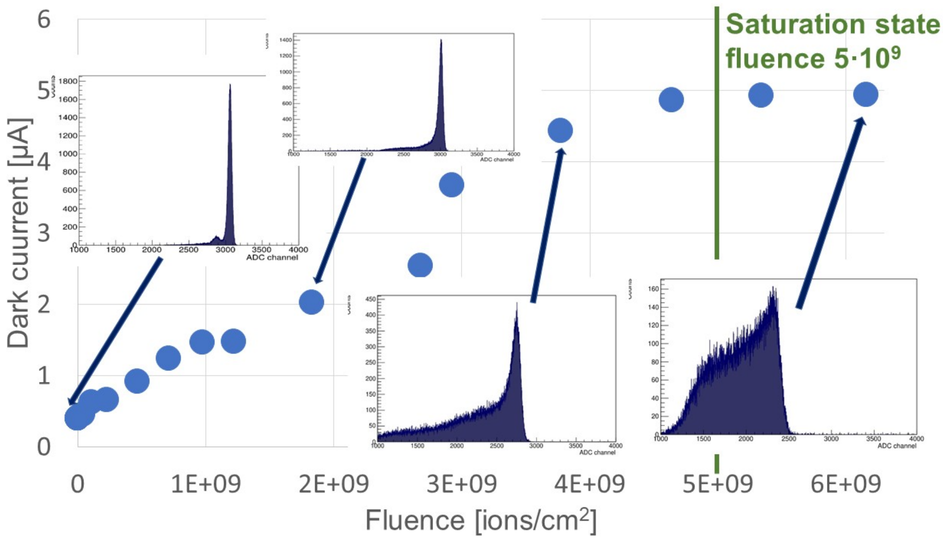

Figure 1: Irradiation of the PIN diode – heavy ion fluence as a function of the dark current. The insets present particle spectra controlled at the various stages of detector destruction and at the dark current saturation level.

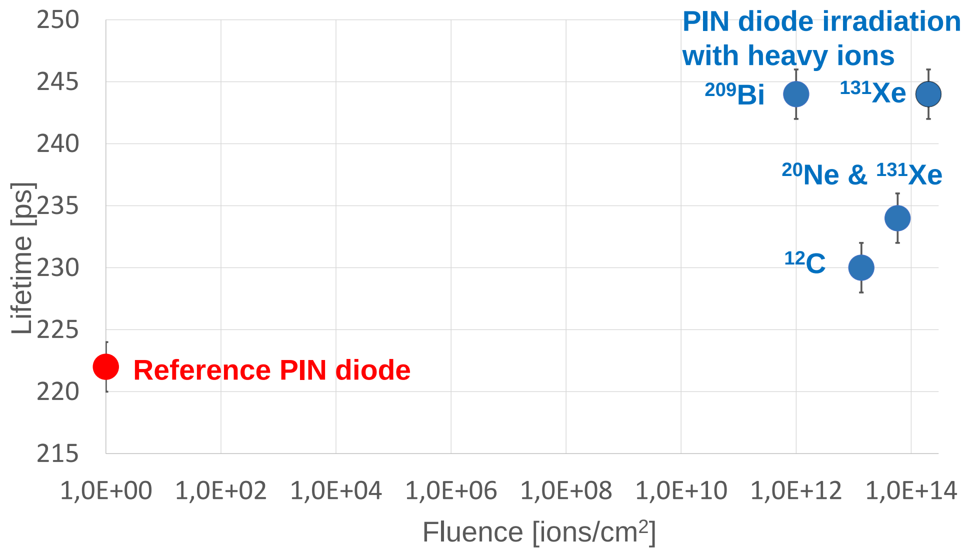

Figure 2: Results of positron annihilation spectroscopy measurement - positron lifetime observed for the irradiated samples (marked in blue) as a function of fluence. The red point corresponds to the reference PIN diode which was not exposed to a heavy ion beam with a high fluence.

We observed:

- The positron LT measured in the four irradiated samples are longer than LT measured in the reference PIN diode (Fig. 2).
- Increase in LT with fluence proves the existence of radiation-induced defects.
- The rapid increase in LT with the fluence of the bombarding ions indicates a small expansion in the size of the defects.

- Registered positron lifetimes are lower than those reported in the literature for monovacancies [8, 9].

Damage of the PIN diode detector manifests itself in changes of the dark current, broadening of the spectrum and a clear upward trend of the LT as a function of the ion fluence.

- The increase of the particle spectrum observed as a growth of the alpha peak tail compared to its maximum with a simultaneous shift of the maximum towards lower energies indicates a decrease in the charge collection efficiency of the irradiated detector.

- Fluences of less than 10^9 ions/cm^2 not completely destroy the detector, although its spectroscopic properties deteriorate.

- Further studies aimed at determining the types of structural damage caused by heavy ion irradiation and examining the properties of detectors made of other materials are currently ongoing.

Bibliography

[1] K. Z. Krutul, M.Sc. thesis, University of Białystok, 2017
[2] K. Krutul *et al.*, Acta Phys. Pol. Proc. Supp. **13**, (2020) 861.
[3] K. Z. Krutul *et al.*, Poster: "The radiation damage of PIN diode detectors irradiated with heavy ions studied with the positron annihilation spectroscopy". Conference "New trends in nuclear Physics Detectors" (2021).
[4] K. Z. Krutul *et al.*, Presentation: " The radiation damage of PIN-diode detectors irradiated with heavy ions studied with the positron annihilation spectroscopy". Conference: "YOUNG MULTIS 2021" (2021).
[5] F. Tuomisto *et al.*, Rev. Mod. Phys. **85**, (2013) 1583.
[6] R. Krause-Rehberg *et al.*, "Positron Annihilation in Semiconductors", Springer, Berlin (1998).
[7] P. Horodek, Vacuum **164**, (2019) 421 .
[8] J.M. Campillo Robles *et al.*, J. Phys.: Conf. Ser. **265**, (2011) 012006.
[9] J.M. Campillo Robles *et al.*, J. Phys.: Condens. Matter **19**, (2007) 176222 .

C.8 Elastic scattering differential cross section for ^{6}He on protons at 26MeV/n

B Zalewski[1], M.C. Golovkov[2], K. Rusek[1], S.G. Belogurov[2,3], A.A. Bezbakh[2], V. Chudoba[2,4], A.S. Fomichev[2], E.M. Gazeeva[2], A.V. Gorshkov[2], G. Kaminski[1,2], S.A. Krupko[2], B. Mauyey[2,5], I.A. Muzalevsky[2,4], P. Napiorkowski[1], E.Yu. Nikolskii[2,6], W. Piątek[1,2], P. Pluciński[1], A. Serikov[2], S.I. Sidorchuk[2], R.S. Slepnev[2], P.G. Sharov[2], N. Sokołowska[7], G.M. Ter-Akopian[2], A. Trzcińska[1], R. Wolski[2]

1) Heavy Ion Laboratory, University of Warsaw, Warszawa, Poland
2) Joint Institute for Nuclear Research, Dubna, Russia
3) Moscow Engineering Physics Institute "MEPhI", Moscow, Russia
4) Institute of Physics, Silesian University in Opava, Opava, Czech Republic
5) Institute of Nuclear Physics of the National Nuclear Center, Almaty, Kazakhstan
6) National Research Center "Kurchatov Institute", Moscow, Russia
7) Faculty of Physics, University of Warsaw, Warszawa, Poland

In 2018 the ^{6}He + ^{1}H elastic scattering reaction was studied at the ACCULINNA-2 fragment separator in the Flerov Laboratory of Nuclear Reactions of the Joint Institute for Nuclear Research, Dubna [1]. The aim of the experiment was the measurement of the angular distribution of the differential cross section. In the experiment, a ^{6}He beam at an incident energy of 26 MeV/n impinged on a cryogenic gas target filled with hydrogen gas at 500 mbar. The gas target was rotated by 33° ensuring clear passage of protons scattered at low scattering angles. The thickness of the target was $1.75{*}10^{21}\frac{atoms}{cm^2}$. The experimental setup consisted of a Time of Flight detector (ToF), two Multi-wire Proportional Chambers (MWPC), two telescopes for reaction product detection and the cryogenic gas target. The ToF detector consisted of two fast scintillating detectors separated by a distance of 12 m. The MWPCs were used for beam tracking in the X and Y axes, where the Z-axis was set by the direction of the beam. The first telescope consisted of a 58x58mm^2 x 300 micron Silicon Strip Detector (SSD) and a 61x61mm^2 x 1000 micron Double Sided Strip Detector (DSSD). It covered laboratory angles in the range from 60° to 80° and was used for the detection of the scattered protons.

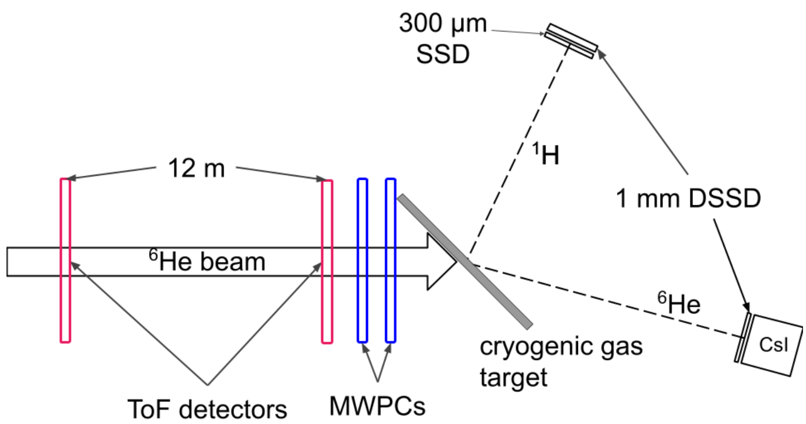

Figure 1: Schematic of the experimental setup for the ^{6}He + p differential cross section measurement.

The second telescope consisted of a 61x61mm^2 x 1000 micron DSSD and a CsI detector, which consisted of a 4x4 array of CsI crystals, each coupled to a Photo-multiplier tube.

This telescope was used for the detection of ^{6}He. The telescopes allowed for the detection of the position as well as particle identification with the use of ΔE-E spectra. A schematic of the experimental setup is presented in Figure 1. The experimental setup allowed for a complete kinematical reconstruction of the studied process.
The elastic scattering was identified by means of simultaneous detection of ^{6}He ions and protons. ^{6}He ions were identified with the use of ΔE-E spectra. At low scattering angles the proton energy was insufficient to identify the particle with the use of ΔE-E spectra. Instead, a locus of the relation between the laboratory angles of the ions was used for reaction identification. The reconstructed laboratory angle of the scattered protons was used to calculate of the CM angle. A monte Carlo simulation of the experiment was performed within the GEANT4 framework[2]. This allowed for detection efficiency calculation and error estimation. The elastic scattering differential section obtained is presented in Figure 2.

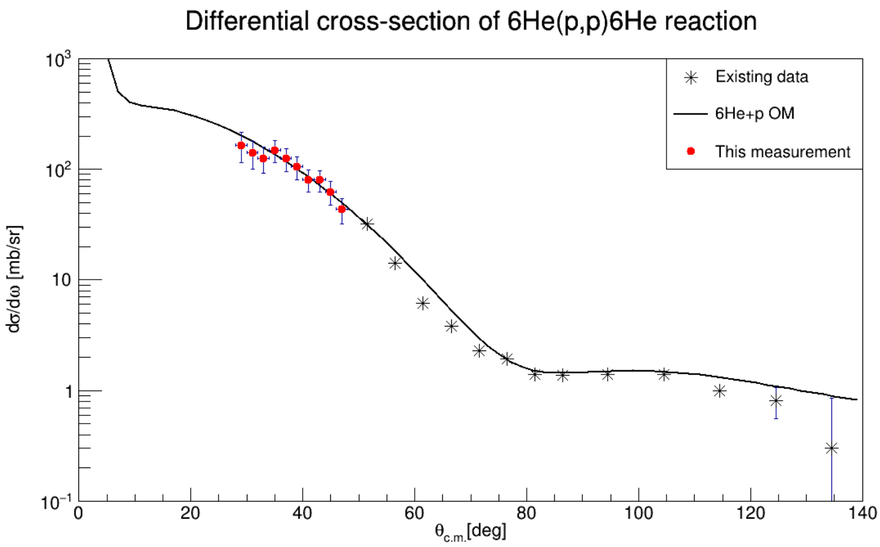

Figure 2: Differential cross-section for ^{6}He + p elastic scattering at E(CM)=22MeV. The newly acquired data set is in good agreement with the data collected previously [3] and with optical model predictions.

The obtained data set is in good agreement with optical model predictions and the cross sections measured previously by Wolski et al. [3] at the same energy. The same experimental setup was later used to measure the ^{6}He + ^{2}H elastic scattering cross section.

Bibliography

[1] A.S. Fomichev *et al.*, Eur. Phys. J. **A54** (2018) 97.
[2] S. Agostinelli *et al.*, Nucl. Inst. and Meth. **A506** (2003) 250-303.
[3] R. Wolski *et al.*, Phys. Lett. **B467** (1999) 8-14.

C.9 Collective bands in ^{128}Xe as seen from the 'beyond mean field' perspective

L. Próchniak
Heavy Ion Laboratory, University of Warsaw, Warszawa, Poland

I present here theoretical results concerning positive parity collective bands in ^{128}Xe. Properties of the collective bands are described within the general Bohr Hamiltonian model where all quadrupole degrees of freedom are treated on an equal footing. The potential energy and six inertial functions (also called mass parameters) are calculated from the microscopic mean field theory using the Adiabatic Time Dependent HFB approach, hence the phrase 'beyond mean field' in the title. The general theory is covered in detail in [5], while a specific application to even-even Xe isotopes is presented in [6]. This latter paper contains a general look at the evolution of spectroscopic properties in a long chain of $^{114\text{-}144}$Xe isotopes. Herein I treat the quadrupole collectivity of ^{128}Xe in a more detailed way showing results based on the UNEDF0 version of the mean field.

Collective levels dominate in the low-energy spectrum of ^{128}Xe but due to a small number of valence protons other degrees of freedom can also influence excited states, e.g. the 0^+ level at 1877 keV is strongly excited in a two-proton transfer reaction [7] which suggests a possible connection with the so-called pairing vibrations. As can be seen in [6], the applied theoretical methods work better for isotopes not very close to the semimagic ^{136}Xe, so a proper description of ^{128}Xe is still a challenge to the theory.

A plot of the collective potential energy is shown in Fig. 1. The potential energy weakly depends on the γ variable having a shallow minimum close to the prolate axis with a β deformation around 0.15. It is interesting that even when the potential resembles qualitatively that of the harmonic oscillator and in the theoretical spectrum (Fig. 3) one can easily see multi-phonon patterns, the electromagnetic properties deviate from the harmonic oscillator. As an example I show in Fig. 3 diagonal matrix elements of the E2 operator, the values of which differ substantially from 0, expected for the oscillator.

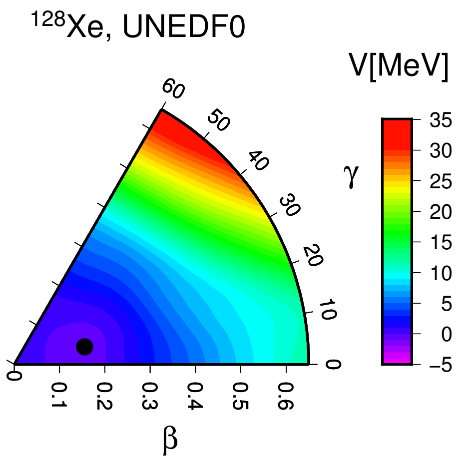

Figure 1: Theoretical collective potential energy.

The experimental and theoretical spectrum of the ^{128}Xe nucleus is shown in Figs. 2 and 3, respectively. One may note a rather good agreement between experiment and theory, especially if one takes into account that no theoretical parameters have been fitted to the spectroscopic properties of the isotope considered. The existence of several low spin levels not included in the four lowest bands (labelled as extra levels in Fig. 3) suggests that the calculated energy is too soft against the β deformation. Another mean field version (the SLy4 Skyrme interaction) gives a more rigid shape [6] but the overall agreement with the experimental data is worse.

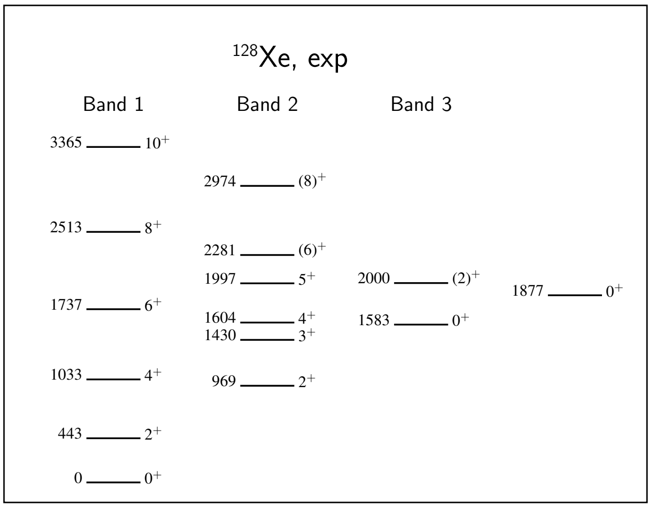

Figure 2: Partial experimental spectrum of ^{128}Xe, i.e. collective positive parity bands plus the 0^+ level at 1877 keV, see text.

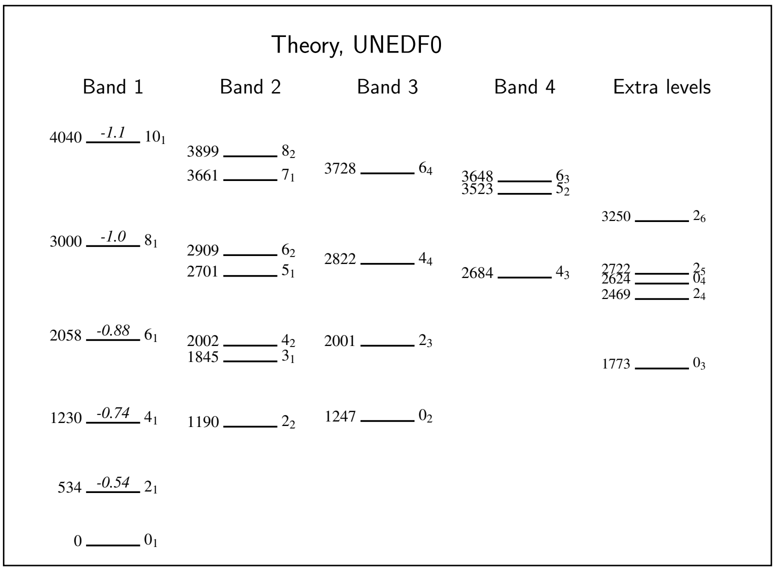

Figure 3: Theoretical spectrum of ^{128}Xe. Levels not included in bands are labelled as 'Extra'. Value of the diagonal element of the $E2$ operator for Band 1 (g.s.) levels are shown above each level.

Table 1 contains experimental and calculated values of the $E2$ reduced transition probabilities. I include here data from two experimental papers [1, 2] and from two evaluations [3, 4] to show that for some transitions the experimental results differ significantly.

Unfortunately there is no experimental information on the spectroscopic moments of the excited levels in ^{128}Xe. Again, one may note quite good agreement between theory and experiment. However, a marked discrepancy is seen for the $0_2 \to 2_2$ and $0_2 \to 2_1$ transitions. The too small value of $B(E2)$ for the $2_1 \to 0_1$ transition is an additional hint that the predicted shape of ^{128}Xe is too soft against the β deformation. Another interesting case is the $10_1 \to 8_1$ transition. The much smaller value given in the recent evaluation [4] in comparison with Ref. [1] suggests a possible loss of collectivity in the g.s. band at spin 10.

J_i	E_i	J_f	E_f	Exp [1]	Exp [2]	Eva [3]	Eva [4]	Th, UNEDF0
2_1	442.9	0_1	0.0	47 (5)	42.6 (64)	40.2 (21)	48 (10)	31.8
2_2	969.5	2_1	442.9	49 (5)	50.1 (97)	48 (5)	57 (4)	41.6
2_2	969.5	0_1	0.0	0.63 (5)	0.65 (8)	0.64 (6)	0.76 (5)	0.35
4_1	1033.1	2_1	442.9	60 (6)	63.5 (52)	59 (5)	62 (3)	57.0
3_1	1429.6	4_1	1033.1		31.8 (59)		72 (10)	17.9
3_1	1429.6	2_2	969.5		91 (16)		210 (30)	53.2
3_1	1429.6	2_1	442.9		1.45 (26)		3.3 (5)	0.75
0_2	1583.0	2_2	969.5		52.8 (76)			4.6
0_2	1583.0	2_1	442.9		3.69 (58)			39.4
4_2	1603.5	4_1	1033.1	30 (3)	30.2 (32)		28 (3)	26.4
4_2	1603.5	2_2	969.5	31 (5)	29.6 (29)		27.7 (18)	36.6
4_2	1603.5	2_1	442.9	0.52 (4)	0.52 (6)			0.01
6_1	1737.3	4_1	1033.1	79 (7)	106 (13)	78 (7)	61 (3)	77.4
0_3	1877.3	2_2	969.5		22.2 (46)			12.3
0_3	1877.3	2_1	442.9		10.4 (23)		11 (3)	0.04
2_3	1999.6	2_1	442.9		0.035(54)		0.05 (8)	0.3
8_1	2512.9	6_1	1737.3	97 (10)			95 (11)	96.0
10_1	3364.6	8_1	2512.9	110 (31)			37 (13)	114.0
6_2	2280.9	4_2	1603.5	97 (10)				62.7
6_2	2280.9	6_1	1737.3	8 (5)				21.9
6_2	2280.9	4_1	1033.1	3 (1)				0.02
4_1	1033.1	2_2	969.5	4 (1)				0.1

Table 1: Theoretical and experimental $B(E2)$ values for ^{128}Xe. Spins and energies in columns 1-4 are from experiment [4]. Subscripts in columns 1 and 3 number states of a given spin in the theoretical spectrum, see Fig. 3.

Bibliography

[1] J. Srebrny, T. Czosnyka, W. Karczmarczyk, P. Napiorkowski et al., Nucl. Phys. A **557** (1993) 663c
[2] L. Coquard, N. Pietralla, T. Ahn, G. Rainovski et al., Phys. Rev. C **80** (2009) 061304
[3] M. Kanbe and K. Kitao, Nucl. Data Sheets **94** (2001) 227
[4] Z. Elekes and J. Timar, Nucl. Data Sheets **129** (2015) 191
[5] L. Próchniak, S.G. Rohoziński, J. Phys. G: Nucl. Phys. **36** (2009) 123101
[6] L. Próchniak, Physica Scripta **90** (2015) 114005
[7] W.P. Alford, R.E. Anderson, P.A. Batay-Csorba, R.A. Emigh et al., Nucl. Phys. A **323** (1979) 339

C.10 Comparison of Coulomb breakup effects on the elastic scattering of ^{6}He and ^{8}He using a Coulomb dipole polarization potential

H.M. Maridi[1], K. Rusek[1], N. Keeley[2]

1) Heavy Ion Laboratory, University of Warsaw, Warszawa, Poland

2) National Centre for Nuclear Research

A recent new expression for the Coulomb dipole polarization potential (CDPP) [1] was applied to different cluster structures of ^{6}He and ^{8}He. The CDPPs were used to compare the effect of breakup coupling on the elastic scattering of these projectiles from a ^{208}Pb target at incident energies of 14 and 16 MeV, below the Coulomb barrier. None of the cluster structures investigated for ^{8}He gave a significant CDPP, supporting previous inferences that the breakup coupling is much less important for ^{8}He than for ^{6}He at energies close to the Coulomb barrier, despite the significantly larger absorption observed in the measured ^{8}He elastic scattering at 16 MeV compared to that for ^{6}He. Coupled reaction channels calculations of the one-neutron stripping reaction indicate a much enhanced role for this reaction in the elastic scattering of ^{8}He compared to ^{6}He, alone sufficient to account for the observed significant deviation from Rutherford scattering for ^{8}He+^{208}Pb elastic scattering even at this sub-barrier energy (Figure 1).

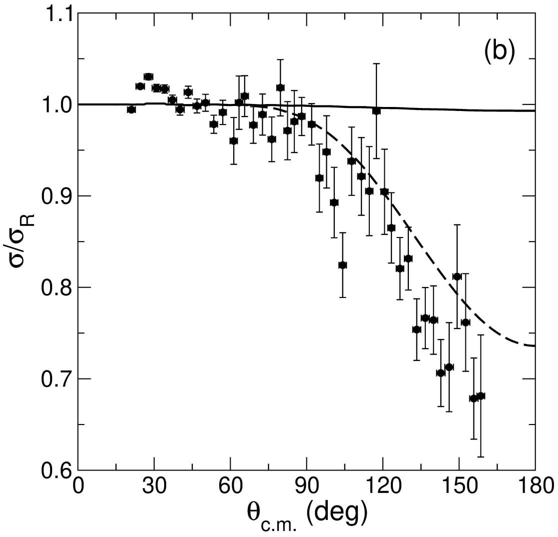

Figure 1: Angular distribution for elastic scattering of ^{8}He+^{208}Pb at 16 MeV compared to the results of calculations (solid curve - CDPP only included, dashed curve - CDPP plus one-neutron stripping).

This work was funded by the Polish National Agency for Academic Exchange (NAWA) within the Ulam Programme under grant agreement No. PPN/ULM/2019/1/00189/U/00001.

Bibliography

[1] H.M. Maridi, K. Rusek, N. Keeley, Phys. Rev. C **104**, 024614 (2021).

Part D
Appendices

D.1 List of experiments performed at HIL in 2021

A list of the experiments performed in 2021 is presented in the following pages. The following acronyms of institution names are used in the list:

- HIL — Heavy Ion Laboratory, University of Warsaw, Warszawa, Poland;
- CEA Saclay — IRFU/SPhN, CEA Saclay, Gif-sur-Yvette, France;
- FP UW — Faculty of Physics, University of Warsaw, Warszawa, Poland;
- IKP TU Darmstadt — IKP, Technical University Darmstadt, Darmstadt, Germany;
- INP Kraków — The H. Niewodniczański Institute of Nuclear Physics PAN, Kraków, Poland;
- IP JKU Kielce — Institute of Physics, Jan Kochanowski University, Kielce, Poland;
- JINR — Joint Institute for Nuclear Research, Dubna, Russia;
- NCNR Świerk — National Centre for Nuclear Research, Otwock, Poland
- ORNL — ORTEC, Oak Ridge, Tennessee, USA;
- PW — Warsaw University of Technology, Warszawa, Poland;
- SOPh Atlanta — School of Physics, Georgia Institute of Technology, Atlanta, GA, USA;
- U. Guelph — University of Guelph, Ontario, Canada;
- UF INFN Florence —University of Florence, INFN Sezione di Firenze, Italy;
- U. Kentucky — Department of Chemistry, University of Kentucky, Lexington, KY, USA;
- U. Sofia— Sofia University "St. Kliment Ohridski", Sofia, Bulgaria
- US Surrey — Department of Physics, University of Surrey, Guildford, UK;

For each experiment the following information is provided: ion, energy, setup/beam line information, date, proposal number, subject, spokespersons and institutions.

^{14}N — 35 MeV — EAGLE 10.05 – 14.01
HIL094 — Electromagnetic structure of low-lying states in 110Cd - complementary Coulomb excitation measurements with a 14N beam (K.Wrzosek-Lipska)
HIL, U. Guelph, ORNL, CEA Saclay, US Surrey, UF INFN Florence, INP Kraków, U. Kentucky, SOPh Atlanta

^{12}C — 40 MeV — Exposure station 17.05 - 21.05
HIL — Studies of the radiation defects in the Cu and Ag foils, and in the semiconductor detectors irradiated with 12C beam of 40 MeV energy (K. Krutul)
HIL, INP Kraków, JINR

^{12}C^{2+} — 45 MeV — Radiobiology 28.06 - 02.07
HIL — Study of the biological response of the glioblastoma cell lines and investigations of mechanisms of radiochromic response in gel dosimeters to ionizing radiation with high LET (U. Kaźmierczak)
HIL, FP UW, IP JKU Kielce, PW, NCNR Świerk

^{32}S — 144 MeV — EAGLE 29.11 - 10.12
HIL088 — Collective Isovector Quadrupole Excitation in 142Sm – Identification via a $\gamma\gamma$-Correlation Measurement after $\varepsilon/\beta+$-Decay (R. Kern)
GIKP TU Darmstadt, U. Sofia, HIL

D.2 Degrees and theses completed in 2021 or in progress

D.2.1 PhD theses of students affiliated to HIL, of HIL staff members, and supervised by HIL staff

Michalina Komorowska, Faculty of Physics, University of Warsaw
Korelacje oktupolowe w jądrach atomowych z obszaru $N \sim 88$
Pear-shaped Nuclei in the $N \sim 88$ *region*
Supervisors: dr hab. L. Próchniak, dr P. Napiorkowski, dr W. Korten, dr M. Zielińska. (program cotutelle) Expected completion time: 2022.

Łukasz Standyło, National Centre for Nuclear Research, Świerk
Badanie mechanizmu wychwytu i termalizacji strumieni jonów i atomów wprowadzonych do plazmy wytwarzanej metodą elektronowego rezonansu cyklotronowego
Investigation of capture and thermalization mechanisms of ions and atomic beams injected into plasma produced by the electron cyclotron resonance
Supervisor: prof. dr hab. K. Rusek, dr K. Sudlitz. Expected completion time: 2022.

Mateusz Filipek, Faculty of Physics, University of Warsaw
Badanie przeżywalności komórek DU-145 poddanych działaniu promieniowania alfa, ze źródła płaskiego Am-241
Studies of DU-145 cell survival after irradiation with alpha particles from a flat Am-241 source
Supervisors: dr hab. Z. Szefliński. Expected completion time: 2023.

Marcin Pietrzak, Faculty of Physics, University of Warsaw
Nanodosimeric characteristics of a carbon ion beam - experiments and monte Carlo simulations
Supervisor: dr hab. Z. Szefliński. Expected completion time: 2023.

Olga Saeed Mohamed Nassar, Faculty of Physics, Warsaw University of Technology
Optyka jonowa w centrum cyklotronu U-200P
Ion trajectories in the central region of the U-200P cyclotron
Supervisors: dr hab. M. Palacz, dr I. Ivanenko. Expected completion time: 2024.

Bogumił Zalewski, Faculty of Physics, University of Warsaw
Badanie oddziaływania ^{6}***He+d***
Study of the ^{6}*He+d interaction*
Supervisor: prof. dr hab. K. Rusek. Expected completion time: 2024.

D.2.2 Other PhD theses based on experiments performed at HIL

Daniel Andrzej Piętak, Faculty of Electronics and Information Technology, Warsaw University of Technology
Metoda oceny jakości wyników z eksperymentów wzbudzeń kulombowskich z wykorzystaniem algorytmu genetycznego
Evaluation method based on a genetic algorithm for results of Coulomb excitation experiments
Supervisors: dr hab. inż. P. Bilski. Thesis completed in September 2021.

Feruzjon Ergashev, Institute of Nuclear Physics, Academy of Sciences of the Republic of Uzbekistan, Tashkent, Uzbekistan
Study of nucleon transfer reactions in the $^{10}B+^{16}O$ interaction at energies near the Coulomb barrier for nuclear astrophysics
Supervisors: prof. S. Artemov. Expected completion time: 2022.

Gani Yergaliuly, L.N. Gumilyov Eurasian National University, Astana, Kazakhstan
Research into the mechanisms of the elastic scattering of accelerated ions of ^{15}N and ^{13}C with a ^{9}Be nucleus at low energies
Supervisors: asociated. prof. Amangeldi Nurlan. Expected completion time 2022.

Oleksandr Chepurnov, Institute for Nuclear Research, National Academy of Sciences of Ukraine
Nuclear reactions in the interaction of ^{15}N and ^{10}B ions with ^{6}Li nuclei
Supervisor: prof. A.T. Rudchik. Expected completion time: 2023.

Oleksandr Kutsyk, Institute for Nuclear Research, National Academy of Sciences of Ukraine
Nuclear reactions in the interaction of ^{15}N ions with ^{12}C and ^{13}C nuclei
Supervisor: prof. A.T. Rudchik. Expected completion time: 2023.

Maria Pęgier, Faculty of Chemistry, University of Warsaw
Macrocyclic compounds labeled with metallic isotopes for application in positron emission tomography
Supervisors: prof. dr hab. K. Pyrzyńska, dr hab. K. Kilian. Expected completion time: 2024.

Auganbek Sabidolda, Al-Farabi Kazakh National University, Almaty, Kazakhstan
Study of nucleon transfer reactions in the $^{10}B+^{12}C$ interaction at energies near the Coulomb barrier for nuclear astrophysics
Supervisors: prof. N. Burtebayev. Expected completion time: 2024.

D.2.3 MSc and BSc theses supervised by HIL staff members

Michał Smolarek, Jakub Krauz, Jakub Łaguna, Krzysztof Witczyński, Faculty of Mathematics, Informatics and Mechanics, University of Warsaw
System sterowania warszawskim cyklotronem
Control system for the Warsaw Cyclotron
Supervisors: mgr G. Grudziński, mgr inż. J. Miszczak. Thesis completed in July 2021

Jakub Gotlib, Faculty of Physics, University of Warsaw
Application of silicon position-sensitive detector in nanodosimetric studies
Supervisor: dr hab. Z. Szefliński. Thesis completed in Sepember 2021

Kinga Kitlińska, Faculty of Chemistry, University of Warsaw
Extraction of selenium species from samples of various matrices
Supervisors: prof. dr hab. K. Pyrzyńska, dr A. Sentkowska. Thesis completed in Ocober 2021

Klaudia Koszel, Faculty of Physics, University of Warsaw
Kontrola jakosci radiofarmaceutyku 18FHBG
Quality control of the 18FHBG radiopharmaceutical
Supervisor: dr hab. K. Kilian. Thesis completed in November 2021

Ewa Kulis, Faculty of Physics, University of Warsaw
Dozymetria promieniowania alfa płaskiego źródła 241-Am i odpowiedź komórkowa na jego działanie
Flat 241-Am alpha source dosimetry and the cellular response to this radiation
Supervisors: dr B. Brzozowska, dr U. Kaźmierczak. Thesis completed in December 2021

Natalia Grabińska, Faculty of Chemistry, University of Warsaw
Przeżywalność komórek nowotworowych napromienianych cząstkami alfa ze źródła 241Am
Cancer cell survival after irradiation with 241Am alpha particles
Supervisor: dr hab. A. Korgul. Thesis completed in December 2021

Krzysztof Domański, Faculty of Physics, University of Warsaw
Zastosowanie uczenia maszynowego do automatycznej analizy testu klonogennego przeprowadzonego na komórkach ssaków
Application of machine learning to automatic clonogenic test analysis of mammal cells
Supervisors: dr hab. Z. Szefliński, dr U. Kaźmierczak. Expected completion time: 2022.

Klaudia Koszel, Faculty of Physics, University of Warsaw
Wytwarzanie i kontrola jakości amoniaku znakowanego izotopem 13N
Production and quality control of ammonia tagged with 13N
Supervisor: dr hab. K. Kilian. Expected completion time: 2022.

Justyna Sykuła, Faculty of Physics, University of Warsaw
Badanie zanieczyszczeń radionuklidowych w procesie produkcji radiofarmaceutyków znakowanych 18F
Investigation of radionuclide impurities in 18F tagged radiopharmaceutical production
Supervisor: dr hab. K. Kilian. Expected completion time: 2022.

Łukasz Łysakowski, Faculty of Physics, University of Warsaw
Badanie korelacji kątowych kwantów γ ***pochodzących z rozpadu*** $^{152}\boldsymbol{Eu}$
Study research of angular correlations of gamma radiation from the radioactive decay of Eu-152
Supervisors: dr J. Samorajczyk-Pyśk, dr G. Jaworski. Expected completion time: 2022.

D.3 Publications

D.3.1 Publications in Web of Knowledge and/or Scopus data bases

J.C. Batchelder, C. Apgar, N.T. Brewer, C.J. Gross, R.K. Grzywacz, S. Ilyushkin, M. Madurga, K. Miernik, S.W. Padgett, S.V. Paulauskas, W.A. Peters, B.C. Rasco, K.P. Rykaczewski, D.W. Stracener, J.A. Winger, M. Wolińska-Cichocka, E.F. Zganjar, D.W. Bardayan, M.E. Howard, B. Manning, M. Matos, A.J. Mendez, D. Miller, A. Ratkiewicz, and E.H. Wang *Levels in ^{125}Cd populated by the β decay of ^{125m}Ag and ^{125}Ag* Phys. Rev. C **104**, 024308(2021).

A. Camaiani, G. Casini, S. Piantelli, A. Ono, E. Bonnet, R. Alba, S. Barlini, B. Borderie, R. Bougault, C. Ciampi, A. Chbihi, M. Cicerchia, M. Cinausero, J.A. Dueñas, D. DellAquila, Q. Fable, D. Fabris, C. Frosin, J.D. Frankland, F. Gramegna, D. Gruyer, K. I. Hahn, M. Henri, B. Hong, S. Kim, A. Kordyasz, M.J. Kweon, H.J. Lee, J. Lemarie, N. LeNeindre, I. Lombardo, O. Lopez, T. Marchi, S.H. Nam, P. Ottanelli, M. Parlog, G. Pasquali, G. Poggi, J. Quicray, A.A. Stefanini, S. Upadhyaya, S. Valdre, E. Vient *Isospin diffusion measurement from the direct detection of a Quasi-Projectile remnant* Phys. Rev. C **103**, 014605(2021).

S. Capra, S. Ziliani, A.Goasduff, S. Leoni, B. Fornal, D. Mengoni, G. Benzoni, I. Zanon, A. Compagnucci, M. Luciani, J. Skowronski, D. Brugnara, N. Cieplicka-Oryńczak, G. Colucci, M.L. Cortes, G. Gosta, A. Gottardo, K. Hadyńska-Klęk, G. Pasqualato, F. Recchia, M. Siliciano, J.J. Valiente-Dobón and A. Pullia. *First in-beam test of GALTRACE innovative silicon detector array* Nuovo Cimento C **44**, 34(2021).

J. Choiński, K. Kilian, P.J. Napiorkowski, M. Pęgier, A. Sentkowska, A. Stolarz, A. Trzcińska. *Radiopharmaceuticals Production and Research Center at Heavy Ion Laboratory of University of Warsaw* Acta Physica Polonica A **139**, 413(2021).

M. Ciemała, S. Ziliani, F.C.L. Crespi, S. Leoni, B. Fornal, A. Maj, P. Bednarczyk, G. Benzoni, A. Bracco, C. Boiano, S. Bottoni, S. Brambilla, M. Bast, M. Beckers, T. Braunroth, F. Camera, N. Cieplicka-Oryńczak, E. Clement, S. Coelli, O. Dorvaux, S. Erturk, G. De France, C. Fransen, A. Goldkuhle, J. Grębosz, M.N. Harak, L.W. Iskra, B. Jacquot, A. Karpov, M. Kicińska-Habior, Y.H. Kim, M. Kmiecik, A. Lemasson, S.M. Lenzi, M. Lewitowicz, H. Li, I. Matea, K. Mazurek, C. Michelagnoli, M. Matejska-Minda, B. Million, C. Muller-Gatermann, V. Nanal, P. Napiorkowski, D.R. Napoli, R. Palit, M. Rejmund, Ch. Schmitt, M. Stanoiu, I. Stefan, E. Vardaci, B. Wasilewska, O. Wieland, M. Zięblinski and M. Zielińska *Accessing tens-to-hundreds femtoseconds nuclear state lifetimes with low-energy binary heavy-ion reactions* Eur. Phys. J. A **57**, 156(2021).

B. Ding, C.M. Petrache, S. Guo, E.A. Lawrie, I. Wakudyanaye, Z.H. Zhang, H.L. Wang, H.Y. Meng, D. Mengoni, Y.H. Qiang, J.G. Wang, C. Andreoiu, A. Astier, A. Avaa, T. Bäck, R.A. Bark, D. Bazzacco, A. Boso, T.D. Bucher, B. Cederwall, M.V. Chisapi, H.L. Fan, F. Galtarossa, F.H. Garcia, A. Goasduff, G. Jaworski, P. Jones, I. Kuti, J.J. Lawrie, G.S. Li, R. Li, M.L. Liu, Z. Liu, B. Lomberg, B.F. Lv, T. Marchlewski, L. Mdletshe, L. Msebi, S.H. Mthembu, D.R. Napoli, A. Netshiya, M.F. Nkalanga, J.N. Orce, K. Ortner, F. Recchia, S. Riccetto, A. Rohilla, T.W. Seakamela, M. Siciliano, M.A. Sithole, D. Sohler, J. Srebrny, D. Testov, A. Tucholski, J.J. Valiente-Dobón, F. Wentzel, K. Whitmore, Y.H.

Zhang, K.K. Zheng, X.H. Zhou, and B.R. Zikhali. *Signature splitting of the* $g7/2[404]7/2^{+}$ *bands in* ^{131}*Ba and* ^{133}*Ce* Phys. Rev. C **104**, 064304(2021).

L. De Dominicis, F. Barbaro, L. Canton, M.P. Carante, A. Colombi, A. Fontana, L. Mou, G. Pupillo, A. Stolarz and P.J. Napiorkowski *Production of* ^{117}*Sn in nat.Cd and nat.In targets with an* α*-beam* IL NUOVO CIMENTO C **44**, 129 (2021).

J. Dobaczewski, P. Baczyk, P. Becker, M. Bender, K. Bennaceur, J. Bonnard, Y. Gao, A. Idini, M. Konieczka, M. Kortelainen, L. Próchniak, A.M. Romero, W. Satuła, Y. Shi, T.R. Werner, L.F. Yu. *Solution of universal nonrelativistic nuclear DFT equations in the Cartesian deformed harmonic-oscillator basis. (IX) HFODD (v3.06h): a new version of the program* Journal of Physics G **48**, 102001(2021).

X. Fabian, G. Baulieu, L. Ducroux, O. Stezowski, A. Boujrad, E. Clément, S. Coudert, G. de France, N. Erduran, S. Ertürk, V. González, G. Jaworski, J. Nyberg, D. Ralet, E. Sanchis, R. Wadsworth *Artificial neural networks for neutron/*γ *discrimination in the neutron detectors of NEDA* Nucl. Inst. and Meth. A **986**, 164750(2021).

A. Goasduff, D. Mengoni, F. Recchia, J.J. Valiente-Dobón, R. Menegazzo, G. Benzoni, D. Barrientos, M. Bellato, N. Bez, M. Biasotto, N. Blasi, C. Boiano, A. Boso, S. Bottoni, A. Braccod, S. Brambill, D. Brugnara, F. Camera, S. Capra, A. Capsoni, P. Cocconi, S. Coelli, M.L .Cortes, F.C.L. Crespi, G .de Angelis, F.J. Egea, C. Fanin, S. Fantinel, A. Gadea, E.R. Gamba, A. Gambalonga, C. Gesmundo, G. Gostad, A. Gottardo, A. Gozzelino, E. T. Gregor, M. Gulmini, J. Hab, K. Hadyńska-Klęk, A. Illana, R. Isocrate, G. Jaworski, P.R. John, S.M. Lenzi, S. Leoni, S. Lunardi, M. Magalini, N. Marchini, B. Million, V. Modamio, A. Nannini, D.R. Napoli, G. Pasqualato, J. Pellumaj, R.M. Perez-Vidal, S. Pigliapoco, M. Polettini, C. Porzio, A. Pullia, L. Ramina, G. Rampazzo, M. Rampazzo, M. Rebeschini, K. Rezynkina, M. Rocchinil, M. Romanato, D. Rosso, A. Saltarelli, M. Scarcioffolo, M. Siciliano, D.A. Testov, D. Tomasell, F. Tomasi, N. Toniolo, C.A .Ur, S. Ventura, F. Veronese, E. Viscione, V. Volpe, O. Wieland, I. Zanon, S. Ziliani, G. Zhang, D. Bazzacco *The GALILEO* γ*-ray array at the Legnaro National Laboratories* Nucl. Inst. and Meth. A **1015**, 165753(2021).

G. Gosta, A. Mentana, F. Camera, A. Bracco, S. Ceruti, G. Benzoni, N. Blasi, S. Brambilla, S. Capra, F.C.L. Crespi, A. Giaz, S. Leoni, B. Million, S. Riboldi, C. Porzio, S. Ziliani, O. Wieland, A. Nannini, M. Rocchini, N. Marchini, M. Ciemała, M. Kmiecik, A. Maj, B. Wasilewska, M. Zięblinski, D. Filipescu, J. Kaur, N. Marginean, S. Pascu, T. Glodariu, D. Ghita, V. Zamfir, J.J. Valiente-Dobón, G. de Angelis, F. Galtarossa, A. Goasduff, T. Bayram, A. Gadea, A. Montaner, I. Zanon, D. Brugnara, A. Gozzelino, G. Pasqualato, R. Menegazzo, A. Gottardo, G. Jaworski, S. Lenzi, D. Napoli, D. Testov, M. Siciliano, T. Marchi, D. Mengoni, D. Bazzacco, A. Boso, P.R. John, F. Recchia, R. Raabe, O. Poleshchuk, and J. Yang *Probing isospin mixing with the giant dipole resonance in the* ^{60}*Zn compound nucleus* Phys. Rev. C **103**, L041302(2021).

O. Hall, T. Davinson, A. Estrade, J. Liu, G. Lorusso, F. Montes, S. Nishimura, V.H. Phong, P.J. Woods, J. Agramunti, D.S. Ahn, A. Algora, J.M. Allmond, H. Baba, S. Bae, N.T. Brewer, C.G. Bruno, R. Caballero-Folch, F. Calvino, P.J. Coleman-Smith, G. Cortes, I. Dillmann, C. Domingo-Pardo, A. Fijałkowska, N. Fukuda, S. Go, C.J. Griffin, R. Grzywacz, J. Ha, L.J. Harkness-Brennan, T. Isobe, D. Kahl, L.H. Khiem, G.G. Kiss, A. Korgul, S. Kubono, M. Labiche, I. Lazarus, J. Liang, Z. Liu, K. Matsui, K.

Miernik, B. Moon, A.I. Morales, P. Morrall, M.R. Mumpower, N. Nepal, R.D. Page, M. Piersa, V.F.E. Pucknell, B.C. Rasco, B. Rubio, K.P. Rykaczewski, H. Sakurai, Y. Shimizu, D.W. Stracener, T. Sumikama, H. Suzuki, J.L Tain, H. Takeda, A. Tarifeno-Saldivia, A. Tolosa-Delgado, M. Wolińska-Cichocka & R. Yokoyama, *β-delayed neutron emission of r-process nuclei at the N=82 shell closure* Phys. Lett. B **816**, 136266 (2021).

N. Keeley, K.W. Kemper, K. Rusek *Influence of halo single-neutron transfer on near barrier ^{15}C + ^{12}C total fusion* Eur. Phys. J. A **57**, 168(2021)

A.R.L. Kennington, G. Lotay, D.T. Doherty, D. Seweryniak, C. Andreoiu, K. Auranen, M.P. Carpenter, W.N. Catford, C.M. Deibel, K. Hadyńska-Klęk, S. Hallam, D. Hoff, T. Huang, R.V.F. Janssens, S. Jazrawi, J. José, F.G. Kondev, T. Lauritsen, J. Li, A.M. Rogers, J. Saiz, G. Savard, S. Stolze, G.L. Wilson, and S. Zhu *Level structure of the Tz=-1 nucleus ^{34}Ar and its relevance for nucleosynthesis in ONe novae* Phys. Rev. C **103**, 035805(2021).

A. Kubiela, H. Suzuki, O.B. Tarasov, M. Pfützner, D.S. Ahn, H. Baba, A. Bezbakh, A.A. Ciemny, W. Dominik, N. Fukuda, A. Giska, R. Grzywacz, Y. Ichikawa, Z. Janas, Ł. Janiak, G. Kamiński, K. Kawata, T. Kubo, M. Madurga, C. Mazzocchi, H. Nishibata, M. Pomorski, Y. Shimizu, N. Sokołowska, D. Suzuki, P. Szymkiewicz, A. Świercz, M. Tajima, A. Takamine, H. Takeda, Y. Takeuchi, C.R. Thornsberry, H. Ueno, H. Yamazaki, R. Yokoyama, and K. Yoshida *Production of the most neutron-deficient Zn isotopes by projectile fragmentation of ^{78}Kr* Phys. Rev. C **104**, 064610(2021).

B.F. Lv, C.M. Petrache , E.A. Lawrie, A. Astier, E. Dupont, K.K. Zheng, P. Greenlees, H. Badran, T. Calverley, D.M. Cox, T. Grahn, J. Hilton, R. Julin, S. Juutinen, J. Konki, J. Pakarinen, P. Papadakis, J. Partanen, P. Rahkila, P. Ruotsalainen, M. Sandzelius, J. Saren, C. Scholey, J. Sorri, S. Stolze, J. Uusitalo, B. Cederwall, A. Ertoprak, H. Liu, S. Guo, J.G. Wang, H.J. Ong, X.H. Zhou, Z.Y. Sun, I. Kuti, J. Timár, A. Tucholski, J. Srebrny, and C. Andreoiu *Tilted precession bands in ^{135}Nd* Phys. Rev. C **103**, 044308(2021).

X. Liu, B. Cederwall, C. Qi, R.A. Wyss, O. Aktas, A. Ertoprak, W. Zhang, E. Clement, G. de France, D. Ralet, A. Gadea, A. Goasduff, G. Jaworski, I. Kuti, B.M. Nyako, J. Nyberg, M. Palacz, R. Wadsworth, J.J. Valiente-Dobón, H. Al-Azri, A. Atac Nyberg, T. Back, G. de Angelis, M. Doncel, J. Dudouet, A. Gottardo, M. Jurado, J. Ljungvall, D. Mengoni, D.R. Napoli, C.M. Petrache, D. Sohler, J. Timar, D. Barrientos, P. Bednarczyk, G. Benzoni, B. Birkenbach, A.J. Boston, H.C. Boston, I. Burrows, L. Charles, M. Ciemala, F.C.L. Crespi, D.M. Cullen, P. Desesquelles, C. Domingo-Pardo, J. Eberth, N. Erduran, S. Erturk, V. Gonzalez, J. Goupil, H. Hess, T. Huyuk, A. Jungclaus, W. Korten, A. Lemasson, S. Leoni, A. Maj, R. Menegazzo, B. Million, R.M. Perez-Vidal, Zs. Podolyak, A. Pullia, F. Recchia, P. Reiter, F. Saillant, M.D. Salsac, E. Sanchis, J. Simpson, O. Stezowski, C. Theisen, M. Zielińska *Evidence for enhanced neutron-proton correlations from the level structure of the N=Z+1 nucleus $^{87}_{43}Tc_{44}$* Phys. Rev. C **104**, L021302(2021).

H.M. Maridi, A. Pakou, K. Rusek. *The p+^{9}Be elastic scattering below 30MeV: Optical model analysis and data normalization* Int. J. Mod. Phys. E **30**, 2150024(2021).

H.M. Maridi, K. Rusek, N. Keeley *Coulomb dynamical polarization potential and the electric dipole polarizability for weakly bound and neutron-rich light nuclei* Phys. Rev. C **104**, 024614(2021).

S.Y. Mezhevych, A.T. Rudchik, A.A. Rudchik, K.W. Kemper, K. Rusek, O.A. Ponkratenko, E.I. Koshchy, S.B. Sakuta. *$^{14}C(^{11}B,^{10}B)^{15}C$ REACTION at $E_lab = 45MeV$ AND THE $^{10}B+^{15}C$ OPTICAL POTENTIAL* Acta Phys. Pol. B **52**, 109(2021).

I.A. Muzalevskii, A.A. Bezbakh, E.Yu. Nikolskii, V. Chudoba, S.A. Krupko, S.G. Belogurov, D. Biare, A.S. Fomichev, E.M. Gazeeva, A.V. Gorshkov, L.V. Grigorenko, G. Kamiński, O. Kiselev, D.A. Kostyleva, M.Yu. Kozlov, B. Mauyey, I. Mukha, Yu.L. Parfenova, W. Piątek, A.M. Quynh, V.N. Schetinin, A. Serikov, S.I. Sidorchuk, P.G. Sharov, N.B. Shulgina, R.S. Slepnev, S.V. Stepantsov, A. Świercz, P. Szymkiewicz, G.M. Ter-Akopian, R. Wolski, B. Zalewski, M.V. Zhukov *Resonant states in ^{7}H: Experimental studies of the $^{2}H(^{8}He,^{3}He)$ reaction* Phys. Rev. C **103**, 044313(2021).

M. Paluch-Ferszt, U. Kaźmierczak, Z. Szefliński *Radiation-induced bystander effect research: Literature review* Acta Phys. Pol. A **139**, 266(2021)

M. Pęgier, P. Dróżdż, P. Pomaranski, K. Pyrzyńska *Magnetic hybrid nanoparticles modified with morin for the removal of Sc (III) from aqueous solutions* Molecular Journal **170**, 106683(2021).

S. Piantelli, G. Casini, A. Ono, G. Poggi, G. Pastore, S. Barlini, M. Bini, A. Boiano, E. Bonnet, B. Borderie, R. Bougault, M. Bruno, A. Buccola, A. Camaiani, A. Chbihi, C. Ciampi, M. Cicerchia, M. Cinausero, M. Degerlier, J.A. Dueñas, Q. Fable, D. Fabris, J.D. Frankland, C. Frosin, F. Gramegna, D. Gruyer, A. Kordyasz, T. Kozik, J. Lemarié, N. Le Neindre, I. Lombardo, O. Lopez, G. Mantovani, T. Marchi, M. Henri, L. Morelli, A. Olmi, P. Ottanelli, M. Pârlog, G. Pasquali, J. Quicray, A.A. Stefanini, G. Tortone, S. Upadhyaya, S. Valdre, G. Verde, E. Vient, and M. Vigilante *Isospin transport phenomena for the systems $^{80}Kr + ^{40,48}Ca$ at 35 MeV/nucleon* Phys. Rev. C **103**, 014603(2021).

M. Plodowska, M. Lopez-Riego, P. Akuwudike, D. Sobota, M. Filipek, M. Kłosowski, U. Kaźmierczak, B. Brzozowska, A. Baliga, H. Lisowska, J. Braziewicz, P. Olko, L. Lundholm, A. Wójcik *Small is beautiful: low activity alpha and gamma sources for small-scale radiation protection research experiments* Int. J. Radiat. Biol. **97**, 541(2021)

K. Pyrzyńska, A. Sentkowska. *Selenium in plant foods: speciation analysis, bioavailability, and factors affecting composition* Critical Reviews in Food Science and Nutrition **61**, 1340(2021).

M. Rocchini, K. Hadyńska-Klęk, A. Nannini, A. Goasduff, M. Zielinska, D. Testov, T.R. Rodriguez, A. Gargano, F. Nowacki, G. de Gregorio, H. Naïdja, P. Sona, J.J. Valiente-Dobón, D. Mengoni, P. John, D. Bazzacco, G. Benzoni, A. Boso, P. Cocconi, M. Chiari, D. Doherty, F. Galtarossa, G. Jaworski, M. Komorowska, N. Marchini, M. Matejska-Minda, B. Melon, R. Menegazzo, P. Napiorkowski, D. Napol,i M. Ottanelli, A. Perego, L. Ramina, M. Rampazzo, F. Recchia, S. Riccetto, D. Rosso, M. Siciliano *Onset of triaxial deformation in ^{66}Zn and properties of its first excited 0^{+} state studied by means of Coulomb excitation* Phys. Rev. C **103**, 014311(2021).

M. Rocchini, M. Chiari, E. Pasquali, A. Nannini, K.Hadyńska-Klęk, P. Sona, D. Bazzacco, G. Benzoni, F. Camera, C. Czeluśniak, D.T. Doherty, A. Goasduff, P.R. John, M.Komorowska, N. Marchini, M. Matejska-Minda, B. Melon, D. Mengoni, P.J. Napiorkowski, M. Ottanelli, A. Perego, F. Recchia, M. Siciliano, L. Sottili, D.

Testov, J.J. Valiente-Dobón, K. Wrzosek-Lipska, M. Zielińska, *Applications of Rutherford backscattering analysis methods to nuclear physics experiments* Nucl. Inst. and Meth. B **486**, 68(2021).

A.T. Rudchik, A.A. Rudchile, O.E. Kutsyk, K. Rusek, K.W. Kemper, E. Piasecki, A. Stolarz, A. Trzcińska, W.M. Pirnak, O.A. Ponkratenko, I. Strojek, E.I. Koshchiy, R. Siudak, S.B. Sakuta, S.A. Vozniuk, A.P. Ilyin, Y.M. Stepanenko, V.V. Uleshchenko, Y.O. Shyrma. *ELASTIC AND INELASTIC SCATTERING OF ^{15}N IONS BY ^{13}C NUCLEI AT ENERGY 84 MeV* Nucl. Phys. Atom. Energy **22**, 10(2021).

A.T. Rudchik, A.A. Rudchik, O.O. Chepurnov, K. Rusek, N. Keeley, K.W. Kemper, S. Kliczewski, E. Piasecki, A. Trzcińska, V.M. Pirnak, O.A. Ponkratenko, I. Strojek, E.I. Koshchy, R. Siudak, S.B. Sakuta, A.P. Ilyin, Y.M. Stepanenko, Y.O. Shyrma, V.V. Uleshchenko, K.A. Chercas, H.M. Maridi, N. Burtebayev. *$^{6}Li + ^{15}N$ interaction at $E_c.m. = 23.1 MeV$: Validation of the $\alpha + d$ cluster model of ^{6}Li* Phys. Rev. C **103**, 044614(2021).

K. Rusek, M. Mazzocco, N. Keeley, K.W. Kemper. *Mechanism of the $^{144}Sm(^{7}Li,^{6}Li^{*}_{3+})^{145}Sm$ reaction at 30 MeV* Eur. Phys. J. A **57**, 10(2021).

J. Samorajczyk-Pyśk, Ch. Droste, L. Próchniak, J. Srebrny, S.G. Rohoziński, J. Andrzejewski, S. Dutt, A. Gawlik, K. Hadyńska-Klęk, Ł. Janiak, M. Klintefjord, M. Kowalczyk, J. Kowalska, R. Kumar, T. Marchlewski, P.J. Napiorkowski, J. Perkowski, W. Piątek, M. Piersa-Siłkowska, T. Rogiński, M. Saxena, A. Stolarz, A. Tucholski. *Low-spin levels in ^{140}Sm: Five 0^{+} states and the question of softness against nonaxial deformation* Phys. Rev. C **104**, 024322(2021).

A. Sentkowska. *Content of selenoaminoacids and catechins in Chinese green teas* European food research & technology **247**, 613(2021).

A. Sentkowska, K. Pyrzyńska. *Analytical Problems in Separation of Selenomethionine and Its Oxidative Product in HILIC HPLC* MOLECULES **26**, 5073(2021).

M. Siciliano, J.J. Valiente-Dobón, A. Goasduff, T.R. Rodríguez, D. Bazzacco, G. Benzoni, T. Braunroth, N. Cieplicka-Oryńczak, E. Clément, F.C.L. Crespi, G. de France, M. Doncel, S. Ertürk, C. Fransen, A. Gadea, G. Georgiev, A. Goldkuhle, U. Jakobsson, G. Jaworski, P.R. John, I. Kuti, A. Lemasson, H. Li, A. Lopez-Martens, T. Marchi, D. Mengoni, C. Michelagnoli, T. Mijatović, C. Müller-Gatermann, D.R. Napoli, J. Nyberg, M. Palacz, R.M. Pérez-Vidal, B. Sayği, D. Sohler, S. Szilner, D. Testov *Lifetime Measurements in the Even-Even $^{102\text{-}108}Cd$ Isotopes* Phys. Rev. C **104**, 034320(2021).

M. Stukel, B. C. Rasco, N. T. Brewer, P. C. F. Di Stefano, K. P. Rykaczewski, H. Davis, E. D. Lukosi, L. Hariasz, M. Constable, P. Davis, K. Dering, A. Fijalkowska, Z. Gai, K. C. Goetz, R. K. Grzywacz, J. Kostensalo, J. Ninkovic, P. Lechner, Y. Liu, M. Mancuso, C. L. Melcher, F. Petricca, C. Rouleau, P. Squillari, L. Stand, D. W. Stracener, J. Suhonen, M. Wolińska-Cichocka, I. Yavin *A novel experimental system for the KDK measurement of the ^{40}K decay scheme relevant for rare event searches* Nucl. Inst. and Meth. A **1012**, 165593(2021).

D.A. Testov , S. Bakes, J.J. Valiente-Dobón, A. Goasduff, S. Frauendorf, F. Nowacki, T.R. Rodriguez, G. de Angelis, D. Bazzacco, C. Boiano, A. Boso, B. Cederwall, M. Cicerchia, P.

Colovic, G. Colucci, F. Didierjean, M. Doncel, J.A. Dueñas , F. Galtarossa, A. Gozzelino, K. Hadyńska-Klęk, G. Jaworski, P.R. John, S. Lenzi, H. Liu, S. Lunardi, R. Menegazzo, D. Mengoni, A. Mentana, D.R. Napoli, G. Pasqualato, F. Recchia, S. Riccetto, L.M. Robledo, M. Rocchini, B. Saygi, M. Siciliano, Yu. Sobolev, and S. Szilner *Octupole correlations near ^{110}Te* Phys. Rev. C **103**, 044321(2021).

D.A. Testov, A. Boso, S.M. Lenzi, F. Nowacki, F. Recchia, G. de Angelis, D. Bazzacco, G. Colucci, M. Cottini, F. Galtarossa, A. Goasduff, A. Gozzelino, K. Hadyńska-Klęk, G. Jaworski, P.R. John, S. Lunardi, R. Menegazzo, D. Mengoni, A. Mentana, V. Modamio, A. Nannini, D.R. Napoli, M. Palacz, M. Rocchini, M. Siciliano, and J.J. Valiente-Dobón *High-spin intruder states in the mirror nuclei ^{31}S and ^{31}P* Phys. Rev. C **104**, 024309(2021).

E.H. Wang, J.M. Eldridge, N.T. Brewer, J.H. Hamilton, J.C. Batchelder, Y.X. Liu, Y. Sun, C. Brown, C.J. Zachary, B.M. Musangu, A.V. Ramayya, K.P. Rykaczewski, C.J. Gross, R. Grzywacz, M. Madurga, D. Miller, D.W. Stracener, C. Jost, E.F. Zganjar, J.A. Winger, M. Karny, S.V. Paulauskas, S.H. Liu, M. Wolińska-Cichocka, S.W. Padgett, A.J. Mendez II, K. Miernik, A. Fijałkowska, and S.V. Ilyushkin *Long-lived isomeric states and quasiparticle band structures in neutron-rich $^{162,164}Gd$ nuclei from β decay* Phys. Rev. C **103**, 014317(2021).

S. Ziliani, M. Ciemała, F.C.L. Crespi, S. Leoni, B. Fornal, T. Suzuki, T. Otsuka, A. Maj, P. Bednarczyk, G. Benzoni, A. Bracco, C. Boiano, S. Bottoni, S. Brambilla, M. Bast, M. Beckers, T. Braunroth, F. Camera, N. Cieplicka-Oryńczak, E. Clément, S. Coelli, O. Dorvaux, S. Erturk, G. De France, C. Fransen, A. Goldkuhle, J. Grębosz, M.N. Harakeh, Ł. W. Iskra, B. Jacquot, A. Karpov, M. Kicińska-Habior, Y. Kim, M. Kmiecik, A. Lemasson, M. Lewitowicz, S. Lenzi, H. Li, I. Matea, K. Mazurek, C. Michelagnoli, M. Matejska-Minda, B. Million, C. Muller-Gatermann, V. Nanal, P. Napiorkowski, D.R. Napoli, R. Palit, M. Rejmund, Ch. Schmitt, M. Stanoiu, I. Stefan, E. Vardaci, B. Wasilewska, O. Wieland, M. Zięblinski, M. Zielińska *Complete set of bound negative-parity states in the neutron-rich ^{18}N nucleus* Phys. Rev. C **104**, L041301(2021).

D.4 Seminars

D.4.1 Seminars co-organised by HIL

Warsaw Nuclear Physics Seminar

Seminars organised jointly by the divisions of Nuclear Physics and Nuclear Structure Theory of the Faculty of Physics, University of Warsaw and the Heavy Ion Laboratory, University of Warsaw

C. Michelagnoli — Institut Laue Langevin, Grenoble, France 7 January 2021
Gamma-ray spectroscopy after slow neutron induced reactions: FIPPS I

Y. Kim — Institut Laue Langevin, Grenoble, France 7 January 2021
Future of FIPPS with gas-filled magnet: FIPPS II

L. Próchniak — Heavy Ion Laboratory, University of Warsaw, Warszawa, Poland 14 January 2021
^{140}Sm - wyzwania dla teorii
^{140}Sm - a challenge to theory

P. Napiorkowski — Heavy Ion Laboratory, University of Warsaw, Warszawa, Poland 21 February 2021
Algorytm genetyczny dla fizyków: przykład zastosowania w analizie wzbudzeń kulombowskich
Genetic algorithms for physicists: an example of applications in the analysis of Coulomb excitations

S. Bottoni — University of Milan, Milano, Italy 04 March 2021
Structure of Ca isotopes between doubly closed shells

J. W. Mietelski — The H. Niewodniczański Institute of Nuclear Physics PAN, Kraków, Poland 11 March 2021
Redukcja tła dla detekcji śladowych aktywności sztucznych emiterów promieniowania alfa, beta i gamma w środowisku
Background reduction for the detection of trace activities of artificial alpha, beta and gamma radiation emitters in the environment

H. Maridi — Heavy Ion Laboratory, University of Warsaw, Warszawa, Poland 18 March 2021
Proton elastic scattering from light nuclei at low and intermediate energies using microscopic optical model and the eikonal approximation

M. Pomorski — CENBG, Bordeaux-Gradignan, France 25 March 2021
WISArD - Probing beyond SM with beta delayed protons

M. Sitarz — Aarhus University, Dania 8 April 2021
Badania w Sali Eksperymentalnej w Duńskim Centrum Protonoterapii
Activities in the experimental room at the Danish Centre of Particle Therapy

M. Pfützner — Faculty of Physics, University of Warsaw, Warszawa, Poland 15 April 2021
Oda do fragmentacji pocisku
Ode to projectile fragmentation

S. Wronka — National Centre for Nuclear Research 22 April 2021
Testy zachowania się antymaterii w ziemskim polu grawitacyjnym - eksperyment GBAR
Tests of antimatter behavior in the Earth's gravitational field - the GBAR experiment

A. Kozela — The H. Niewodniczański Institute of Nuclear Physics PAN, Kraków, Poland 29 April 2021
Eksperyment BRAND - na tropie Nowej Fizyki
The BRAND experiment - on the trail of New Physics

M. Biesiada — National Centre for Nuclear Research 6 May 2021
Nowe zastosowania soczewek grawitacyjnych
New applications for gravity lenses

S. Harabasz — IKP, Technical University Darmstadt, Darmstadt, Germany 13 May 2021
Statistical hadronization model for heavy-ion collisions in the few-GeV energy regime

I. Martel — University of Huelva, Huelva, Spain 20 May 2021
Low energy reactions of halo nuclei

K. Sieja — IPHC, Strasbourg, France 27 May 2021
Spectroscopy and shape change in neutron-rich Sr and Zr isotopes

J. Dobaczewski — Department of Physics, University of York, York, UK 10 June 2021
Electromagnetic moments in nuclei within nuclear DFT

J. Wiśniewski — Faculty of Physics, University of Warsaw, Warszawa, Poland 7 October 2021
Rola orbitali typu ekstruder w powstawaniu deformacji
The role of extruder orbitals in deformation

Z. Janas — Faculty of Physics, University of Warsaw, Warszawa, Poland 14 October 2021
Studies of gamma-ray and neutron induced reactions with an active-target Time Projection Chamber

K. Piasecki — Faculty of Physics, University of Warsaw, Warszawa, Poland — 21 October 2021

Co to jest model statystyczny i jak go użyliśmy do opisu reakcji p+p przy 158 GeV/c

What is a statustical model and how we used it to describe the p+p reaction at 158 GeV/c

G. Jaworski — Heavy Ion Laboratory, University of Warsaw, Warszawa, Poland — 28 October 2021

Filtr krotności neutronów NEDA w Warszawie

The NEDA neutron multiplicity filter in Warsaw

H. Albers — GSI Helmholtz Center for Heavy Ion Research, Darmstadt, Germany — 4 November 2021

DESPEC experiments in FAIR Phase-0: from commissioning to early physics

W. Trzaska — Department of Physics, University of Jyväskylä, Finland — 18 November 2021

Dark Matter or Doesn't Matter

J. Srebrny — Heavy Ion Laboratory, University of Warsaw, Warszawa, Poland — 25 November 2021

Podatność na trójosiową deformację kwadrupolową. Modele kolektywne od prostych modeli fenomenologicznych do mikroskopowego Uogólnionego Hamiltonianu Bohra. Seminarium poświęcone pamięci S.G. Rohozińskiego

Quadrupole Triaxiality Softness - collective models. (In Memory of S.G. Rohoziński) From simple phenomenological models to a fully microscopic General Bohr Hamiltonian

C. Schmitt — IPHC, Strasbourg, France — 2 December 2021

New insights into fission from recent experiments. What drives fission across the nuclear chart?

M. Piersa-Siłkowska — Faculty of Physics, University of Warsaw, Warszawa, Poland — 9 December 2021

Rozpad beta bardzo neutronowo-nadmiarowych izotopów indu

β-decay study of very neutron-rich indium isotopes

M. Maćkowiak-Pawłowska — Faculty of Physic, Warsaw University of Technology, Warszawa, Poland — 16 December 2021

News from the NA61/SHINE strong-interactions program

D.4.2 Other seminars organised at HIL

Internal semi-formal HIL seminars

G. Jaworski — Heavy Ion Laboratory, University of Warsaw, Warszawa, Poland 23 June 2021

NEDA w ŚLCJ
NEDA at HIL

D.4.3 External seminars given by HIL staff

A. Sentkowska 22 March 2021
Beetroot juice as a source of selenium, vitamin B and polyphenols
Webinar on Food Science and Obesity, online

J. Choiński 20 May 2021
Możliwości produkcji radioizotopów stosowanych w procedurach teranostycznych
Possibilities of producing radioisotopes used in theranostic procedures
Polish Society of Nuclear Medicine, online

K. Krutul 5 July 2021
The radiation damage of PIN-diode detectors irradiated with heavy ions studied with the positron annihilation spectroscopy
Young Multis 2021 - Multi-scale Phenomena in Condensed Matter - conference for young researchers, online

G. Jaworski 8 July 2021
NEDA @ HIL
NEDA Management Board Meeting, online

K. Hadyńska-Klęk 22 September 2021
The GOSIA Code – Simulation and the data analysis tool
Nuclear structure using gamma-ray spectroscopy – Inter-University Accelerator Centre (IUAC) online school, New Delhi, India

K. Hadyńska-Klęk 22 September 2021
The GOSIA Code – Nuclear shapes from COULEX
Nuclear structure using gamma-ray spectroscopy – Inter-University Accelerator Centre (IUAC) online school, New Delhi, India

K. Wrzosek-Lipska 22 September 2021
GOSIA - a Coulomb excitation data analysis code; theoretical description and approximations used
Nuclear structure using gamma-ray spectroscopy – Inter-University Accelerator Centre (IUAC) online school, New Delhi, India

G. Jaworski 20 October 2021
NEDA @ HIL
NEDA@HIL PrePAC Workshop, Warszawa, Poland

M. Palacz 20 October 2021
Welcome. NEDA - the story and performance of
NEDA@HIL PrePAC Workshop, Warszawa, Poland

G. Jaworski 25 October 2021
NEDA @ HIL
New Trends in Nuclear Physics Detectors, Warszawa, Poland

M. Palacz 11 November 2021
Studies of excited states in ^{102,103}Sn to deduce two-body neutron interactions, single-particle energies and N=Z=50 core excitations
AGATA Collaboration Meeting 2021, Legnaro, Italy

K. Hadyńska-Klęk 8 November 2021
Coulomb excitation of the super-deformed structure in ^{36}Ar
Pre-PAC workshop of AGATA@LNL, Legnaro, Italy

U. Kaźmierczak 1 December 2021
Challenges in radiobiology research with heavy ion beams in Poland
Global Nuclear Physics Innovation, Warszawa, Poland

M. Paluch-Ferszt 1 December 2021
How to test electronics used in the Cosmos?
Nuclear Physics and Innovative Technologies, Warszawa, Poland

P.J. Napiorkowski 2 December 2021
Software development for nuclear physics
Nuclear Physics and Innovative Technologies, Warszawa, Poland

P.J. Napiorkowski 10 December 2021
A "Nuclear microscope" at the Heavy Ion Laboratory
Joint Institute for Nuclear Research, Dubna, Russia, Dubna, Russia

D.4.4 Poster presentations

U. Kaźmierczak, M. Paluch-Ferszt, Z. Szefliński 25 October 2021
Investigation of the biological response of human glioma cell lines after exposure to carbon-ion radiation
New Trends in Nuclear Physics Detectors, Warszawa, Poland

U. Kaźmierczak, M. Paluch-Ferszt, Z. Szefliński 20 September 2021
Investigation of the biological response of human glioma cell lines after exposure to carbon-ion radiation
Second Edition of the Virtual Scientific Conference of the Ochota Campus, online

M. Komorowska, P.J. Napiorkowski 20 September 2021
Study of Octupole Collectivity in ^{146}Nd and ^{148}Sm
Second Edition of the Virtual Scientific Conference of the Ochota Campus, online

K. Krutul, P.J. Napiorkowski, K. Hadyńska-Klęk, K. Wrzosek-Lipska, M. Komorowska, M. Paluch-Ferszt, Z. Szefliński 26 June 2021
Badanie odporności radiacyjnej detektorów typu PIN-dioda na oddziaływanie z ciężkimi jonami
Studies of radiation resistance of PIN-diode detectors to interaction with heavy ions
IX edycja Ogólnopolskiej Konferencji Młodych Naukowców nt. Dokonania naukowe doktorantów IX edycja -Wielka Sesja Posterowa, online

K. Krutul, P.J. Napiorkowski, K. Hadyńska-Klęk, K. Wrzosek-Lipska, M. Komorowska, M. Paluch-Ferszt, Z. Szefliński 20 September 2021
Badanie odporności radiacyjnej detektorów typu PIN-dioda na oddziaływanie z ciężkimi jonami przy wykorzystaniu spektroskopii anihilacji pozytonów
Studies of radiation damage of PIN diode detectors irradiated with heavy ions with positron annihilation spectroscopy
Second Edition of the Virtual Scientific Conference of the Ochota Campus, online

K. Krutul, P.J. Napiorkowski, K. Hadyńska-Klęk, K. Wrzosek-Lipska, M. Komorowska, M. Paluch-Ferszt, Z. Szefliński 25 October 2021
The radiation damage of PIN diode detectors irradiated with heavy ions studied with positron annihilation spectroscopy
New Trends in Nuclear Physics Detectors, Warszawa, Poland

D.4.5 Lectures for students and student laboratories

K. Kilian summer semester of the academic year 2020/2021, 15 hours
Radiofarmaceutyki — synteza, wytwarzanie i zastosowania
Radiopharmaceuticals — synthesis, production and applications
Faculty of Chemistry, University of Warsaw, Warszawa, Poland

K. Kilian winter semester of the academic year 2020/2021, 30 hours
Metody izotopowe i chemia radiofarmaceutyków
Radiochemistry and radiopharmacy
Faculty of Physics, University of Warsaw, Warszawa, Poland

K. Kilian summer semester of the academic year 2020/2021, 60 hours
Pracownia radiofarmaceutyków
Laboratory of Radiopharmaceuticals
Faculty of Physics, University of Warsaw, Warszawa, Poland

K. Kilian winter semester of the academic year 2020/2021, 30 hours
Metody izotopowe i chemia radiofarmaceutyków
Radiochemistry and radiopharmacy
Faculty of Chemistry, University of Warsaw, Warszawa, Poland

Z. Szefliński summer semester of the academic year 2020/2021, 30 hours
Techniki jądrowe w diagnostyce i terapii medycznej
Nuclear Techniques in Medical Diagnostics and Therapy
Faculty of Physics, University of Warsaw, Warszawa, Poland

Z. Szefliński summer semester of the academic year 2020/2021, 45 hours
Pracownia Fizyczna II stopnia
Physics Laboratory for 2nd Level
Faculty of Physics, University of Warsaw, Warszawa, Poland

A. Sentkowska winter semester of the academic year 2020/2021, 45 hours
Analityka środowiska - laboratorium
Environmental Analysis Laboratory
Faculty of Chemistry, University of Warsaw, Warszawa, Poland

A. Sentkowska winter semester of the academic year 2020/2021, 45 hours
Pracownia specjalizacyjna
Specialization Laboratory
Faculty of Chemistry, University of Warsaw, Warszawa, Poland

D.5 Honours and Awards

The Rector of the University of Warsaw awards

In 2021 the following employees of the Heavy Ion Laboratory received the Rector of the University of Warsaw award:

Eliza Balcerowska,
Jarosław Choiński,
Bartosz Kalisiewicz,
Urszula Kaźmierczak,
Marian Kopka,
Wojciech Kozaczka,
Katarzyna Krutul,
Piotr Krysiak,
Ireneusz Mazur,
Jan Miszczak,
Paweł Napiorkowski,
Anna Odziemczyk,
Monika Paluch-Ferszt,
Krzysztof Pietrzak,
Anna Ratyńska,
Justyna Samorajczyk-Pyśk,
Nurullo Sobirov,
Lech Szeląg,
Roman Tańczyk.

D.6 Laboratory staff

Director: Krzysztof Rusek
Deputy director: Paweł Napiorkowski
Director proxy for technical issues: Jarosław Choiński
Financial executive: Eliza Balcerowska

Senior scientists:

Krzysztof Kilian, Andrzej Kordyasz[a], Marcin Palacz, Ernest Piasecki[a], Leszek Próchniak, Krzysztof Rusek, Anna Stolarz, Zygmunt Szefliński[a]

Scientific staff and engineers:

Tomasz Abraham, Andrzej Bednarek, Jarosław Choiński, Giulia Colucci, Przemysław Gmaj, Katarzyna Hadyńska-Klęk,Grzegorz Jaworski, Grzegorz Kamiński[d], Urszula Kaźmierczak, Marian Kopka, Michał Kowalczyk, Katarzyna Krutul,Ireneusz Mazur, Jan Miszczak, Paweł Napiorkowski, Wojciech Okliński[a], Monika Paluch-Ferszt, Mateusz Pęgier, Wojciech Piątek[b], Bogdan Radomyski, Olga Saeed Mohamed Nassar, Justyna Samorajczyk-Pyśk, Aleksandra Sentkowska, Julian Srebrny[a], Łukasz Standyło, Roman Tańczyk, Agnieszka Trzcińska, Andrzej Tucholski, Marzena Wolińska-Cichocka, Katarzyna Wrzosek-Lipska, Bogumił Zalewski

Doctoral candidates:

Michalina Komorowska,

Technicians:

Mariusz Antczak, Tomasz Bracha, Piotr Jasiński, Bartosz Kalisiewicz, Wiesław Kalisiewicz, Robert Kopik, Wojciech Kozaczka, Zbigniew Kruszyński[a], Piotr Krysiak, Krzysztof Łabęda, Kamil Makowski, Mariusz Matuszewski Bogusław Paprzycki, Krzysztof Pietrzak, Łukasz Świątek

Administration and support:

Eliza Balcerowska, Anna Błaszczyk-Duda, Marek Budziszewski [c], Barbara Kowalska[a], Joanna Kowalska, Jolanta Matuszczak, Anna Odziemczyk, Jolanta Ormaniec, Anna Ratyńska, Ewa Sobańska, Nurullo Sobirov[d], Lidia Strzelczyk, Lech Szeląg, Andrzej Wiechowski, Katarzyna Włodarczyk[a], Magdalena Zawal

Voluntary scientists:

Jędrzej Iwanicki, Maciej Kisieliński, Jan Kownacki, Andrzej Wojtasiewicz, Irena Żejmo

[a] part time
[b] on leave
[c] until 16 September
[d] since 1 June

D.7 Laboratory Council

1. Prof. dr hab. Józef Andrzejewski
Nuclear Physics Division
University of Łódź, Łódź
2. Prof. dr hab. Mieczysław Budzyński
Institute of Physics
Maria Curie-Skłodowska University, Lublin
3. Prof. dr hab. Ewa Bulska
Biological and Chemical Research Centre
University of Warsaw, Warszawa
4. Dr Jarosław Choiński
Heavy Ion Laboratory
University of Warsaw, Warszawa
5. Prof. dr hab. Zbigniew Czerski
Institute of Physics
University of Szczecin, Szczecin
6. Prof. dr hab. inż. Andrzej Chmielewski
(**Member of the Council Presidium**)
Institute of Nuclear Chemistry
and Technology, Warszawa
7. Prof. dr hab. Bogdan Fornal
The Henryk Niewodniczański
Institute of Nuclear Physics
Polish Academy of Sciences, Kraków
8. Dr hab. Krzysztof Kilian
Heavy Ion Laboratory
University of Warsaw, Warszawa
9. Prof. dr hab. Stanisław Kistryn
(**Member of the Council Presidium**)
M. Smoluchowski Institute of Physics
Jagiellonian University, Kraków
10. Dr hab. Agnieszka Korgul
Faculty of Physics
University of Warsaw, Warszawa
11. Dr hab. inż. Michał Kowal, prof. NCBJ
The National Centre for Nuclear Research
Świerk k/Warszawy
12. Prof. dr hab. Leszek Królicki
Department of Nuclear Medicine
Medical University of Warsaw, Warszawa
13. Prof. dr hab. inż. Krzysztof Kurek
(**Member of the Council Presidium**)
The National Centre for Nuclear Research
Świerk k/Warszawy
14. Prof. dr hab. Adam Maj
(**Chairman of the Council**)
The Henryk Niewodniczański
Institute of Nuclear Physics
Polish Academy of Sciences, Kraków
15. Prof. dr hab. inż Piotr Magierski
Faculty of Physics
Warsaw University of Technology,
Warszawa
16. Dr hab. Krzysztof Miernik
Faculty of Physics
University of Warsaw, Warszawa
17. Dr Paweł Napiorkowski
(**Director of HIL**)
Heavy Ion Laboratory
University of Warsaw, Warszawa
18. Dr hab. Marcin Palacz
Heavy Ion Laboratory
University of Warsaw, Warszawa
19. Dr hab. Leszek Próchniak
Heavy Ion Laboratory
University of Warsaw, Warszawa
20. Prof. dr hab. Krzysztof Rusek
Heavy Ion Laboratory
University of Warsaw, Warszawa
21. Prof. dr hab. Wojciech Satuła
(**Deputy Chairman of the Council**)
Faculty of Physics
University of Warsaw, Warszawa
22. Dr hab. Elżbieta Stephan, prof. UŚ
Institute of Physics
University of Silesia, Katowice
23. Dr Agnieszka Trzcińska
(representative of the HIL staff)
Heavy Ion Laboratory
University of Warsaw, Warszawa

D.8 Programme Advisory Committee

PAC members

- Piotr Bednarczyk (The H. Niewodniczański Institute of Nuclear Physics PAN, Kraków, Poland)
- Gilles de France (GANIL, Caen, France)
- Nicholas Keeley (National Centre for Nuclear Research, Otwock, Poland)
- Marco Mazzocco (Padova University, Padova, Italy)
- Chiara Mazzocchi (Faculty of Physics, University of Warsaw, Warszawa, Poland)
- Leszek Próchniak (Heavy Ion Laboratory, University of Warsaw, Warszawa, Poland)
- Władysław Trzaska (Department of Physics, University of Jyväskylä, Finland)
- Galina Knyazheva (Joint Institute for Nuclear Research, Dubna, Russia)

The international Programme Advisory Committee of the Heavy Ion Laboratory usually meets twice a year, in spring and autumn. The deadline for submitting proposals is 3 - 4 weeks before a PAC meeting . PAC approved experiments are scheduled at the meetings of the Users' Committee, which also serves as a link between cyclotron users and the Laboratory. The Users' Committee is chaired by Jarosław Perkowski (the University of Łódź).

D.9 External HIL users

In 2021 there were **46** external HIL users and visitors from **15** scientific institutions, including 14 people from 5 institutes in Poland, 16 people from 5 institutions in the European Union and associated countries and 16 people from 6 institutes in other countries.

External HIL users and visitors were from:

Poland

- Faculty of Physics, University of Warsaw, Warszawa, Poland
- The H. Niewodniczański Institute of Nuclear Physics PAN, Kraków, Poland
- National Centre for Nuclear Research, Otwock, Poland
- Institute of Physics, Jan Kochanowski University, Kielce, Poland
- Warsaw University of Technology, Warszawa, Poland

European Union and associated countries

- IRFU/SPhN, CEA Saclay, Gif-sur-Yvette, France
- IKP, Technical University Darmstadt, Darmstadt, Germany
- University of Florence, INFN Sezione di Firenze, Italy
- Sofia University “St. Kliment Ohridski”, Sofia, Bulgaria

Other countries

- Joint Institute for Nuclear Research, Dubna, Russia
- ORTEC, Oak Ridge, Tennessee, USA
- School of Physics, Georgia Institute of Technology, Atlanta, GA, USA
- University of Guelph, Ontario, Canada
- Department of Chemistry, University of Kentucky, Lexington, KY, USA
- Department of Physics, University of Surrey, Guildford, UK

List of Authors

Abraham T., 15, 28, 30, 65
Ahmed U., 65
Akopian G.M., 75
Araszkiewicz M., 30, 43

Bednarek A., 9
Belogurov S.G., 75
Bezbakh A.A., 75
Bilewicz A., 50
Bracha T., 9, 18, 50

Chepurnov O.O., 60
Chercas K.A., 60
Choiński J., 9, 18, 25, 50
Chudoba, 75
Cichacka M., 48
Colucci G., 25, 28, 57, 65
Cortes M.L., 65
Czubek J., 48

Droste Ch., 62

Fomichev V., 75

Gazeeva E.M., 75
Gmaj P., 9
Gniazdowska E., 50
Golovkov M.C., 75
Gorshkov A.V., 75
Gumiela M., 50

Hadyńska-Klęk K., 28, 30, 65, 72
Hagino K., 57
Horodek P., 72

Ilyin A.P, 60

Jakubowski A., 9
Jankowski D., 32
Jasiński P., 9
Jaworski G., 16, 28, 65
Jia H. M., 25

Kalisiewicz W., 9
Kamiński G., 75
Kaźmierczak U., 19, 30, 43, 48
Keeley N., 60, 61, 80
Kemper K.W., 60, 61
Kern R., 65
Kilian K., 30, 37, 46
Kisieliński M., 15, 25, 65
Kliczewski S., 60
Komorowska M., 28, 30, 65, 72
Kopka M., 9
Kordyasz A., 69
Korgul A., 43
Koshchyi E.I., 60, 61
Koszel K., 37
Kowalczyk M., 15, 25, 28, 30, 65, 69
Kowalska J., 18, 50
Kozaczka W., 9
Koźmiński P., 50
Krawczyk T.J. , 32
Krupko S.A., 75
Krutul K.Z., 28, 30, 72
Krysiak P., 9

Lankoff A., 43
Le T.N.M., 72
Lin C. J., 25

Łabęda K., 9
Łyczko M., 50

Majka E., 50
Majkowska-Pilip A., 50
Makowski K., 9
Maliszewska-Olejniczak K., 43
Maridi H.M, 60, 80
Marszewska M., 48
Maryański M.J., 48
Matuszczak J., 32
Matuszewski M., 25
Matuszyńska A., 50
Mauyey B., 75
Mazur I., 9
Ma N. R., 25
Mezhevych S.Yu., 60, 61
Mielewska B., 48
Milewska K., 37

Mishchenko B.V., 60
Miszczak J., 9
Muzalevsky I.A., 75

Napiorkowski P.J., 28, 30, 65, 69, 72, 75
Nickel C., 65
Nikolskii E.Yu., 75

Okliński W., 15
Olejniczak A., 72

Palacz M., 15, 16, 28, 30, 65
Paluch-Ferszt M., 19, 22, 30, 32, 43, 48, 69, 72
Paprzycki B., 9
Piasecki E., 25, 57
Piasecki K., 25
Pietralla N., 65
Pietrzak K., 9
Pirnak V.M., 60
Piątek W., 75
Piętka I., 28
Pluciński P., 75
Ponkratenko O.A., 60, 61
Próchniak L., 62, 77
Pyrzyńska K., 39, 41, 46
Pęgier M., 46

Quỳnh A.M., 28

Radomyski B., 9
Rainovski G., 65
Rudchik A.A., 60, 61
Rudchik A.T., 60, 61
Rusek K., 30, 32, 60, 61, 75, 80

Saeed Mohamed Nassar O., 9, 30
Sakuta S.B., 61
Samorajczyk-Pyśk J., 28, 30, 62, 65
Sentkowska A., 30, 39, 41
Serikov A., 75
Sharov P.G., 75
Shyrma Yu.O., 60
Sidorchuk S.I., 75
Siemek K., 72
Siudak R., 60
Slepnev R.S., 75
Sokołowska N., 75
Sosnowski K., 9
Srebrny J., 62, 65
Standyło Ł., 9, 12
Stepanenko Yu.M., 60
Stetz T., 65
Stolarz A., 18, 30, 50
Stoyanova M., 65
Sudlitz K., 12
Szefliński Z., 19, 22, 30, 43, 48, 69, 72

Świątek Ł., 18, 50

Tańczyk R., 18, 30, 50
Trzcińska A., 25, 28, 30, 57, 65, 75
Tucholski A., 28
Tymińska K., 43

Uleshchenko V.V., 60

Walczak R., 50
Wawrowicz K., 50
Wen P. W., 57
Werner V., 65
Wojewódzka M., 43
Wolińska-Cichocka M., 25
Wolski R., 75
Wrzosek-Lipska K., 28, 30, 65, 72

Yang L., 25

Zalewski B., 25, 30, 60, 65, 75
Zhang H. Q., 25
Zidarova R., 65

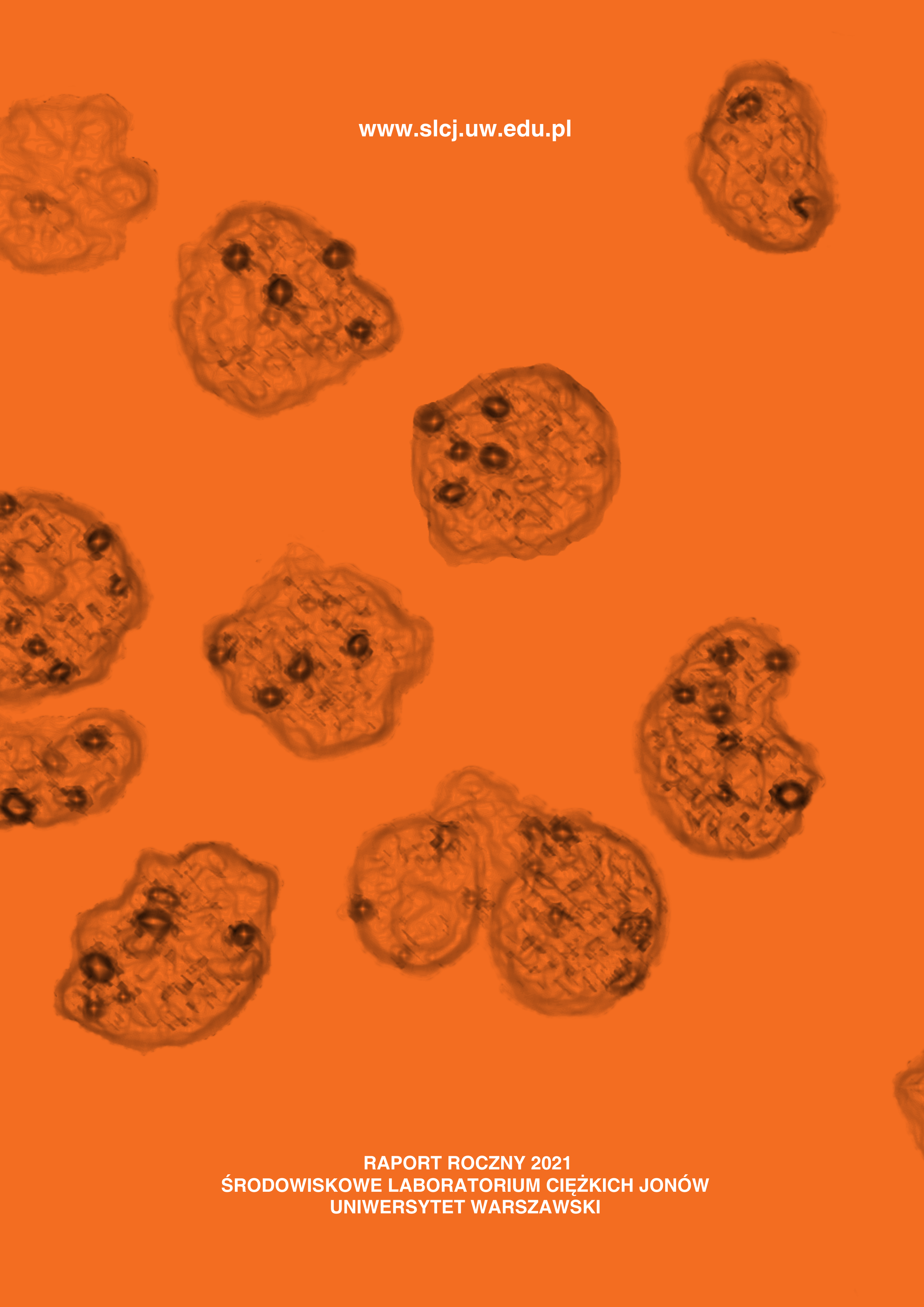

www.slcj.uw.edu.pl

RAPORT ROCZNY 2021
ŚRODOWISKOWE LABORATORIUM CIĘŻKICH JONÓW
UNIWERSYTET WARSZAWSKI